SSD
SCIENCE FOR A SUSTAINABLE DEVELOPMENT

DEVELOPMENT OF A NEW LOW-COST AND REGENERABLE
DETECTION DEVICE FOR MICROBIAL COMPOUNDS

"MIC-ATR"

A. Van Cauwenberge, E. Noël, J. De Coninck, M. Voué,
O. Denis, K. Huygen
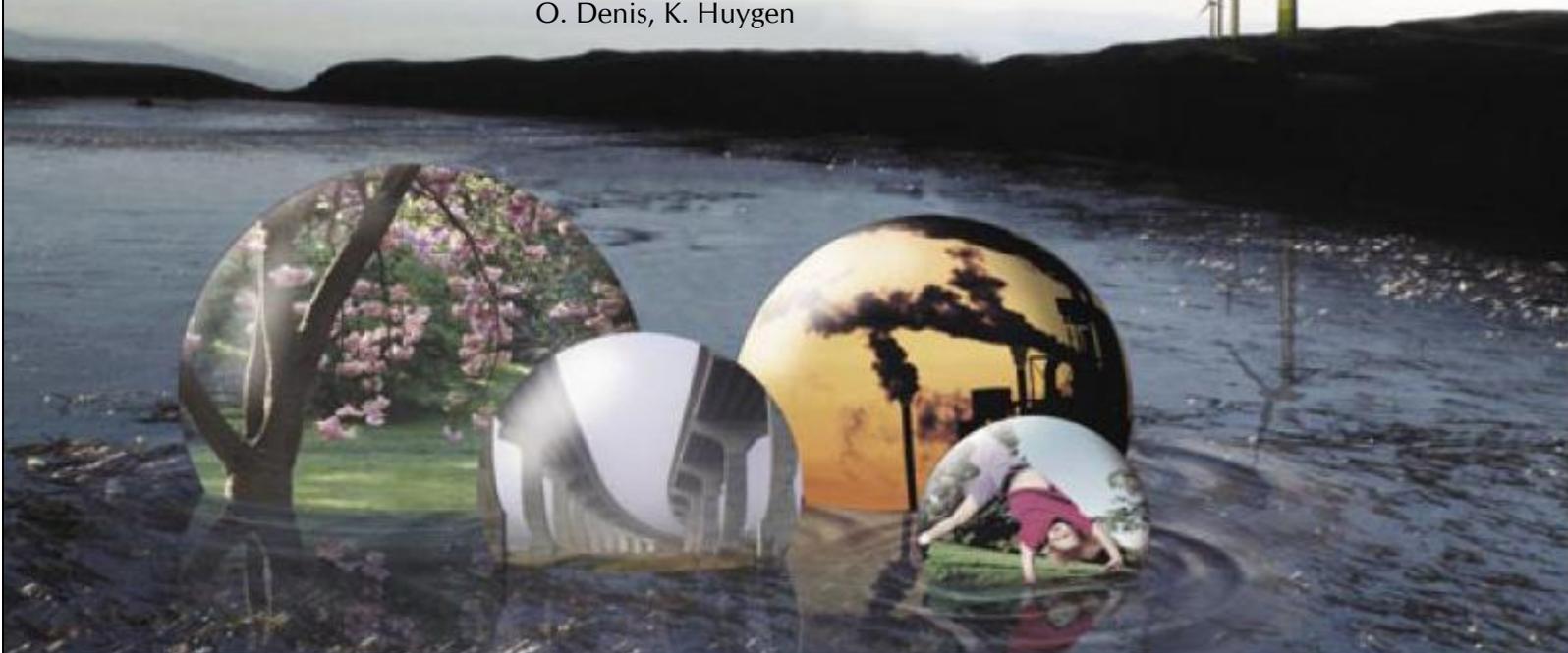
ENERGY

TRANSPORT AND MOBILITY

AGRO-FOOD

HEALTH AND ENVIRONMENT

CLIMATE

BIODIVERSITY

ATMOSPHERE AND TERRESTRIAL AND MARINE ECOSYSTEMS

TRANSVERSAL ACTIONS

.be

SCIENCE FOR A SUSTAINABLE DEVELOPMENT
(SSD)
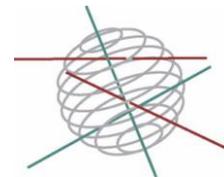
Health and Environment

FINAL REPORT

Development of a new low-cost and regenerable detection device for microbial compounds

"MIC-ATR"

SD/HE/04

Coordinator
A. Van Cauwenberge & E. Noël
Hygiène Publique en Hainaut
Hainaut Vigilance Sanitaire
Boulevard Sainctelette, 55
7000 Mons

Partners
J. De Coninck & M. Voué
Université de Mons
Laboratoire de Physique des Surfaces et des Interfaces
Place du Parc, 20
7000 Mons

O. Denis & K. Huygen
ISP-WIV
Département Maladies Transmissibles et Infectieuses
Programme d'Allergologie
Engelandstraat, 642
1180 Bruxelles

belspo

A. Van Cauwenberge, E. Noël, J. De Coninck, O. Denis, K. Huygen - ***Development of a new low-cost and regenerable detection device for microbial compounds "MIC-ATR"-*** Final Report. Brussels : Belgian Science Policy 2012 – 111 p. (Research Programme Science for a Sustainable Development)

TABLE OF CONTENT

ACRONYMS, ABBREVIATIONS AND UNITS

AFLA-B1:	Aflatoxin B1
AFLA-ALB:	Aflatoxin B1 coupled to albumin
ATR:	Attenuated Total Reflexion
BIA-ATR:	Biological Interaction Analysis using Attenuated Total Reflexion
BSA :	Bovine Serum Albumin
DNP :	2,4-DiNitroPhenol
DNP-ALB:	2,4-DiNitroPhenol coupled to albumin (equiv. to DNP-HSA)
ELISA:	Enzyme Linked Immunosorbent Assay
FITC:	Fluorescein IsoThioCyanate
FTIR:	Fourier-Transform Infra-Red
HSA:	Human Serum Albumin
IRE:	InfraRed Element
KLH:	Keyhole Limpet Hemocyanin
LOD:	Limit of detection
LPS:	Lipopolysaccharides
mAb:	Monoclonal Antibody
NHS:	N-hydroxysuccinimidyl
OTS:	OctadecylTrichloroSilane
OVA:	Ovalbumin
PBS:	Phosphate-Buffered Saline
PEG:	PolyEthyleneGlycol
VERRU-A	Verrucarin-A

SUMMARY

There is crucial concern about the presence of moulds in indoor environments and their adverse effects on human health. The indoor moulds, omnipresent in 60% of the dwellings, have indeed the potential to produce components that have been associated to several severe human health problems like allergic hypersensitivity responses, bronchitis, symptoms of asthma, pulmonary haemorrhage, potentially mortal. For instance, in Belgium, according to the Scientific Institute of Public Health, the prevalence for asthma is about 4% in the global population and is relatively stable between 2001 and 2004.

Fungal spores are universal atmospheric components and are recognized as important causes of respiratory allergies. Fungi grow on most substrates if enough moisture is available, frequently colonize indoor damp places and their spores are commonly found in house dust. People living in these environments often complain about a variety of health problems probably resulting from chronic exposure to mold components.

Four of them have been identified as components of interest: VOCs, fungal spores, airborne mycelium fragments, mainly containing glycan wall fragments and mycotoxins, which are non - or weakly volatile stable secondary metabolites. The links between the presence in the environment of these compounds and identified and declared pathologies is most of the time indirect. Visual inspection does not allow to fully asses any adverse health effect. The risk associated to mould should be characterised by the presence of mycotoxins in ambient air and in dust. The most dangerous ones belong to the family of aflatoxins and trichothecenes.

Up to now, mycotoxins have been intensively studied in the context of food safety. They have been implicated as causative agents of pathologies in humans and animals that have consumed fungus-infected agricultural products. In this context, the link between the amount of toxin and the observed pathology is more direct. In such a way, normalization actions were carried out, defining the upper admitted levels of such compounds in foodstuffs. However, these limits are not defined for airborne mycotoxins, due to the lack of experimental data and the absence of reliable sampling and testing procedures. To date, studies have mostly focused on detecting mycotoxins on bulk materials or in settle dust but there is an urgent need, driven by the guidelines of Public Health policy, to develop specific and sensitive tests to measure airborne macrocyclic trichothecenes mycotoxins in indoor environments, for which no specific nor enough sensitive detection method exists.

Classical diagnosis and monitoring techniques for the study of mould contamination indoors are still commonly based on fungal cultures and spores counts.
While straightforward, these techniques are time-consuming, dependent from a skilled investigator, very often lack reproducibility.

In the field of indoor mould surveillance, there is a need to develop objective monitoring and standardized sample analyses techniques for exposure determination. In this project, one approach towards the development of objective monitoring assays was based on the detection of fungi or their toxins using monoclonal antibody (mAb)-based assays. These antibodies were used in ELISA assays and in the development of a regenerable low-cost biosensor of high sensitivity and selectivity based on FTIR/ATR spectroscopy. The biosensor uses optical elements, transparent in the IR spectral domain, modified by wet chemistry to allow the coupling of molecular receptors. Our strategy was to develop new rat mAb directed against mould antigens to allow their easier quantification in dwellings using immunoassays as compared to the conventional culture techniques still in use nowadays. We also developed a rat mAb specific for the verrucarin A, an important trichothecene. This mAb allowed the development of new immunoassays and was used in the construction of a new biosensor using optical elements.

The comparative detection of low molecular weight molecule like DNP has first served as model for detection of haptens and for optimization of the sensor. Results obtained by competitive ELISA and by FTIR were compared, with the use of 6 different rat monoclonal antibodies specific for the DNP. All the tested antibodies responded in a similar manner to the coupled DNP molecules (DNP-HSA) but significant differences were observed for the recognition of free DNP molecules. With coupled DNP molecules, the limits of detection were equivalent between both techniques but for the free DNP molecules, the limits of detection were different: 1 µg/ml with ELISA and 4 ng/ml with the FTIR assays, using the LO-DNP34 antibody.

Going further with the experiments, we realized that the biosensors had to be optimized for the direct detection by FTIR-ATR. Therefore a new system of gas purge has been installed to obtain cleaner background spectra and improve signal to noise ratio. Miniaturization and robotization of the detection system have also been achieved in order to increase the sample throughput and reduce the costs of functionalization, with the use of new crystals named "toblerone". A new antifouling coating has also been developed, considering the possibility of grafting a novel amphiphilic silanization reagent composed of a very short alkyl chain and a short PEG chain, in order to detect analytes of interest in complex matrix and media. Validation of this new device has been performed with the detection of FITC and aflatoxin B1 which share some chemical similarity. Spectral references of aflatoxin B1 and verrucarin A were obtained using the Smart Golden Gate accessory which offers better sensitivity and versatility.

In this way, FTIR fingerprints of aflatoxin B1 and verrucarin A were obtained, showing a good correlation between the chemistry of these molecules and their infrared signature. FTIR technology has then been used for quantitative analyses. By analyzing the amide band of BSA coupled aflatoxin, the limit of detection was about 2,7 ng/ml. For free toxin, obtained by analyzing the evolution of the hydroxyl bands, the limit of detection was about 10 pg/ml. These infrared elements are relatively expensive but demonstration was made that a cleaning procedure by elution is possible to reuse the coated element but optimization of elution conditions is very complex and requires further study. Mechanical polishing is also possible to remove all the graftings onto the infrared elements.

A competitive ELISA has also been set up with success to detect aflatoxin B1 in solutions, but it seemed not sensitive enough to detect the presence of airborne aflatoxin in the air of the analysed dwellings.

As moulds are very common outdoor but are also present indoor in damp places, quantification of the mould biomass in the ambient air turned out to be interesting in order to better appreciate the level of indoor contamination. Therefore, a sandwich ELISA was set up using monoclonal antibodies specifically developed for the project. Among the numerous antibodies obtained, some of them were clearly species specific while LO-MO-5 turned out to detect the presence of the recognized antigen into various mould extract preparations i.e. *Alternaria alternata, Cladosporium herbarum, Stachybotrys chartratum* and *Penicillium chrysogenum. Aspergillus niger, Acremonium strictum and Fusarium oxysporum* extracts were moderately recognized while extracts from *Candida albicans* and *Saccharomyces cerevisiae* were not or almost not recognized. This assay was optimalized (coating of the antibody, saturation solution, incubation times, concentrations of revealing antibodies and peroxydase streptavidin) and we used an extract of *Cladosporium herbarum* spores as an internal standard for the quantification of field samples. The sensitivity of this assay was estimated to be between 2000 and 1000 equivalent *C. Herbarum* spores per ml.

The next part of the work was dedicated to the production of monoclonal antibodies against mycotoxins. As mycotoxins are small non proteinic components, they are not able to induce the production of antibodies when injected "as this" in animals since the production of antibodies (at least for non repetitive antigens) requires the help of T helper cells recognizing linear peptides. Therefore Roridin A and Verrucarin A were conjugated to BSA and OVA and fusion experiments were conducted with LOU/c rats immunized in the footpads with 50 μg of verrucarin A conjugated BSA. Of the 553 tested clones, 70 clones (13%) produced antibodies recognizing the verrucarin A bound to OVA. Only one of these clones produced antibodies which were inhibited by the free verrucarin A.

After optimization of a competitive ELISA test using this antibody (F24-1G2), we obtained sensitivity between 3.9 and 1.95 ng/ml of free verrucarin A. This antibody was used in both competitive ELISA and FTIR-ATR techniques. With the latter, it was possible to detect verrucarin A at 1pg/ml, reaching a thousand times better sensitivity compared to competitive ELISA.

These new tools have been implemented in environmental samplings that were coupled to the standard activities of the "Laboratoire de Prévention des Pollutions Intérieures" (LPI) in indoor pollution prevention and diagnosis. The LPI is intervening on request of the general practitioner in the dwellings suspected to be the cause of health problems to their occupants. A visit is including systematic sampling for both chemical and microbiological pollutants and measuring of physical parameters. A questionnaire is filled-up with the patient and first advices are provided. After the analysis of the samples, a report is send to the patient and a copy to the medical practitioner with specific advices related to the results. During the sampling campaign, 84 visits were made to symptomatic dwellings and 17 to control dwellings. 95 dust samples from the Laboratory of Allergology in Strasbourg were also considered. The conclusions and recommendations arising from this study are the following:

The investigations made on fungal flora in symptomatic dwellings shows that on surfaces, tenant's dwellings are far more contaminated by molds than owners ones (92% vs. 55%). This discrepancy has not been observed in air. However, the presence of mycotoxins has been clearly associated with the development of molds. Three major genera of molds have been found (*Cladosporium, Penicillium and Aspergillus*) but a larger diversity and representativeness is observed with the tenants, among which *Stachybotrys*, *Ulocladium* and *Alternaria,* known to cause adverse health effects, represent 12% of the total contamination. A very simple recommendation to prevent this situation would be to avoid mould proliferation before health problems occur. Ideally, owners should be obliged to solve the problems of dampness and mold contamination before putting a property for rent and tenants should also be better informed about issues related to dampness. This is maybe even more crucial in these times of repeated floods that promote mold growth in dwellings where dampness problems are becoming recurrent.

Air contamination is massive (>90%) in symptomatic dwellings while in control houses, the air presents a very low contamination (only in 6% of the houses). The three major pathologies declared by the inhabitants are asthma, bronchitis and rhinitis but we were not able in this study to find a direct correlation between a specific pathology and the presence of one or several specific mold genera.

Investigations made in dust showed an indoor mold biomass in all investigated dwellings, but the means values are significantly lower in control than symptomatic dwellings. However, no correlation could be made between mold pollutants and dust mites pollutants, showing the large diversity of contaminants and situations.

The spore antigens are present everywhere but it can reasonably be drawn from our data that recommended values for mattresses and floor should not exceed 30 10^6 Eq clado sp/m2 and 85 10^6 Eq clado sp/m2 respectively.

In air, mycotoxins have been detected by LC-MS/MS in 18% of symptomatic dwellings but not in control dwellings. This value is of high concern since these compounds are the potential source of severe adverse effects on human health. The major mycotoxins present in the analyzed samples are Roridin A and Verrucarin A. However, because of the lack of commercial standards for LC-MS/MS only a panel of 17 mycotoxins has been used and we have no idea of the possible presence of other ones. Verrucarin A and Roridin A are thus considered as indicators of a potential mycotoxin contamination. The commercial kit Quantitox (Envirologix) overestimates mycotoxins in air, when compared to the results obtained by LC-MS/MS. In more difficult matrix like dust samples, LC-MS/MS has shown its limits, with inadequate limit of detection (LOD) for environmental samples.

The existing tests and methods have thus all shown their limits and drawbacks and we therefore investigated the presence of Verrucarin A in environmental samples using FTIR biosensors grafted with the anti-verrucarin A mAb F24 developed during this project. We first focused on a frequency in agreement with chemical structure of the verrucarin A (CH strectching region around 3000 cm^{-1}) when analysing dust samples known to be positive. All the results were consistent with the ones obtained by ELISA tests. Regarding air samples, a larger range of frequency had to be explored by FTIR to find a region (hydroxyl stretching region at 3300 cm^{-1}) in agreement with the chemical structure of verrucarin A and with the results previously obtained with our other methods.

In conclusion, we have demonstrated that a regenerable biosensor based on FTIR/ATR spectroscopy and modified by wet chemistry to allow the grafting of specific antibodies is a promising technology able to detect mycotoxins in complex matrix with a high sensitivity. However, the technique still needs further developments in order to validate the method, determine the limit of detection in environmental samples and quantify the ligands.

Keywords: FTIR-ATR spectroscopy, biosensors, indoor pollution, mycotoxins, molds, damp dwellings, allergic diseases, sick building syndrome

1. INTRODUCTION

Since several decades, allergic diseases are proliferating in developed countries. The US CDC (Centre for Disease Control and Prevention) has shown that between 1980 and 1994 the prevalence of asthma in the U.S. increased of 75 % in the overall population and of 74% among children 5-14 years of age (Akinbami *et al.* 2009). Therefore asthma accounts for more than 10 million outpatient clinic visits, and nearly 2 million emergency visits each year. The annual economic cost of asthma in the USA is $19.7 billion. Direct costs make up $14.7 billion of that total, and indirect costs such as lost productivity add another $5 billion (American Lung Association, 2007). The situation and the annual cost of asthma in Europe is very similar (European lung white book. 2003)

In Belgium, according to the Scientific Institute of Public Health, the prevalence for asthma is about 4% in the global population and was relatively stable between 2001 and 2004. In the province of Hainaut, the situation is statistically different and the prevalence reaches levels around 6%, as shown in **figure 1**.
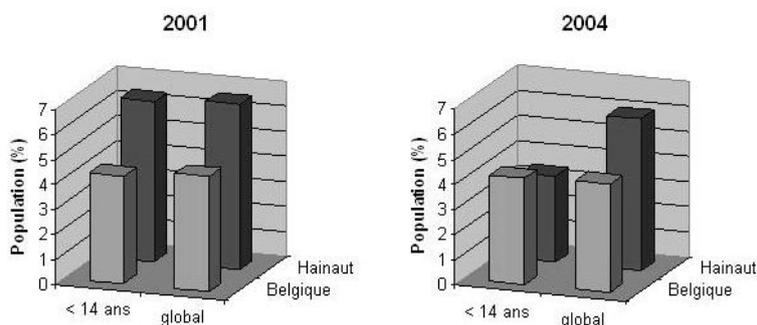
Figure 1 : Asthma prevalence in Belgium for years 2001 and 2004 (data source: WIV-ISP, Brussels)

Moulds are saprophytic or pathogenic fungi found in nearly every environment, indoors and outdoors, all year round. *Alternaria alternata* and *Cladosporium herbarum* are the major mould species found in outdoor environments and their clinical significance regarding allergic sensitizations and diseases has been clearly demonstrated (Perzanowski *et al.* 1998; Resano *et al.* 1998). For instance the cross sectional study from the European Community respiratory health survey showed that the frequency of sensitisation to *A. alternata* or *C. herbarum* increased significantly with increasing asthma severity (Zureik *et al.* 2002) and *A. alternata* sensitization represent a risk factor for respiratory failure (Black *et al.* 2000; Zureik *et al.* 2002).

The exact prevalence of sensitization to *A. alternata* is difficult to determine due to the poor standardization of mould extracts but several epidemiological studies have shown that 10 to 20% of patients with repiratory allergies are sensitized to this mould (Bartra *et al.* 2009).

Exposure to moulds indoor has also been associated with a variety of adverses effects such as allergies, mycotoxicoses and infections (Seltzer and Fedoruk, 2007). *Aspergillus fumigatus* and *versicolor* and *Penicillium brevicompactum* and *chrysogenum* are among the most common species found in damp dwellings and are known to produce many harmful mycotoxins. In addition *A. alternata, S. chartratum* and *Cladosporium spp* are also found indoor (Nolard *et al.* 2001). In sick houses and buildings, high indoor humidity allows fungal growth. People living in this environment often complain from a sick building syndrome probably resulting from chronic exposure to volatile organic compounds and mycotoxins. Living in damp dwellings also increases the frequencies of respiratory allergies (Bornehag *et al.* 2005; Dates *et al.* 2008).

Regarding the connexions between allergy and damp dwellings, recent studies (Bex *et al.*, 2003) whose results are summarized by Prof. F. Squinazi, Head of the Laboratoire d'Hygiène de la Ville de Paris, point out the following sticking features:

In Europe and North America, moulds are present in 20% to 40% of the buildings.
A study carried out in France over the period 2003-2007 on 567 buildings highlighted that 47% of them encountered problems that could be directly related to ambient humidity. In the USA, 20% to 30% of atopic patients are concerned by the allergy to indoor moulds, which corresponds to 6% of the total population.

In these studies, four fungal components have been identified as components of interest:

- the organic volatile compounds (OVCs)
- the fungal spores
- the airborne mycelium fragments, mainly containing glycan wall fragments
- the mycotoxins, which are non- or weakly volatile stable secondary metabolites.

The links between the presence in the environment of these compounds of interest and pathologies is, most of the time, indirect.

Figure 2 : Contaminated dwellings (Source: Laboratoire de prévention des Pollutions Interieures (LPI), HVS, Mons, Belgium)

Among the identified causes of asthma, living in poor indoor environment has often been highlighted. In such kind of environment, dampness is the principal factor of development of mould. Visual inspection doesn't allow to fully assessing any adverse health effect. The risk associated to mould should be characterised by the presence of mycotoxins in ambient air. The indoor moulds have indeed the potential to produce extremely dangerous toxins. Exposure to these factors has been associated to several severe human health problems like allergic hypersensitivity responses, symptoms of asthma, pulmonary haemorrhage, potentially mortal. The most dangerous mycotoxins responsible for these belong to the family of aflatoxines and trichothecenes (Cooley *et al.*, 2004; Jennessen *et al.*, 2005).

Mycotoxins have also been intensively studied in the context of food safety (Scudamore *et al.*, 1998). Mycotoxins, by-products of fungal metabolism, have been implicated as causative agents of adverse health effects in humans and animals that have consumed fungus-infected agricultural products. The fungi are a vast assemblage of living organisms, but mycotoxin production is most commonly associated with the terrestrial filamentous fungi called the moulds. Various genera of toxigenic fungi are capable of producing such diverse mycotoxins as the aflatoxins, rubratoxins, ochratoxins, fumonisins, and trichothecenes. The trichothecenes are a very large family of chemically related toxins produced by various species of Fusarium, Myrotecium, Trichoderma, Cephalosporium, Verticimonosporium, and Stachybotrys. They are markedly stable under different environmental conditions. The distinguishing chemical feature of trichothecenes is the presence of a trichothecene ring, which contains an olefinic bond at C-9, 10; and an epoxide group at C-12, 12 (**Figure 3**). They can be divided into four categories (WHO, 1990) :

Type A   functional group other than a ketone group at C8;
Type B   carbonyl group at C8;
Type C   second epoxide group at C7,8 or C9,10;
Type D   macrocyclic ring system between C4 and C15 with two ester linkage
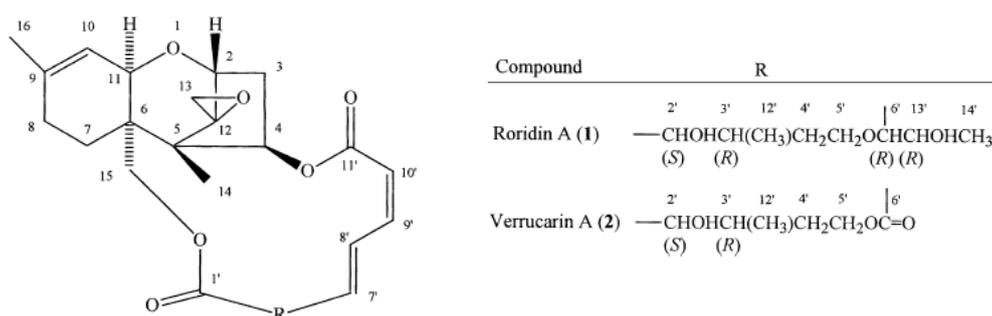
Figure 3 : Molecular structure of some D-class macrocyclic trichothecenes: Roridin A and Verrucarin A.

In addition to their allergic potential, moulds are also plant pathogenic fungi that cause important yield losses in crops. *A. alternata* induces stem cell cancer of tomato. *Alternaria spp* are also causal agents of black or brown spot diseases of fruits and their mycotoxins have been reported in many products such as fruit juices, olives, tomatoes and cereals (Drusch and Ragab, 2003; Ozcelik *et al.* 1990).

Classical diagnosis and monitoring techniques for the study of mould contamination indoors are still commonly based on fungal cultures and spores counts. While straightforward, these techniques are time-consuming, dependent from a skilled investigator, very often lack reproducibility and there is a need for objective monitoring techniques. In the field of indoor mould surveillance and in plant pathology also, there is a need to develop standardized sample analyses techniques for exposure determination. One approach towards the development of objective monitoring assays is based on the detection of fungi or their toxins using monoclonal antibody (mAb)-based assays.

2. METHODOLOGY AND RESULTS

2.1. Methodology

To date there is an urgent need, driven by the guidelines of Public Health policy, to develop specific and sensitive tests to measure airborne mould contaminants and mould toxins like the macrocyclic trichothecenes mycotoxins in indoor environments, for which no rapid, specific nor enough sensitive detection method exists (Institute of Medicine of the National Academy of Sciences). This research project had several goals; in particular to analyse mould contaminations in the context of symptomatic dwellings, meanings dwellings in which people are complaining of various health problems and to develop new techniques including new immunoassays and a regenerable low-cost biosensor of high sensitivity and selectivity based on FTIR/ATR spectroscopy for the monitoring of these contaminated dwellings.

Current assessment methods of indoor mold contamination are based on sample cultivation or microscopic spore counts. Although these techniques may be very informative on a case by case basis they have also major drawbacks. The direct microscopic spore count method is time consuming, subjective, shows a low sensitivity and high data variability. The methods based on culture analysis can overlook fungal species that are not easily cultivable, may give an underestimate of those fungal types that grow slowly because they are overtaken by faster growing colonies and ignore the presence of non cultivable and non-viable spores or mycelia fragments (Niemeier *et al*, 2007). Recent developments in molecular techniques have provided significant advances in rapid detection and characterization of microorganisms irrespective of their viability or cultivability. However these molecular assays, require skilled laboratory personnel, are not easily implemented for routine analysis and more importantly are very expensive. Surrogate markers of mold contamination that measure quantitative loads of fungal biomass indoor such as β-glucan or ergosterol are useful for providing information about the global amount of fungi. However their measurements are also very expensive, require highly trained personnel and sophisticated analyzers (HPLC and mass spectrometer) which can hamper the routine use of these markers (Robine *et al.,* 2005). Therefore there is a need for the development of better techniques able to identify environmental exposure to molds and it is clear that the development of new assays will allow the development of new preventive measures for public health purposes.

Indeed, in its report "Damp Indoor Spaces and Health", the Institute of Medicine of the US National Academy of Sciences identified the development of valid and standardized

quantitative exposure assessment methods (particularly methods based on non-culture techniques and measuring constituents of micro-organisms such as allergens, β-glucans, fungal spores,…) as a high research priority (Institute of Medicine of the US National Academy of Sciences, 2004).

Monoclonal antibodies (mAbs) are powerful tools for the quantification, detection, and targeting of specific molecules and immunoassays have become a common techniques in diagnostic laboratories. Nowadays mAb are frequently used for the detection of numerous compounds and for the exposure assessment to numerous agents. Immunodetection techniques are very flexible, inexpensive, easily implementable and standardizable and could be interesting tools for the development of new assessment methods of indoor fungal contamination.

Our strategy was to develop new rat mAb (Lebacq *et al.*, 1983; Bazin *et al.*, 1984; Digneffe *et al.,* 1990; Acquermans *et al.*, 1990) directed against mould antigens to allow their easier quantification in dwellings using immunoassays as compared to the conventional culture techniques still in use nowadays. We also developed a rat mAb specific for the verrucarin A, an important trichothecene. This mAb allowed the development of new immunoassays and was used in the construction of a new biosensor using optical elements, transparent in the IR spectral domain, modified by wet chemistry to allow the coupling of receptors, in particular mAb directed against macrocyclic trichothecenes (Voué et al, 2007).
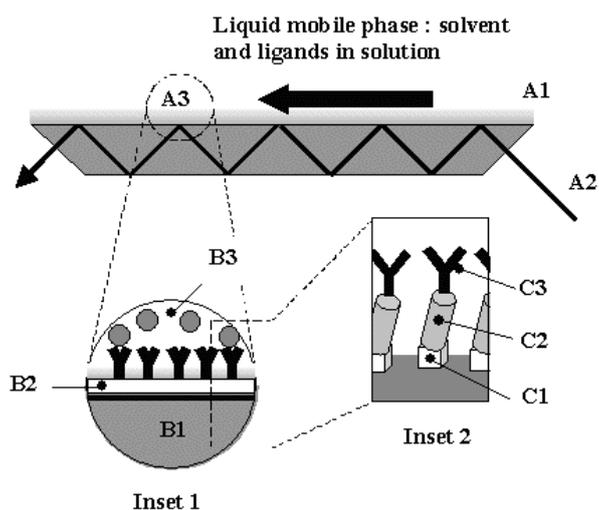
Figure 4 : A1: Total internal reflection element transparent in the infra-red spectral domain; A2: Incident infra-red beam; A3: Ligand/receptor interactions at the crystal surface and evanescent wave). Inset 1: Molecular recognition (B1: ATR element surface; B2: Functionalization layer; B3: Free ligands and ligands bound to receptors). Inset 2: Schematic representation of the molecular construction (C1: anchoring molecule; C2: spacer molecule; C3: receptor).

Biosensors are composite devices that have been bio-functionalized and enable highly specific interactions between a biological molecule and another molecule of its surrounding (Andreescu and Sadik, 2004). They allow the specific recognition of free analyte (the ligand) of interest by a target (the receptor) which is tightly bound to the sensor. Sensors based on the molecular recognition of bio-molecules have already attracted intensive interest in many different fields such as medical diagnostics and control, environmental analysis, and monitoring of biotechnological processes.

Different surface sensitive techniques can be applied to detect the ligand-receptor interactions, depending on the nature of the sensor supports. Among others, they are piezoelectric methods, impedance spectroscopy, fluorescence microscopy, imaging ellipsometry and surface plasmon resonance (SPR) spectroscopy (Jonsson *et al.,* 1991; Malmqvist, 1993). Biosensors based on the SPR spectroscopy, a surface sensitive technique able to probe molecular interactions in real time and on-line, make use of changes in the refractive index of the medium near a thin film of gold evaporated or sputtered on a glass support. The targets or biological receptors are immobilized via the method of self-assembled monolayers based on the chemisorption of thiol-containing molecules or via the interaction with an amorphous Dextran matrix. Intrinsically, this detection technique measures the mass loading on the surface and provides no direct physico-chemical information about the ligand-receptor interaction. Binding of small molecules is therefore difficult to investigate. Alternative techniques are therefore requested to fill the gap between the binding of the ligand on the receptor and the induced conformational modifications of the molecular structures. This physico-chemical information can be obtained from Fourier transform infra-red (FTIR) spectroscopy (Mirabella, 1993), an extremely powerful analytical technique, particularly adapted to the characterization of organic molecules and biological systems (Goormaghtigh *et al.,* 1999 ; Vigano *et al.*, 2005). In addition to the level and kinetics of binding, it provides quantitative information about the structure of molecules investigated. The method has been applied to the study of mono- and multilayers of bio-organic samples in contact with optical element by using the attenuated total internal reflection (ATR) configuration. Due to the propagation of the evanescent wave outside the ATR element, i.e. in its surrounding medium, the ATR configuration allows the study of analytes in water-containing media when they are brought in contact with an optical element.

The specificity of such sensors is obviously related to the existence of specific ligand-receptor couples but, indirectly, this specificity can only be fully exploited if the receptor can be covalently linked to the sensor substrate. This covalent binding highly depends on the chemical nature of the ATR element. The mostly used ATR elements are made of silicon and germanium. The chemical bonding of molecules on silicon substrates via

the activation of the native SiO2 layer has been widely studied. This can be performed either using an oxidation process to increase the density of Si-OH groups at the surface or using a reduction process to passivate the interface by a Si-H layer. The modification of the surface properties using such reaction paths is less obvious when considering germanium ATR elements: contrarily to the SiO2 layer, the GeO2 layer is water soluble and the Ge surface is much less resistant to the oxidation process than the Si one. Vogel and coworkers could get rid of these draw-backs (Liley *et al.*, 1997; Kroger *et al.,* 1999] by using self-assembled monolayers of thiol-terminated molecules on gold coated Ge elements.

To avoid the presence of the gold film, which significantly reduced the efficiency of the FTIR-ATR method due to the attenuation of the evanescent wave in the thin metallic layers, a biosensor technology (BIA-ATR technology) has been developed using an organic layer directly grafted on the chemically activated surfaces of a germanium crystal. The functionalized layer of the ATR device has been build by wet chemistry in a view of covalently binding a receptor, as shown hereafter (Marchand *et al.*, 2002; Devouge *et al.*, 2005).

The biosensor devices that we have developed have been produced on the basis of the patented BIA-ATR technology. Starting from germanium ATR elements (50 x 20 x 2 mm³) with an internal incidence angle of 45°, this production requires a three-step procedure involving (a) the cleaning and activation of the germanium surface, (b) the construction of the organic anchoring layer by wet chemistry and/or photochemistry approaches and (c) the covalent binding or the adsorption of the toxin receptors.

The organic anchoring layer have been obtained by the grafting of small molecules (OTS or APTES) on the activated ATR element surface (Voue *et al.*, 2007) and the binding of bifunctional molecular clips.

These molecules can eliminate N-hydroxysuccinimide and bind proteins via the formation of a covalent amide bound with the sterically available $-NH_2$ groups of the protein. The obtained biosensing device is highly performing. Its performance has been demonstrated at three complementary levels:

Low detection limit: its application in the detection of biotin with immobilized streptavidin showed that concentrations as low as 10^{-13} M to 10^{-12} M could readily be unambiguously detected (Voue *et al.*, 2007). Taking into account the molecular weight of biotin, this result shows that concentrations of 0.25 pg/ml are readily detected by the method, which is 10^3 better than the detection limit reported by Brasel (2005) ;

Ability to detect the binding of small molecules on large receptors: the method has been used to detect the binding of the Rabeprazol, a regulating/inhibiting agent of the H^+-pump, to gastric ATPase (*BIA-ATR Report, WDU Programme, DGTRE*).

High potential of application to the detection in complex environments: Furthermore, the molecular construction involving membrane fragments containing phosphatidylcholine (PC) or phosphatidylserine (PS) allowed us to quantitatively monitor the specific binding of the haemophilia factor VIII as a constituent of a complex protein solution (Goldzstein, 2006).

For these reasons, the combination of the wet chemistry approach and of the FTIR spectroscopic detection method provides us a powerful tool to quantitatively investigate the binding of the mycotoxins to specific receptors.

2.2. DNP detection: ELISA and FTIR analysis.

This part of the report concerns the comparative detection of a low molecular weight molecule (DNP) by ELISA and FTIR. The choice of this molecule has been made because it may be considered as an appropriate model for detection of haptens.

2.2.1. ELISA results

A "classical" competitive ELISA has been used to detect the free DNP in solution and to determine the detection limit of this technique in these particular conditions. Since the detection limit is clearly dependant of the characteristics of the antibodies used in the assay, we performed this competitive ELISA with six different rat mAb specific for the DNP. The characteristics of these antibodies (antigen used for rat immunization, isotype and affinities) are listed in Table I.

To detect the DNP, BSA labelled DNP was coated on ELISA plates; then the plates were saturated and washed. Decreasing concentration of inhibitors (free DNP or BSA labelled DNP) was applied together with a fixed concentration (1 µg/ml) of rat mAb against DNP. After the incubation the plated were washed and the binding of the rat mAb to the coated BSA-DNP was revealed by a mouse mAb labelled with the peroxydase and specific for the rat Kappa light chain.

Name	Antigen	Isotype	Affinity
LO-DNP-1	DNP-OVA	IgG1	8.4 10E10
LO-DNP-2	DNP-Ascaris	IgG1	1.7 10E10
LO-DNP-34	DNP-OVA	IgM	5.5 10E10
LO-DNP-45	DNP-salmonella	IgA	3.2 10E10
LO-DNP-57	DNP-salmonella	IgG2b	1.4 10E10
LO-DNP-61	DNP-salmonella	IgG2a	7.1 10E10

Table I: Characteristics of the rat antibodies specific for DNP used.

The binding of the six rat mAb was inhibited similarly by the free BSA-DNP in solution leading to an assay sensitivity located between 80 and 40 ng/ml. However only the binding of LO-DNP-2 and -61 showed an inhibition of more than 50% at the highest concentration of DNP tested (1 mg/ml) and this assay showed a very poor sensitivity (between 8 to 4 µg/ml).

Therefore we worked to optimize the detection of the free DNP in this assay. We optimized the concentrations of BSA-DNP used for the coating, the concentrations of LO-DNP-61 in solution and the duration of the different incubations. This optimized competitive ELISA assay had a 1000 x higher sensitivity for the free DNP and the level of free DNP detection was located between 8 to 4 ng/ml (**figure 5**).
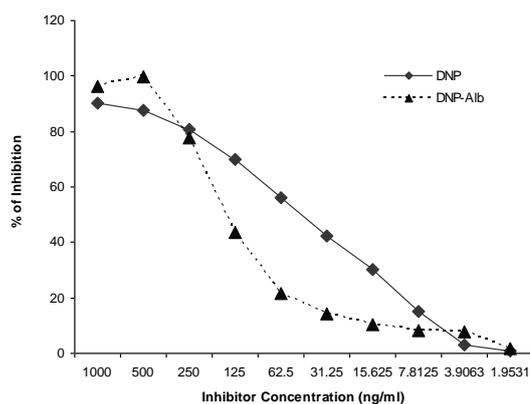
Figure 5: Detection of free DNP and of DNP coupled to albumin molecules – Optimization of the competitive ELISA towards an increased sensitivity for the free DNP

2.2.2. FTIR analysis results

The optical device for the detection of 2,4-DNP is build on a Germanium crystal covered by an octadecyl-trichlorosilane (OTS) self-assembled monolayer coupled to a spacer molecule whose end function is an N-hydroxysuccynimidyl ester (**figure 6**).

As shown on **figure 7**, the binding of LO-DNP1 monoclonal antibody against 2,4-DNP is clearly evidenced by the increase of the intensity of the amide I (1634 cm^{-1}) and II (1543 cm^{-1}), as well as by the decrease of the carbonyl band at 1740 cm^{-1}. Similar binding curves were observed for LO-DNP34 and LO-DNP61 antibodies. The mAb layer was stable under rinsing by a PBS solution.

(A)   **(B)**
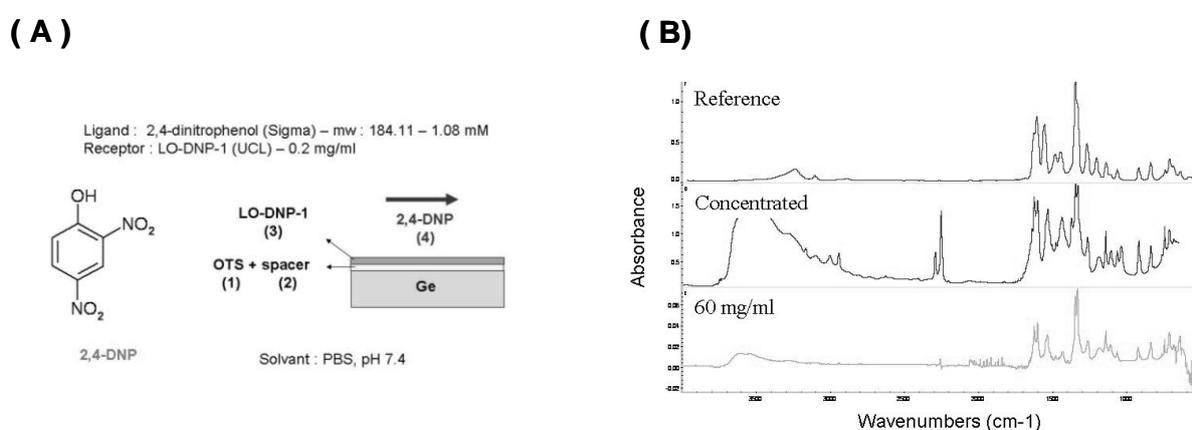
Figure 6: (A) Detection principle for 2,4-DNP using monoclonal antibodies. (B) Reference spectrum of 2,4-DNP – Comparison with DNP spectra in concentrated and diluted (60 mg/ml) solutions.
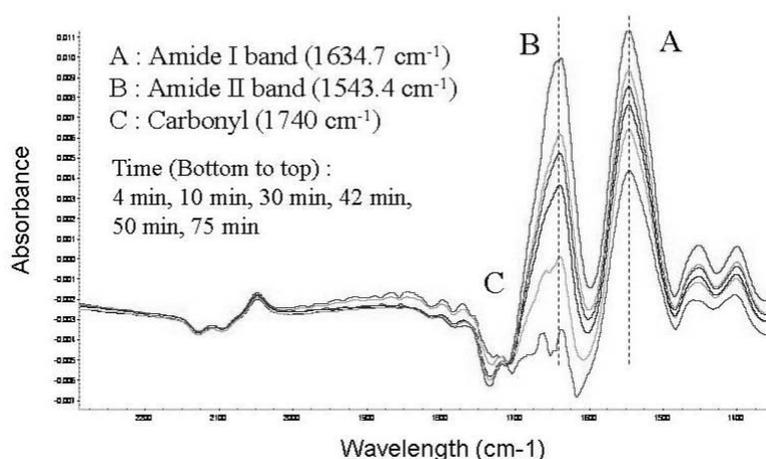
Figure 7: Binding of the LO-DNP1 anti-DNP monoclonal antibody – Time evolution of the amide bands.

The second stage of the experiments concerns the detection of the ligand itself. Solutions of free DNP were flown in the experimental cell but no significant increase of the DNP absorption peaks was observed at 1268, 1346, 1556 and 1607 cm $^{-1}$ (data not shown). An *a posteriori* explanation is given by the poor affinity of the mAb for the free DNP as evidenced by the ELISA results.

Experimental procedure has been reoriented towards the detection of DNP coupled to albumin and towards competition tests. The methodology was therefore the following.

In a first step, a DNP-HSA solution (1 mg/mL in PBS) was injected in the flow cell at a flow rate of 5 to 10 µL/min (discontinuous). After 2 h, buffer solution was injected in the cell to remove the unreacted excess of protein. After the binding of the protein to the sensor surface, monoclonal antibodies (Mabs) (5 µg/mL in PBS) were incubated at room temperature in the presence of either free or coupled DNP. After 20 min of incubation, an aliquot of the Mabs/inhibitor solution was injected in the flow cell and the binding of the antibody to the immobilized protein was monitored as a function of time by recording FTIR spectra.

A series of inhibition tests was carried out to probe the sensitivity of the detection method with respect to the coupled or to the free DNP. After binding the coupled protein to the sensor surface, solutions containing Mabs and inhibitors were injected in the flow cell after 20 min of incubation at room temperature. The absorbance of the sample is easily converted in percentage of inhibition by

$$I = 100\left(1 - \frac{A_i - A_0}{A_{max} - A_0}\right) \qquad (1)$$

where A_i is the absorbance of the sample, A_0 is the absorbance measured after the binding of the protein and the subsequent rinsing with PBS and A_{max} the absorbance measured in the absence of inhibitor. In each case, the absorbance refers to the amide II band.

We considered two types of inhibitors: free DNP and DNP-HSA molecules. Using this experimental scheme, three monoclonal antibodies against DNP were tested: LO-DNP61, LO-DNP34 and LO-DNP01. The results presented in **figure 8** clearly show that these antibodies respond in a different manner to the free or to the coupled molecule. The sensitivity is about 10 to 100 times higher for the coupled molecule than for the free antigen (**figure 8 A**). More interesting is the fact that the response of the test also depends on the antibody for the free antigen, although the responses are equivalent for coupled DNP. In the case of free DNP, the LO-DNP34 has sensitivity about 100 times less than the other types of antibodies.

It should also be pointed out that the LO-DNP61 antibodies interact with the free DNP molecules (**figure 8, filled circles**) in a way similar to the one they interact with the hapten-carrier complexes, at least at low concentration of inhibitors.

Similar experiments were carried out using ELISA technique. Their results are presented the **figure 8 B**. The curves are steeper than for the FTIR sensors. All the tested antibodies respond in a similar manner to the coupled DNP molecules (open symbols) but significant differences are observed for the recognition of free DNP molecules (filled symbols). Sensitivity is about 100 times higher for LO-DNP61 but LO-DNP34 does not recognize the free DNP molecules.

For the DNP-HSA inhibitors, the limits of detection are equivalent between both techniques: in the range 5 – 15 ng/mL (FTIR assays) and about 40 ng/mL (ELISA). For the free DNP molecules, the limits of detection are different: higher than 1 µg/mL (ELISA for all the antibodies and FTIR for LO-DNP34) but detection limit of 4 ng/mL was estimated using FTIR assays and LO-DNP61 antibody, which is a level comparable to those estimated for the coupled molecules.
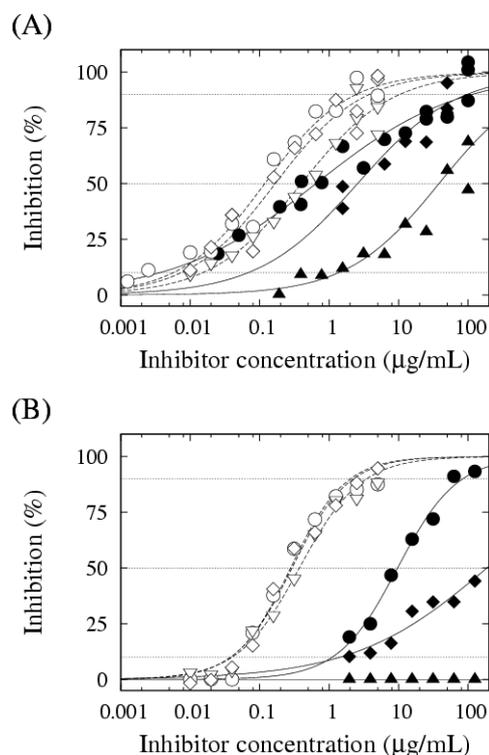
Figure 8: Inhibition curves for DNP-HSA (open symbols) and free DNP (filled symbols) using (A) FTIR immuno-sensors and (B) ELISA – Influence of the antibody (circles: LO-DNP61, triangles: LO-DNP34, diamonds: LO-DNP01).

2.3. Optimization of the sensors surfaces to allow direct detection by FTIR/ATR.

2.3.1. Indirect optimization: A new independent system of purge

FTIR instrumentation requires an environment free of water and CO_2 to protect the optical and electronic components **(Figure 9)** and to assure high signal to noise ratios.
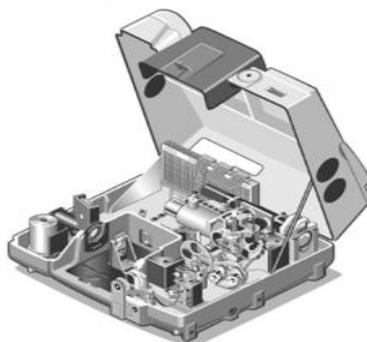
Figure 9: Optical and electronic components inside the spectrometer.

The purge gas must be free of moisture, oil, carbon dioxide and other reactive or infrared-absorbing materials. The old purge system (compressed air initially present in the building) has generated a lot of contaminations and humidity problems. In addition, we have also supported the repair of optical components because we observed a phenomenon of crystallization on the windows used to seal the optics. It seems that these KBr windows and the FTIR source are affected by the poor air quality on old purge system. Hopefully, the other optics elements (mirrors, MCTA and DTGS window, beamsplitters) were still in good condition.
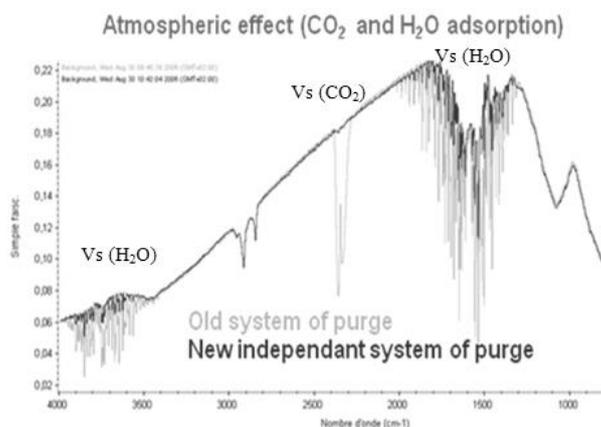
Figure 10: Comparison between old and new systems of purge.

So to avoid this recurring contamination we decided to buy a new system of purge before replacing all windows and the infrared source. The new independent system purge gas source is specifically designed for use with FTIR spectrometers to provide a purified purge gas from compressed air.

This equipment allowed us to obtain cleaner background spectra **(Figure 10)** in a shorter period of time and more accurate analysis by improving the signal-to-noise ratio. This complete system (**Figure 11)** consists of an air compressor, CO_2 and water removal filters, a flow controller and a pressure regulator.

Figure 11: The new system of purge.

2.3.2. Indirect optimization: Miniaturization and robotization development (essential equipments to study environmental samples)

To increase the number of analyses, to reduce the cost of functionalization (**Figure 12 and 13**) and to work with small volumes (**Figure 14**), we have developed a new automatic tool (**Figure 15**) that provides refined measures.

The main features of the multilane sensors (new design) are:

- Smaller flow: 5 to 50 µl/min.
- Smaller volume cell: 0.2 to 20µl.
- Number of lanes: 15.

Single bounce Horizontal Attenuated Total Reflection (optimized IR optics).
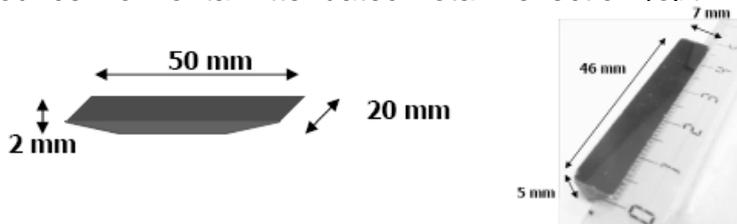
Figure 12: Comparison of dimensions between old IRE and new crystal named toblerone.

Figure 13: Single bounce ATR onto new IRE i.e. toblerone crystal
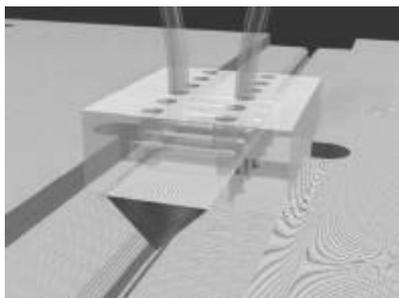
Figure 14: New design
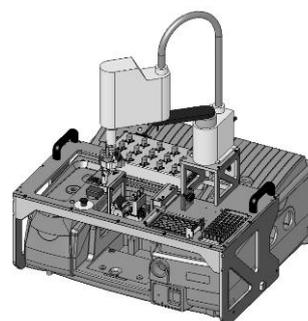
Figure 15: Robotization

2.3.3. Direct optimization: control of the surface (wettability & FTIR measurements)

The quality of the grafted organic layer was assayed by static contact angle measurements with water (θ_w) and FTIR-ATR spectroscopy.

The contact angle is a measure of the ability of a liquid to spread on a surface. The method consists on measuring the angle between the outline tangent of a drop deposited on a solid and the surface of this solid. The contact angle is linked to the surface energy. The contact angle measurements give the affinity of a liquid to a solid surface: if water is used to measure the contact angle one can deduce the hydrophobic (great angle) or hydrophilic (small angle) character of the surface.

The θ_w measurements onto OTS surface equal 105 ± 5 degree and give 45 ± 5 degree onto PEG synthetized (**Figure 16**). The difference is due to surface chemistry and show a low surface energy when grafted successfully. It is a practical tool to control grafting of surfaces.

Figure 16a and **16b**

Figure 16: Grafting controls by wettability. Figure16a: OTS monolayer on germanium; Figure 16b: PEG monolayer synthetized on germanium

The C-H stretching region of the FTIR-ATR spectrum of Si-PEG 1a (commercial PEG) is shown in **Figure 18**. The peaks found at 2956 cm^{-1} (w, CH3 st as), 2923 cm^{-1} (s, CH2 st as) and 2853 cm^{-1} (m, CH3 st sy) are in agreement with chemical structure.

Sample Si-PEG 2b (synthetized PEG) showed similar features in the 2800-3000 cm^{-1} region but this time the carbamate NH stretching was also visible (broad peak at 3330 cm^{-1}). All the vibrational peaks are listed in **Table II.**

The stretching region of OTS aliphatic chains is also located around 3000 cm^{-1} (**Figure 17**).
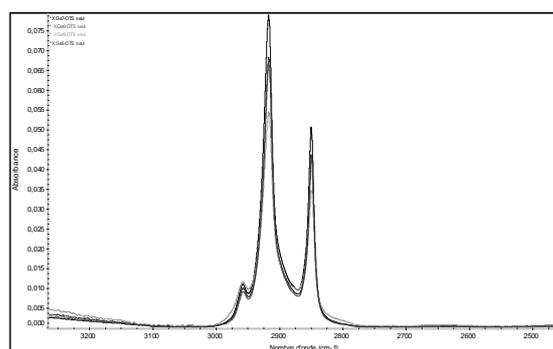
Figure 17: OTS monolayer infrared spectra
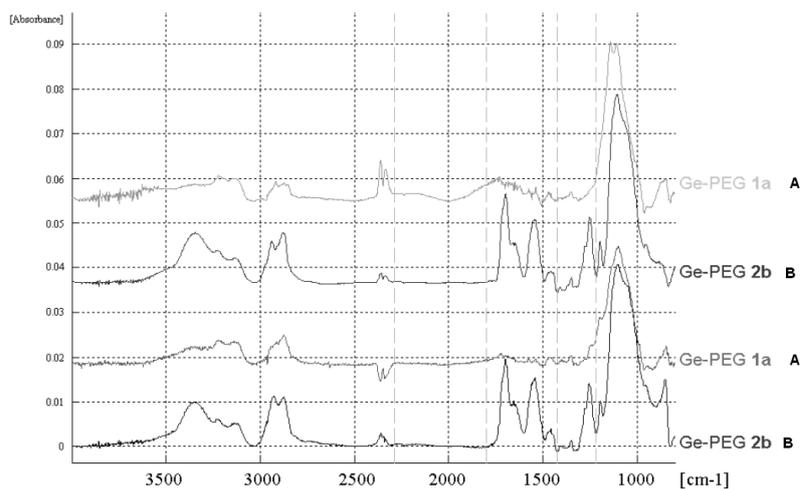
A : Commercial PEG infrared spectra
B : PEG synthetized infrared spectra

Figure 18: Infrared spectra of PEG graftings

Frequency	Intensity [a]	Assignment [b]
3351	m	N-H st (carbamate)
3233	w	oxidized crystal background
3132	w	oxidized crystal background
2930	m	O-CH2, CH2 st as
2879	m	O-CH2, CH2 st sy
1699	s	C=O st (carbamate)
1657	m	C=O st (carbamate)
1565	m	N-H δ (carbamate)
1548	m	N-H δ (carbamate)
1463	w	O-CH2, CH2 bending
1404	v w	CH3 δ sy
1354	w	O-CH2, CH2 wagging
1278	m	(O)C-O st as (carbamate)
1261	m	C-N st
1202	m	CH3 rocking mode
1101	v s	C-O-C st as
1067	v s	Si-O-C st
958	m	C-O-C st sy
856	m	Si-C st

[a]   v s (very strong), s (strong), m (medium), w (weak), v w (very weak)
[b]   st (stretching), sy (symmetric), as (asymmetric), δ (deformation)

Table II: Frequencies (cm^{-1}) and assignments of dominant vibrational modes obtained by FTIR-ATR spectroscopy of Si PEG 2b crystal (synthetized PEG).

2.3.4. Direct optimization: antifouling coating to detect analyte of interest in a complex media

Polyethylene glycols (PEGs) are widely used to reduce non specific adsorption of biomolecules (proteins) on surfaces. When chemical grafting is concerned instead of coating, oligomers of ethylene oxide (chains containing 3 to 9 EO units) are also efficient. Very few studies are devoted to the stability of PEG-derivatized silicon (and none about germanium), under conditions mimicking physiological media used for biosensor detection.

Nevertheless, it appears that such devices are not highly stable in phosphate buffered saline (PBS) and that the loss of PEGs most probably results from basic hydrolysis of the Si-O bonds within the interface oxide layer. (**figure 19 A**)

The problem of long-term stability of self-assembled monolayers (SAMs) in biological fluids could be addressed by using amphiphilic silane derivatives for reaction on oxidized surfaces. Since the hydrolysis of PEGylated silicon is inherent to the PEG hydrophilicity, incorporation of a hydrophobic segment next to the reactive silane function would prevent the access of water molecules to the device surface. This substrate showed a high waterproof durability and a good ability to suppress protein adsorption (**figure 19 B)**

Hydrolysis of commercial PEGs   Stability of self-organizing PEGs
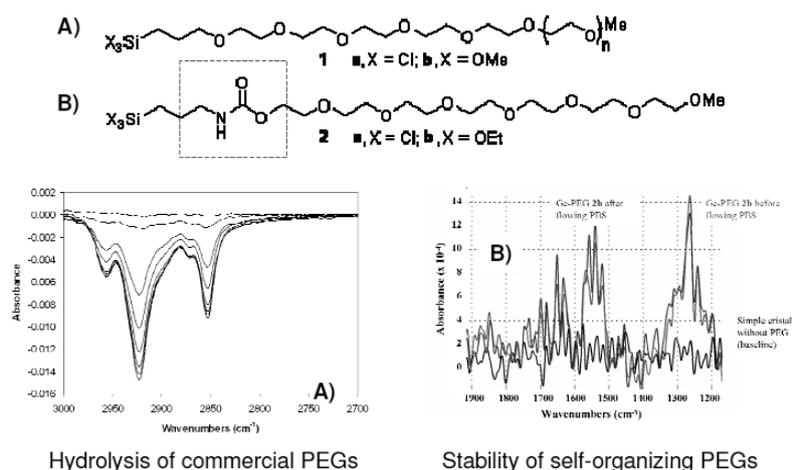
Figure 19: Comparison of a commercial (A) or synthesized (B) PEG.

In our context of FTIR-based sensor, the organic layer covering the ATR element has to be as thin as possible for optimal spectroscopic measurements. Hence, we considered the possibility of using a novel amphiphilic silanization reagent composed of a very short alkyl chain (3 methylene groups) and a short PEG chain (6 Ethylene Oxide units are considered as the minimum length to induce the protein repulsive effect), connected via a carbamate link. This key function, although relatively hydrophobic, is able to establish hydrogen bonds between vicinal chains and, hopefully, prevent water penetration into the resulting network as shown in **Figure 20.**
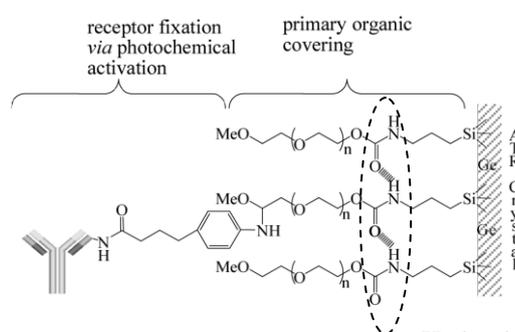
Figure 20: Antifouling coating.

This new antifouling coating has been provided by our colleague Professor J. Marchand from UCL.

2.4. Validation of optimization using a model for AFLATOXIN

We compared two methods of detection (FTIR-ATR spectroscopy and Fluorescence microscopy) using chemical construction of our biosensors.

2.4.1 Chemical similarity
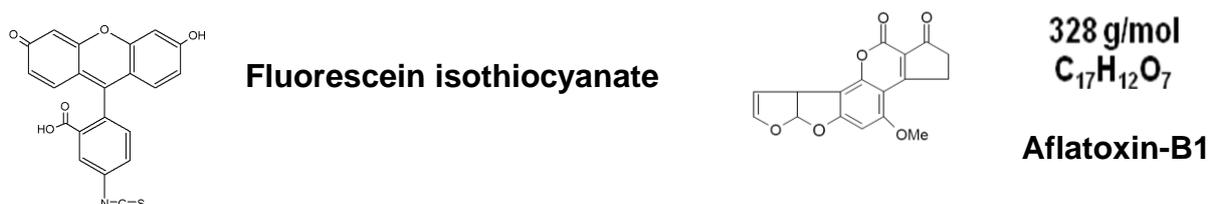
Figure 21: Chemical similarity between fluorescein and Aflatoxin.

Fluorescein is a fluorophore commonly used in microscopy which has a high chemical similarity with Aflatoxin (**Figure 21**).

The fluorescence of this molecule is very high, and excitation occurs at 494 nm and emission at 521 nm.

FITC is the original fluorescein molecule functionalized with an isothiocyanate reactive group (-N=C=S), replacing a hydrogen atom on the bottom ring of the structure.

Fluorescein isothiocyanate (FITC) is widely used to attach a fluorescent label to proteins via the amine group. The isothiocyanate group reacts with amino terminal and primary amines in proteins. It has been used for the labeling of proteins including antibodies and lectins.

FITC is a fluorochrome dye that absorbs ultraviolet or blue light causing molecules to become excited and emit a visible yellow-green light (see picture on **table IIIa**).

This emission ceases upon removal of the light causing the excitation. Fluorochrome labeling provides rapid, accurate localization of antigen-antibody interaction when one of the reactants is part of a cell, tissue or other biological structure. FITC is a commonly used marker for antibodies in immunofluorescent techniques since the conjugation of FITC to proteins is relatively easy and does not, in general, destroy the biological activity of the labeled protein. FITC is widely used as a hapten to label different proteins.

This molecule was considered as a model from Aflatoxin detection, but has also been used as a test molecule to validate the optimization of direct detection. So, we conducted the detection of fluorescein in two different methods and contexts.

2.4.2 Material

Rat anti-FITC monoclonal antibodies and all ligands coupled with FITC and in its free form were purchased from IMEX (Belgium).
The isotype of the LO-FLUO-1, anti-FITC monoclonal antibodies is IgM (rat).
MARK1 FITC (FITC conjugated anti-rat) is a secondary antibody for the specific recognition of constant parts of the receptor.
IR FITC is an immunoglobulin of rat without specificity, a FITC coupled protein.
Phosphate buffer saline solution (PBS) solution was purchased from Sigma-Aldrich.

2.4.3 Procedure

We have worked with a direct or indirect construction using SADP-functionalized silicon wafers surfaces.
Unlike direct system, indirect construction requires additional steps because Biotinylated antibodies need the use of NeutrAvidin. So, first step is NeutrAvidine (1mg/ml in PBS) incubation and after a step of rinsing with PBS. Then, we can bind a biotinylated antibody (LO-FLUO-1-Biotin) at 0.2mg/ml on this avidinylated surface.
For direct construction, a LO-FLUO-1 solution (0.2 mg/ml) in PBS was directly incubated with our sensors surfaces. After 30 min of incubation, to remove the unreacted excess of antibodies, we thoroughly rinsed with a spray containing buffer solution. After the binding of the monoclonal antibody to the sensor surface, a solution of FITC (1 mg/mL in PBS) in its free form or coupled with either protein or secondary antibody was incubated.

2.4.4 Results
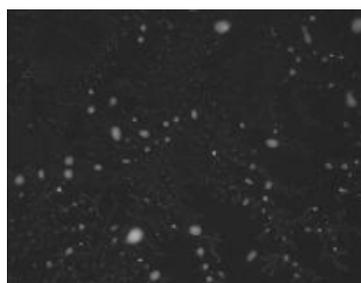
Table IIIa: Image of fluorescence response

Receptors	Ligands	Before incubations	After incubations
LO-FLUO-1	IR863 FITC	16591	21729
	IR863 FITC	16332	27649
	MARK-1 FITC	16348	17184
	MARK-1 FITC	16279	17146
	FITC	15827	18423
	FITC	15777	17165
Average grayscale		**16192**	**19883**
Avidin then LO-FLUO-1-Biotin	IR863 FITC	15973	18525
	IR863 FITC	15978	21620
	MARK-1 FITC	15834	17417
	MARK-1 FITC	15821	29523
	FITC	16050	22682
	FITC	16004	16760
Average grayscale		**15943**	**21088**

Table IIIb: Results of fluorescence response.

On **table III** an increase in gray level can be observed after incubation of our sensors with fluorescent probes whatever construction (direct or indirect). Commercial monoclonal anti-FITC antibody was demonstrated to be specific for both the free and protein-conjugated form of fluorescein. Compared with our FTIR sensors, microscopic fluorescence is less sensitive because we only obtained a fluorescent response from concentration of 1 mg/ml FITC and up.

We have also detected fluorescent probes as ligand with our sensors i.e. functionalized infrared crystal. On the **Figure 22** you can see references spectra by FTIR
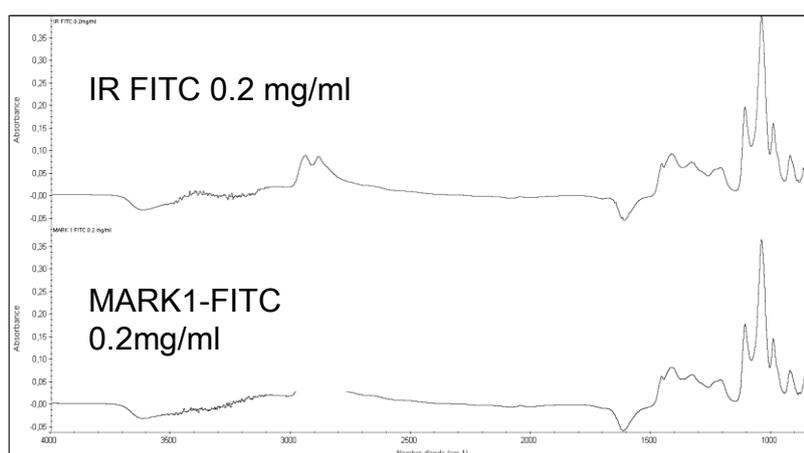
Figure 22: FTIR spectral references.

The detection of FITC is possible with FTIR biosensors. As the fluorescent dye is coupled with secondary antibody or immunoglobulin it is easier to see amides bands as show on **Figure 23**.
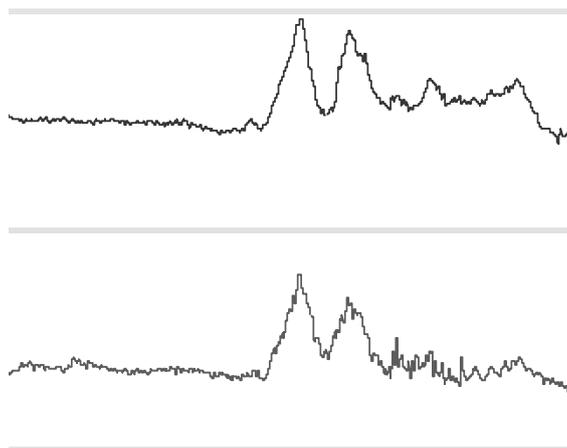
Figure 23: Detection of ligands coupled to FITC by FTIR biosensors. Using LO-FLUO-1 (Anti Fluorescein monoclonal antibody) in direct system (Direct detection of IR-FITC (Immunoglobulin) at 0.2 mg/ml).

This FITC detection by FTIR spectroscopy and Fluorescence microscopy allowed us to validate direct and indirect detection when we used antibodies as receptors in our molecular construction.

2.5. Spectral references

2.5.1 FTIR accessories

To know the location of significant peaks of free aflatoxin-B1 and concentrated verrucarin-A, it is possible to take spectral references in solution thanks to two different infrared accessories available in the LPSI laboratory (Umons), which are described below:

A) Smart Multi-Bounce HATR accessory (For multiple-reflection ATR analysis).

The Smart Multi-Bounce HATR crystal has a pathlength of 10 micrometers, while the smallest pathlength of a typical transmission cell is 15 micrometers. This short pathlength makes the Smart Multi-Bounce HATR accessory suitable for samples that absorb strongly and yields better results than transmission. In addition, this accessory is well suited for providing information about the chemical compound in solution.

Figure 24: Smart Multi-Bounce HATR accessory.

The trough plate kit is useful for analyzing liquids. The ATR crystal is recessed and mounted into a trough-shaped, leak-proof sampling plate (**Figure 24**). The ATR crystal sample plate eliminates the risk of liquid spills damaging the accessory in any way. Also included is a volatile liquid cover that prevents solvent evaporation to improve the infrared measure and reduce the noise of signal.

The standard crystal material is zinc selenide (ZnSe), with a 45 degree angle of incidence. This material is well suited for almost all routine sampling. ZnSe is fairly hard, and is utilized for neutral pH solutions.

Specifications are as follows:
Crystal Material: Zinc Selenide, standard; (4000 – 650 cm-1)
Number of Reflections: 10
Crystal Angle: 45°
Pathlength: Approximately 10 micrometers
Sample Volume (trough): 0.5 millilitres

A second infrared accessory is:
   B) Smart Golden Gate accessory (For single reflection ATR analysis)

The Smart Golden Gate is designed to handle a wide range of sample types, including samples that are normally difficult to analyze by ATR such as corrosive liquids. The accessory features a diamond ATR crystal bonded at high temperature to a tungsten carbide support. The crystal is extremely durable and stable.

The Smart Golden Gate with standard ZnSe focusing optics has the following features:
Crystal material : Type II a diamond mounted on tungsten carbide
Refractive index : 2.4 at 1000 cm-1

Angle of incidence : 45° (one reflection)

Spectral range : 5000 ~ 650 cm-1

Deph of penetration : 2 micrometers at 1000 cm-1 (assumes RI of sample is 1.5 at 1000 cm-1)

Useful pH range : 1 to 14

The Smart Golden Gate offers unprecedented sensitivity, ruggedness and versatility for a single-reflection ATR accessory. Samples are placed directly on the diamond ATR crystal for analysis. A volatile liquid cover is also used for preventing evaporation of the solution samples during the analysis.

The cover shown on **Figure 25** can be placed over a volatile liquid sample to minimize evaporation during the analysis.

Figure 25: Volatile liquid cover   **Figure 26:** Smart Golden Gate optical design
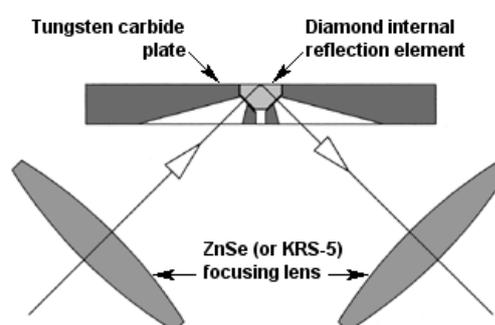
The Smart Golden Gate optical design on **Figure 26** combines a ZnSe focusing lens with a type IIa diamond head that is mounted on a tungsten carbide support. The sample material contacts only the diamond portion of the optical unit. This configuration provides a (diamond) sampling surface that is extremely chemically resistant. The focusing lens reflects the infrared beam at the proper angle for ATR analysis.

2.5.2 Procedure to obtain spectral references:

A background spectrum is needed to process the sample data to an infrared spectrum. The background is a reference spectrum which accounts for the unique optics of the Smart Golden Gate accessory and the spectrometer. Each sample spectrum is ratioed against a background so that the final spectrum is free of these features.
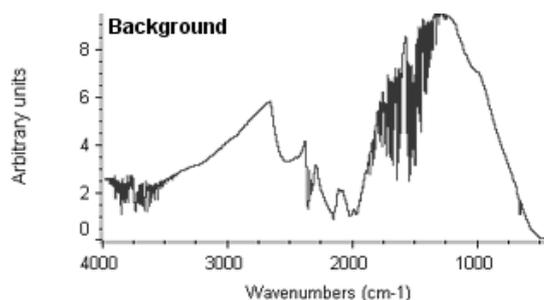
Figure 27: Background without PBS

Figure 27 shows a background spectrum collected with the Smart Golden Gate. Note the diamond absorption at about 2000 cm-1.

Buffer i.e. PBS is placed on the crystal when measuring the background. The background spectrum remains in memory and is selected as the current background. It will be used to process all the collected sample spectra, until its replacement by another one. When background collection with PBS is completed, then the sample can be inserted.

To analyze a liquid sample, a pipette or syringe is used to place a drop or two of the liquid directly onto the ATR crystal (see **Figure 28**). For best results, the crystal has to be covered completely (this is required for quantitative analysis).
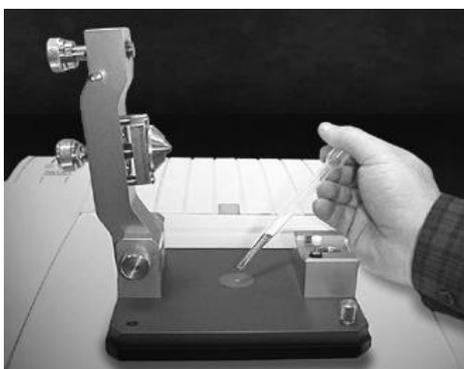
Figure 28: Liquid applied directly onto crystal to obtain the spectrum.

Once the sample is positioned on the sampling area, collection of the sample data can start.

When the system has finished collecting the specified number of scans (32 scans in the experiment), the final spectrum is displayed and shows only the change in IR energy (the background energy has been removed).

The final format of all samples spectra is in absorbance.

Between each sample spectra, the sample is removed and the crystal cleaned with water and ethanol. When the crystal is cleaned, the baseline is very flat and the system is ready to continue measuring samples.

2.5.3 Aflatoxin-B1 FTIR fingerprint:
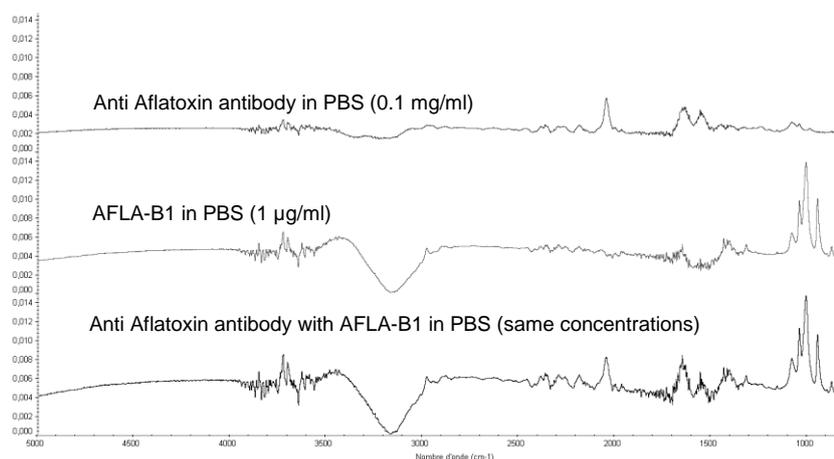
Figure 29: AFLA-B1 and Anti-AFLA-B1 mAb FTIR measurements.

The **Figure 29** shows that there are no chemical differences when Anti-Aflatoxin antibody is coupled to Aflatoxin.

We can see the same significant peaks when receptor and ligand are free or incubated together.
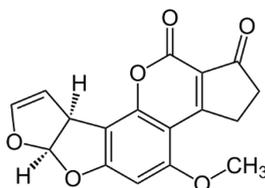
Figure 30: AFLA-B1 chemical structure

The spectrum of AFLA-B1 is a real fingerprint of the chemical structure and we find good consistency between the chemistry composition of the AFLA-B1 (**Figure 30)** and the adsorption regions of infrared measures (**Figure 30**).

The infrared spectrum of AFLA-B1 detailed on **Figure 31** possesses two low intensity bands at 1735 cm^{-1} and 1654 cm^{-1} respectively due to coumarin and ketone carbonyl functions.

These absorption bands in the aflatoxin B1 spectrum are attributable to the unique structural relationship of the coumarin and ketone carbonyl groups in the molecule.

There is also a low intensity band at 1560 cm^{-1} due to stretching vibration bands of (-C=CH-). A broad absorption band around 3400 cm^{-1} for AFLA-B1 indicated the presence of hydroxyl functions.

The vibrations involving the stretching of the C-O bonds give several infrared strong bands around 1000 cm^{-1} . These infrared bands indicate the presence of different compounds including a carboxylate, a cyclopentanone and an aromatic structure. We also find the stretching vibrations (O-CH3) between 3000 and 2890 cm^{-1}. We can see several others bands at 1092 cm- 1 (C-O-C), 2850 cm- 1 (-O-CH3), and others 1439, 1420, and 1321 cm^{-1}.
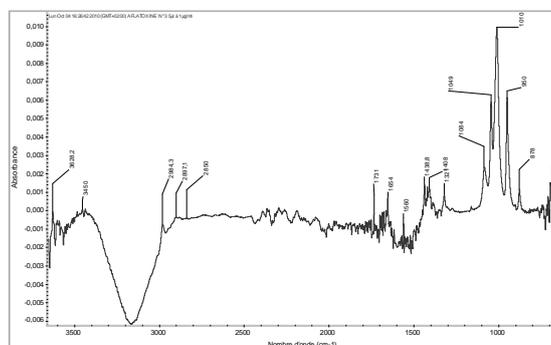
Figure 31: Location of AFLA-B1 peaks

2.5.4 Verrucarin-A FTIR fingerprint

We did the same to accurately determine the significant peak position of Verrucarin-A whose chemical structure is shown on **figure 32**.
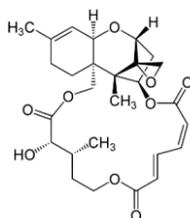
Figure 32: Verrucarin A chemical structure

It is not possible to see Verrucarin-A in solution (PBS/methanol) even for concentrations of about 1 µg/ml but if we evaporate the solvent and thus concentrate the Verrucarin-A onto crystal, in this way significant peaks appeared as shown in **figure 33**.

In fact, the use of infrared spectroscopy for direct detection of chemical and biological targets in water at a low parts per million level is not possible because the opacity of water in the infrared region limits the beam path length to about 25-50 µm.

Attenuated total reflection (ATR) is a common technique used in infrared spectroscopy for aqueous-based studies because the finite penetration of the evanescent wave defines the amount of water probed by the IR beam which, in turn,

circumvents the need for narrow path length cells. However, the use of ATR is limited to detecting and analyzing aqueous samples that are above certain threshold concentrations, e.g., at least millimolar.
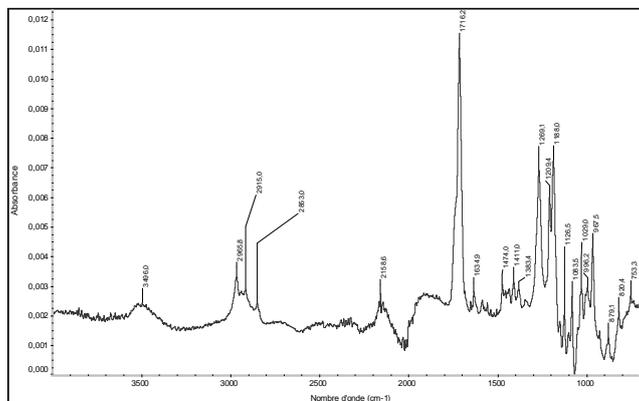
Figure 33: Peaks Location of VERRU-A dried onto infrared element

We found again a good correlation between the chemistry of the VERRU-A molecule (**figure 32**) and the infrared signature (**figure 33**).

Figure 33 shows that the infrared spectra of VERRU-A possesses one strong intensity band at 1716 cm-1 due to ester C=O bond and two low bands at 1635 and 1582 cm-1 corresponding to C=C functions. A broad absorption band around 3500 cm-1 for Verrucarin-A indicated the presence of OH groups. We also show three stretching vibrations of CH3 and CH2 between 3000 and 2850 cm-1.

The vibrations involving the stretching of the C-O bonds give several infrared strong bands below 1000 cm-1 like AFLA-B1 spectra. These infrared bands indicate the presence of different compounds (carboxylate, cyclopentanone and aromatic structures). We can see several others bands at 1083 cm- 1 (C-O-C), 2158 cm-1 (-C-CH3), 1269 (C-O), and 1209 cm-1 (C-O-H), 1188, 1126, 1083, 1029, 996, 967, 879, 820 cm- 1.

We demonstrated that it is possible to obtain references spectra of concentrated samples by adequate infrared technologies but to achieve low detection levels in ATR, the analyte of interest must be concentrated on the internal reflection element (IRE).

2.6. Detection of aflatoxin (B1 and G1) by FTIR-ATR.

Here, we applied the approach of functionalized IRE for the detection of aflatoxins. The prior functionalization of IRE by wet chemistry is required to allow anchoring of the antibody as shown in **figure 34**.
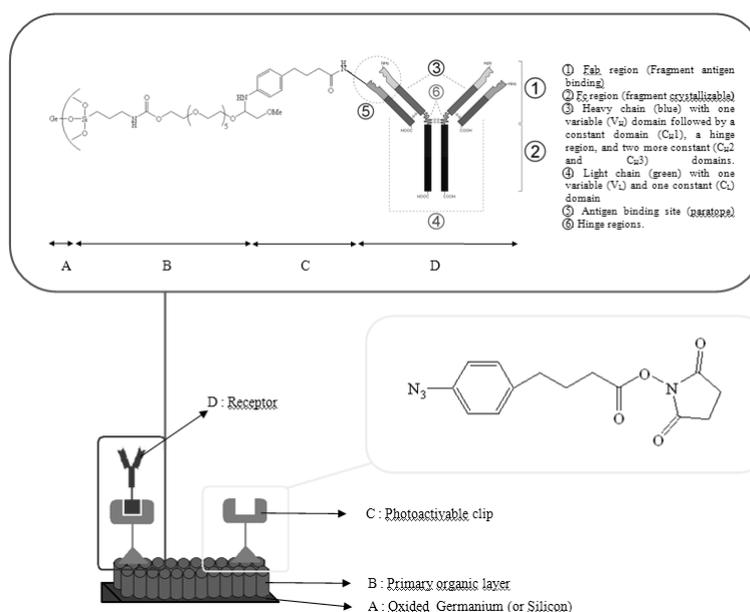
Figure 34: Generic biosensors

Some experiments were run to monitor the binding of an anti-aflatoxin B1-G1 antibody on a functionalized germanium crystal. The molecular layers are equivalent to what has been used for DNP detection (**figure 35**).

Binding of the MoAb was investigated over 4000 s and monitored by the intensity of the amide II band.
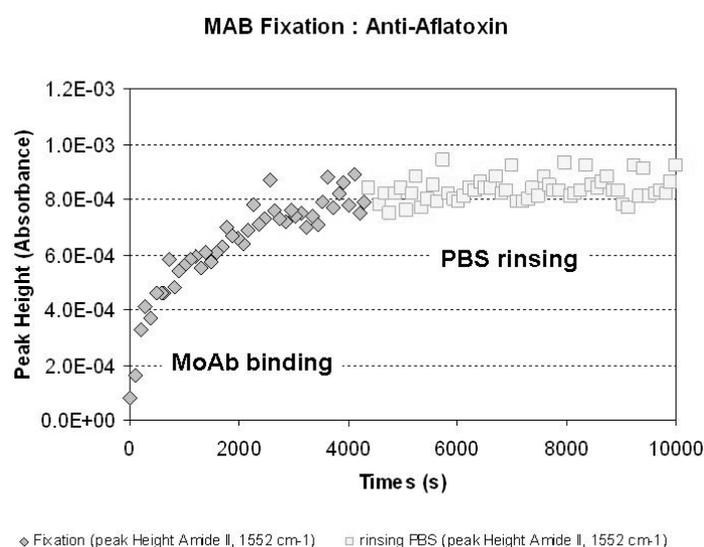
Figure 35: Binding of the anti-aflatoxin B1 antibody – Time evolution of the amide II bands (1552 cm^{-1}).

We can see on **figure 36** the difference between the steps of receptor binding and saturation. Because the strength of the absorption is proportional to the concentration, FTIR can be used for some quantitative analyses.

After rinsing, we can determine the amount ratio composition of our surface construction which is about respectively 3:1 if you measure the peak height of amide II band at 1552 cm^{-1}. Quantitative analysis is possible to determine the fraction composition of our chemical construction.
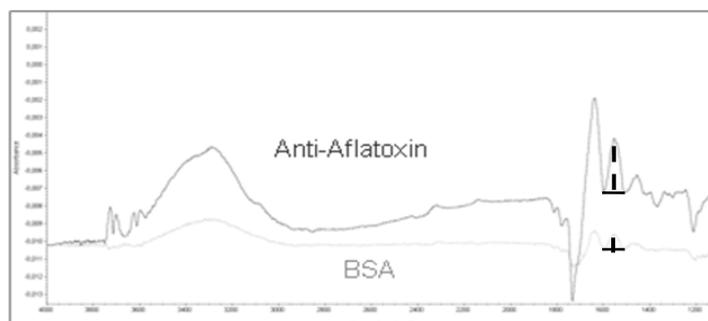
Figure 36: Quantitative comparaison (commun scale) of surface composition
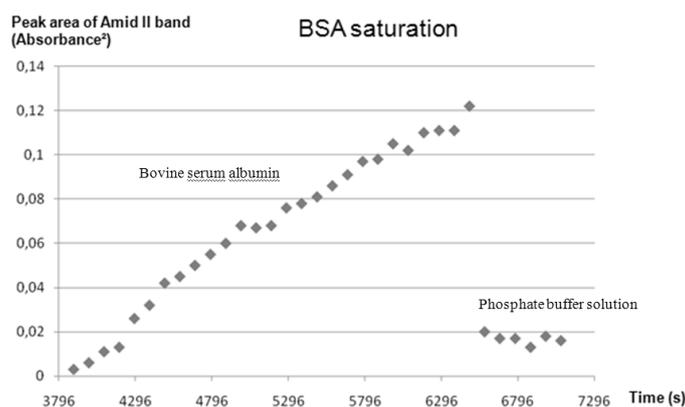
Figure 37: BSA saturation by specific adsorption onto unreacted sites

You can see on **figure 37** the saturation of binding sites with bovine serum albumin at 5 mg/ml. Here we injected 500µl of BSA with a flow rate of 12 µl/min. After rinsing with PBS (Phosphate Buffer Solution) almost all of the BSA is removed. There remains only the BSA which is specific bounded onto a bifunctionnal molecule.

In **figure 38** are also reported some results concerning the detection of Aflatoxin B1. For the toxin coupled to BSA, the limit of detection is about 2.7 ng/mL by analyzing the evolution of the amide bands of proteins.

Figure 38: Detection of Aflatoxin-BSA
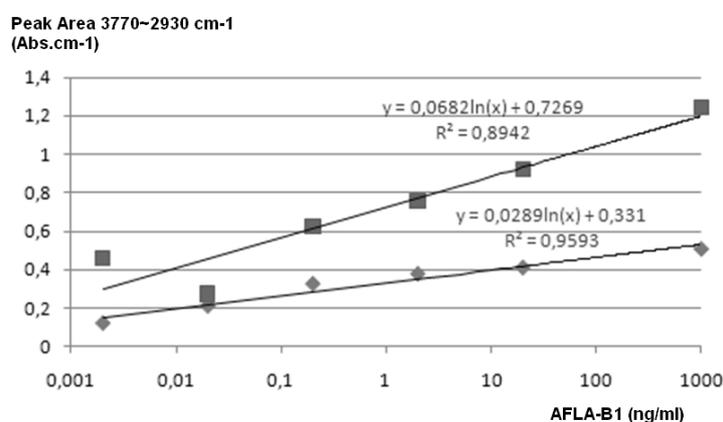
Figure 39: Detection of Aflatoxin under free form.

For the free toxin, the limit of detection is about 10 pg/ml (as shown in **figure 39**) by analyzing the evolution of the hydroxyl bands of AFLA-B1. We determined the limits of detection as being three times the spectral response with PBS. In this region the peak area with PBS equal 0.1 Absorbance.cm^{-1}, and so the corresponding limit of detection is equal at 0.3 Absorbance.cm^{-1}.

Let us here point out that within this field of research, we are subject to the quality of the available commercial receptors. For instance, with the anti-Alfatoxin mAb (SC-57610) from Tebu-Bio Company, we have performed several experiments before realizing that the corresponding receptor was not active in our case (neither in FTIR nor in ELISA).

2.7 Regeneration of Infrared Elements

Infrared elements (IRE) are relatively expensive, and thus a cleaning procedure is required to reuse the coated IRE. Elution methods often used in immunoaffinity chromatography techniques can be applied to our sensors. Elution conditions are intended to break the ionic, hydrophobic and hydrogen bonds that hold the antigen and antibody together. Successful eluting conditions will be dependent upon the specific antigen-antibody interaction that is occurring. Ideally, an elution condition effectively releases the antibody or antigen without causing permanent damage but all eluting conditions result in some loss of functionality.

There are lots of elution buffers on the market but as this part was not included in the initial planning we could only test a mixture solution of Glycine and HCl (Hydrochlorid acid) at low pH and at .0.1M to validate elution.
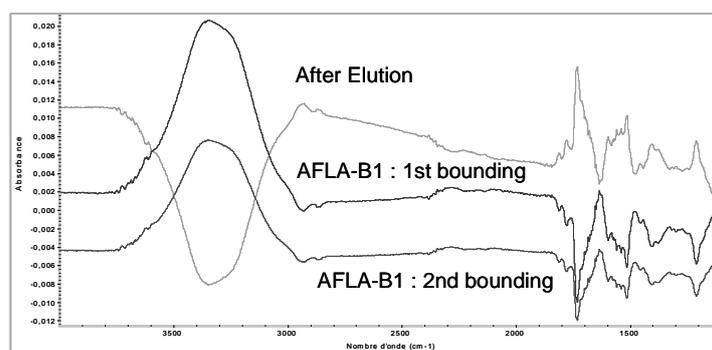
Figure 40: Elution to remove AFLA-B1

Red spectra is Aflatoxin spectra after rinsing, orange spectra is the elution spectra after rinsing, pink spectra is the second bounding of Aflatoxin after PBS.

Elution with Glycine/HCl mixture is efficient to remove antigen as seen with FTIR spectra.
By comparing AFLA-B1 spectra with elution spectra (as shown in **figure 40**), the positive peaks of the first ones are becoming negative and this is showing the possibility to elute antigen. But if you try to bind a second time AFLA-B1 (pink spectra) in the same conditions, there is less bounding (lower peak height) unlike the first bounding of AFLA-B1. The anti-aflatoxin antibody is still able to bound aflatoxin but less effective, indicating a partial damage of the antibody.
So optimization of elution conditions is very complex and requires further study. This may be part of future prospects for reducing the costs for routine analyses.

We have also developed a cleaning method for removing the functionalization on the infrared crystal. The IRE can be removed after experiments and manually cleaned once that all crystal tracks have been used.

For silicon crystal we used piranha solution for cleaning infrared element. Piranha solution is a mixture of sulphuric acid (H_2SO_4) and hydrogen peroxide (H_2O_2), used to clean organic residues off substrates. Because the mixture is a strong oxidizer, it will remove most organic matter, and it will also hydroxylate most surfaces (add OH groups), making them extremely hydrophilic (water compatible). Hydroxylation of surfaces is necessary for the OTS (OctadecylTrichloroSilane) or PEG (PolyEthyleneGlycol) grafting.

For germanium crystal, it is possible to remove contaminants thanks to mechanical polishing (in **figure 41**).
The quality of the finished surface is highly dependent on the equipment and consumables used in the process. To provide an optical polishing of high quality of infrared element we used a polishing machine with a specimen mover for semiautomatic preparation of materialographic specimens associated with high performance diamond products suspension.

Figure 41: Mechanical polishing machine

We can see on **figure 42** that it is possible to remove all graftings onto IRE (thanks to wet chemistry or mechanical remove) because aliphatic bands and NHS bands of bifunctionnal azoture disappear completely after recycling (positive peaks become negative)
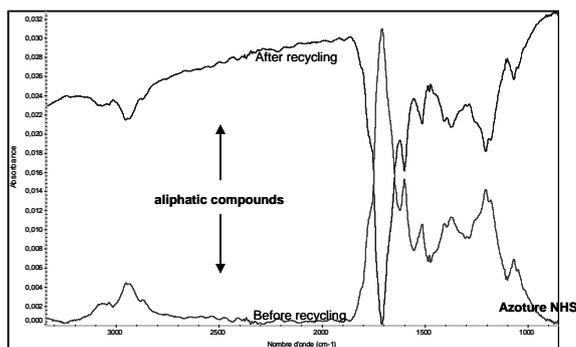
Figure 42 - Recycling effect onto germanium IRE

2.8. Biosensors controls

Figure 43 shows the rinsing with PBS after the binding of monoclonal antibody onto ligands coupled with Albumin.

$m = 19.9 \ 10^{-4}$
$\sigma = 3 \ 10^{-5}$
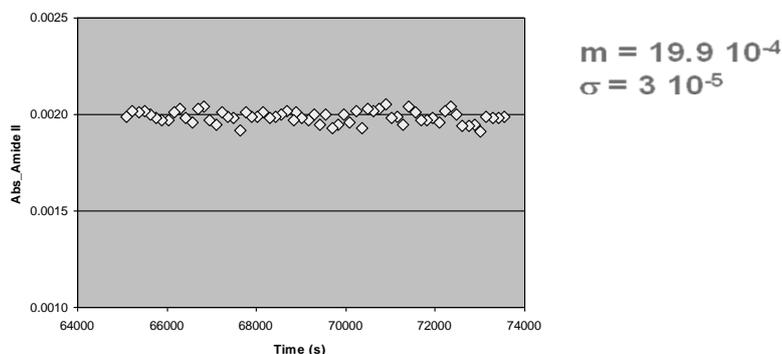
Figure 43: Level of noise.

A series of control experiments were carried out to check the saturation of the binding sites of the sensor. After the binding of the protein to the sensor and the rinsing step with PBS solution, a solution of glycine 0.33M (pH 7.2) was injected in the flow cell. The interaction of glycine with the possible unreacted NHS molecules was monitored at 1332 and 1411 cm -1 as shown in **figure 44**.

These absorption bands are characteristics of the glycine molecules and do not interfere with the amide bands of the protein. If the intensity of the absorption bands comes back to the level of the baseline after the glycine pulse, it can be concluded that the sensor surface is covered at more than 95% by the initially bound protein. This figure also shows the reproducibility of our experiments.
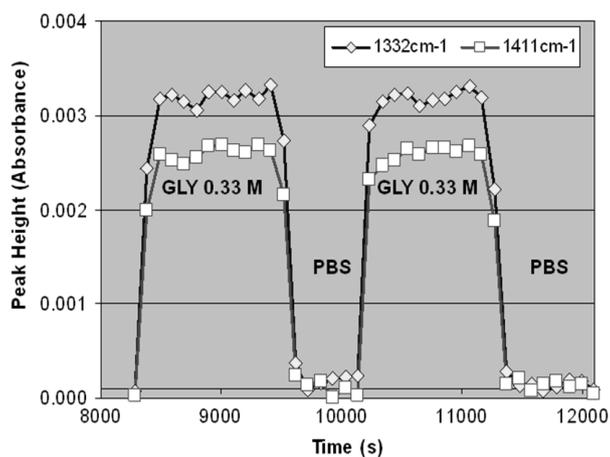
Figure 44 - Saturation of the sensor surface by bound proteins.
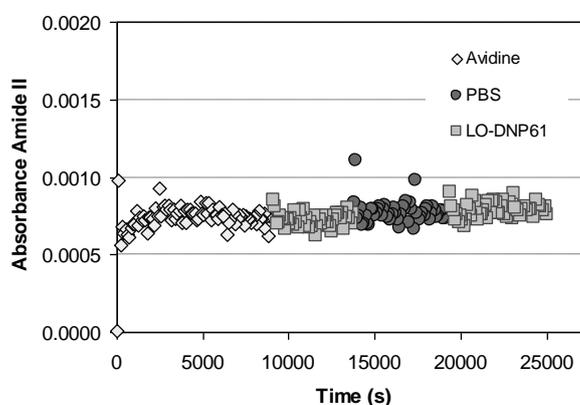
Figure 45 - Unspecific binding - No binding of monoclonal antibody (5 µg/ml) to the protein.

In another set of control experiments, the specificity of the molecular recognition of the Mabs was probed by initially binding avidine on the sensor surface. The absorbance of the amide II band of the avidine molecules rapidly rises and stabilizes after 5000 s. The subsequent pulses of Mabs and of protein-free PBS do not significantly modify its value, confirming the specificity of the antibodies and the stability of the protein layer (**figure 45**).

Without bifunctionnal molecule it is possible to detect DNP-Albumin as shown **in figure 46** but there is no protein binding at 2 mg/ml.
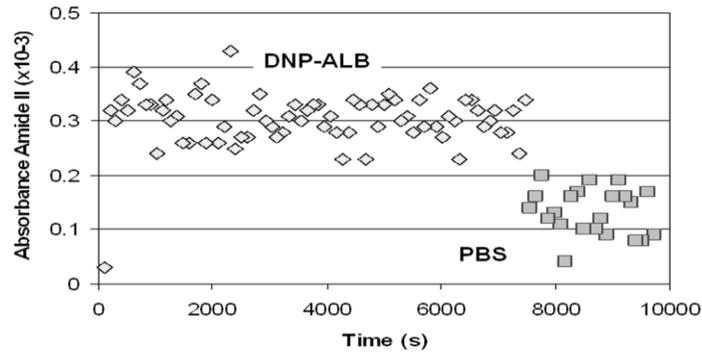
Figure 46 - Unspecific binding

2.9. Biosensors procedure

Firstly, a background acquisition is taken before functionalization. Then the sample spectrum is taken after functionalization, with the aim of controlling grafting (as we can see **in figure 47 and 48**). We can see in **figure 47** the spectral signature of aliphatic chains (CH_2 and CH_3 bands between 3000 and 2800 cm^{-1}) due to OTS grafting onto IRE.
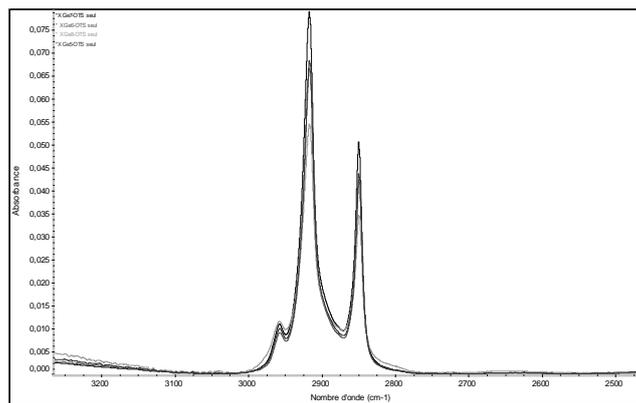
Figure 47 - OTS monolayer grafting on germanium
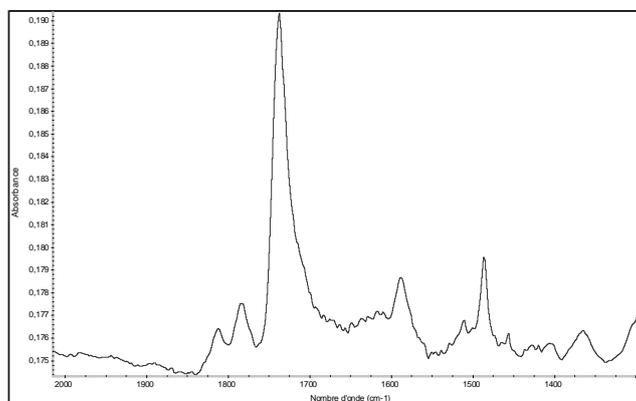
Figure 48: Commercial spacer molecule (N-Succinimidyl (4-azidophenyl) 1,3´-dithiopropionate)

The **figure 48** shows the infrared signature of our bifunctionnal azoture molecule photografted onto IRE including the C=O band at 1737 cm^{-1}.
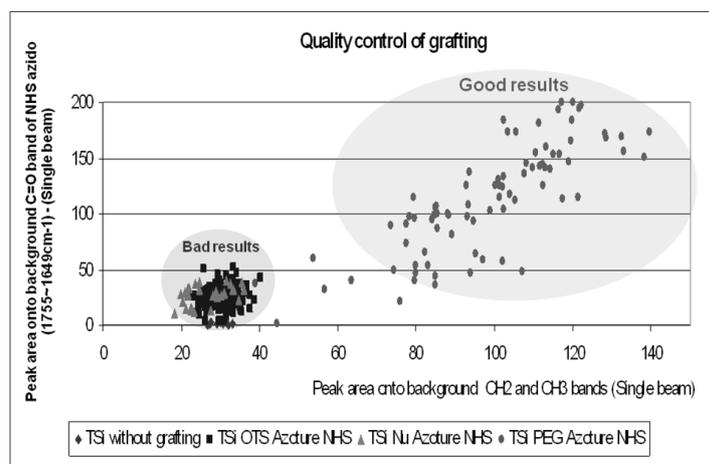
Figure 49: Predictive quality control

We also determined a threshold of acceptability for the quality of grafting (in **figure 49**). This allows us to predict the success in term of detection. Greater is the peak area of aliphatic chains (PEG grafting) and greater will be the peak area of NHS azoture. OTS grafting is less efficient than the PEG grafting in term of azoture quantity and giving poorer results in terms of analyte detection (**figure 49**)
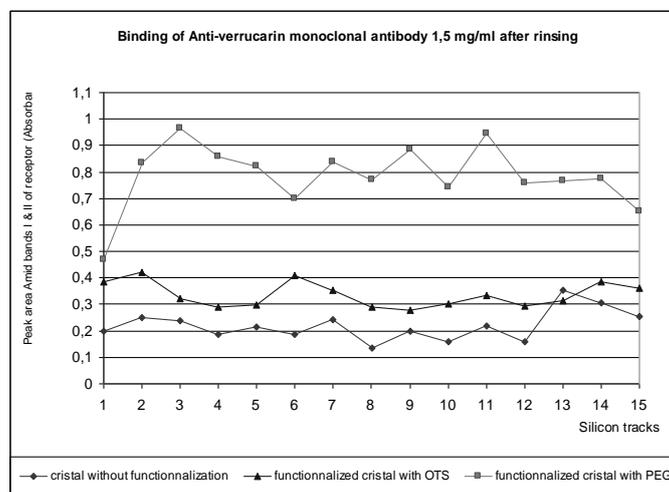
Figure 50: Binding of the Anti-verrucarin mAb with different functionalizations.

Moreover, PEG grafting give the best results in term of receptor anchoring as shown in **figure 50**. The amount of anti-Verrucarin F24 mAb binding is more than twice better with PEG grafting.

The SADP-functionalized surfaces were placed in an ATR flow cell (Specac, UK) connected to a Watson-Marlow 403U/VM2 peristaltic pump (Farmount, UK). Typical flow speed was 20 µL/min.

We acquire (after grafting controls) two backgrounds with or without flow circulation in order to visualize the liquid influence on the infrared signal (**figure 51**).
The second background with Phosphate Buffer Solution (PBS) is very important because it is a real reference for all the following samples. For this reason, it is important to avoid air bubbles or leak if you want to see the binding.
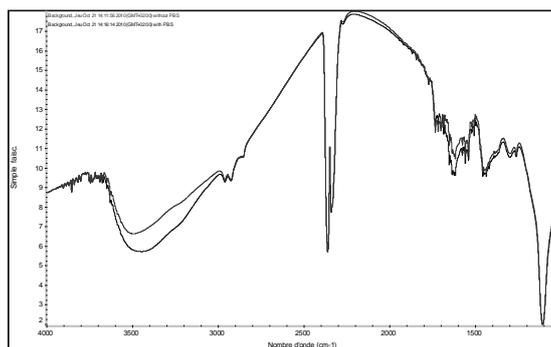
Figure 51: Background acquisition with or without PBS*.*

The red background is before flow circulation and the blue background is a background during flow circulation with PBS. **Figure 51** show that the major difference is the OH stretching vibration bands around 3500 cm-1.
Thus we can launch the macro basic program for taking one sample spectra per minute to visualize the stability in the flow cell.
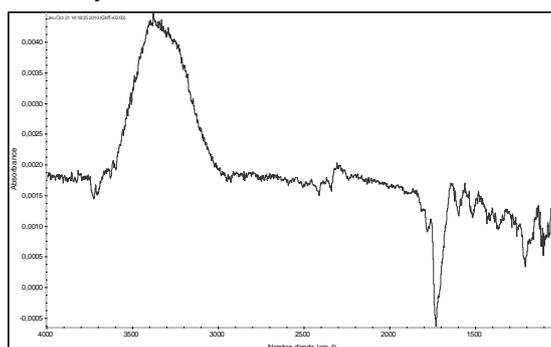
Figure 52: Instability of baseline with our functionalization sensors before saturation.

The **figure 52** shows the partial hydrolysis of the activated ester of the N - succinimidyl group of the bifunctionnal molecule due to the circulation of PBS.
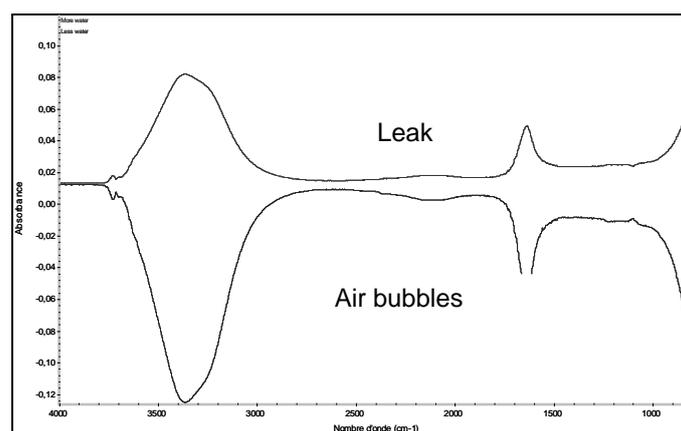
Figure 53: Air bubbles or leak spectra.

The background or the sample may contain more or less water due to air bubbles or leak.

On **figure 53**, the red sample shows more water and the blue sample less water. There are two infrared bands, one at 3365cm-1 and the other at 1635cm-1. So it is very important to work with impermeable cellule and to use degassed solution to avoid the leaks or air bubbles.
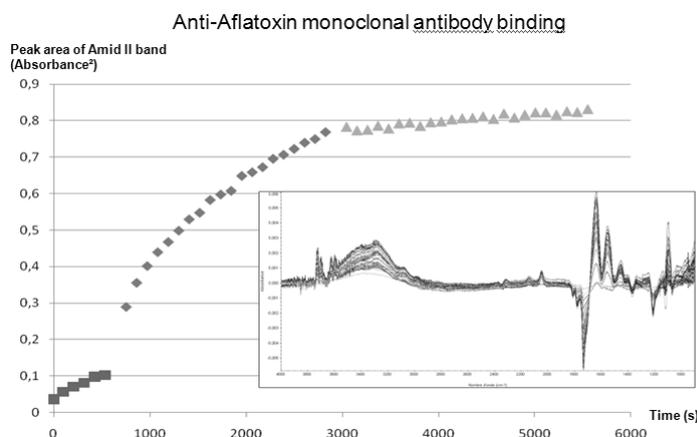
Figure 54: Monitoring the binding of anti-Aflatoxin mAb.

The binding of the mAb to the sensor surface can be quantified and monitored on-line from the FTIR intensity of some specific absorption bands as shown in **figure 54**. We injected 500 µL at a concentration of 0.1 mg/ml with a flow rate of 12 µl/min. When using flow cells, the direction of the flow is tangential to the surface and the time required to achieve maximum specific binding of the monoclonal antibody was about 30 min.

As the coupling between the mAb and the surface requires the hydrolysis of the activated ester of the N-succinimidyl group of the azoture molecule, 4 bands are characteristics of the appropriate anchoring of the mAb at the sensor surface:

the amide I and amide II absorption bands of the mAb and the stretching bands $v(C=O)$ and $v(C-O)$. Taking a baseline (background) of the spectrum recorded on the azoture functionalized crystal surface, the two former bands appear in positive mode as they correspond to the binding of the mAb, while the two latter appear in negative mode as they monitor the hydrolysis of the reactive function of azoture NHS molecules.

After receptor binding, a HSA solution (5 mg/mL in PBS) was injected in the flow cell at a flow rate of 25 µL/min (continuous), in order to saturate the still free sites of bifunctionnal molecules. We can monitor the saturation as function of time as shown in **figure 55**.

After 30 minutes, buffer solution was injected in the cell to remove the unreacted excess of protein.
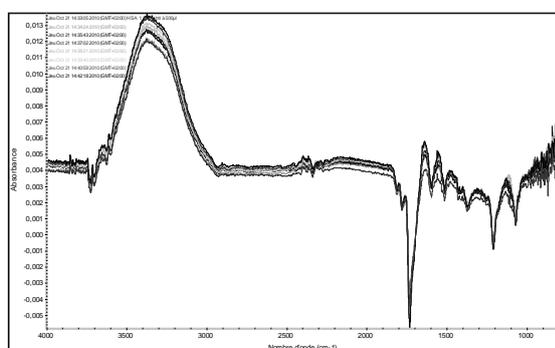
Figure 55: Saturation with protein.
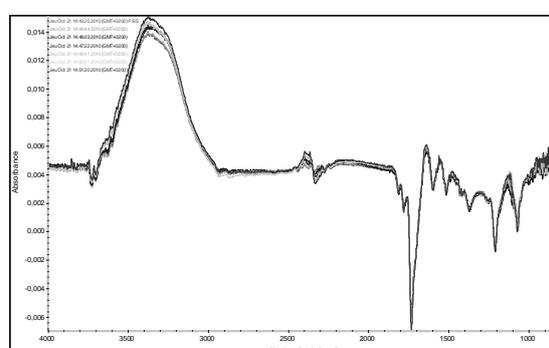
Figure 56: Rinsing after saturation.

The stability of the anchored protein layer is shown: the absorbance of the amide II band and the stretching bands $v(C=O)$ and $v(C-O)$ remains constant during rinsing of the flow cell with PBS solution as shown in **figure 56**.

Thus, taking a new background the baseline is more stable and partial hydrolysis is finished as shown in **figure 57**.
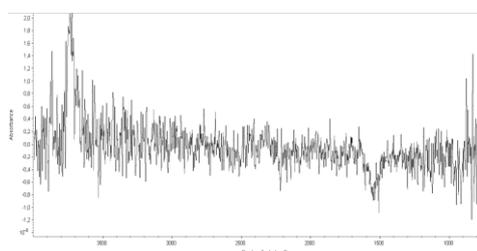
Figure 57: Stability of baseline after saturation step using HSA at 5 mg/ml.

After this step, the infrared sensor is stable and so ready to detect the specific ligand (antigen in solution). We can monitor the binding of toxins onto our sensor as function of time. After rinsing, we can see if the analyte of interest is well anchored.

2.10. Detection of aflatoxins (B1 and G1) by competitive ELISA.

We have set up a competitive ELISA able to quantify the concentration of aflatoxins in solutions. We used bovine serum albumin labelled with aflatoxin B1 (from Sigma-aldrich) as a coating antigen and clone AT-B1 (mouse monoclonal antibody specific for aflatoxin B1-G1, from Sigma-Aldrich) as detecting antibody. We optimalised the concentrations of the coating antigens, detecting antibody and the revelation process in order to improve the sensitivity of this assay. **Figure 58** shows the results from two independent detections of aflatoxin B1 using this optimized assay. We have run six duplicates of the same sample to measure the CV intra-assay. This assay was performed five times during five consecutive days in order to calculate the CV inter-assay. We obtained 15.0, 16.0, 14.8, 25.7 and 13.1 for the CV intra-assay leading to an inter-assay CV of 23.9. The best sensitivity obtained with this assay was between 470 and 235 pg/ml.
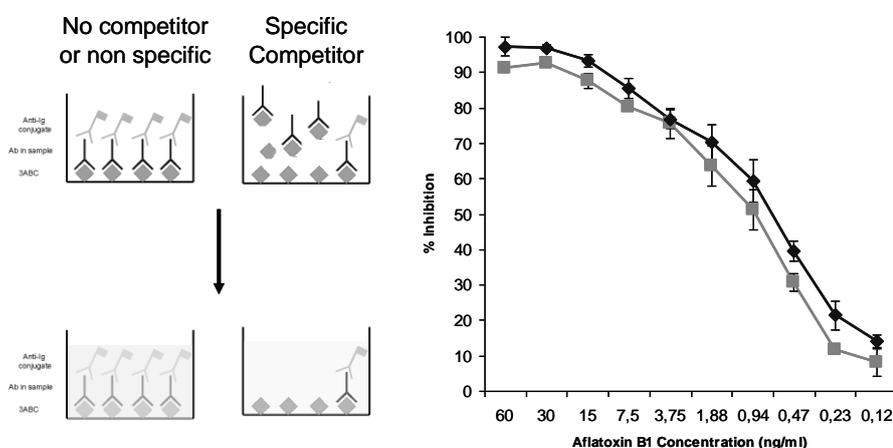
Figure 58: Detection of Aflatoxin B1 using a competiotive immuno-assay

Using this competitive ELISA we next tried to determine the concentrations of aflatoxin-B1 in environmental samples. We analysed 85 air samples carried out in contaminated houses. We found a very low concentration of Aflatoxin B1 (near the detection limit) in 7 samples but these results were not confirmed by the mass spectrometry analysis.
Therefore our ELISA seems not sensitive enough to detect the presence of airborne Aflatoxin B in the air of the analysed dwellings.

2.11. Monoclonal antibodies against mould antigens.

In order to obtain rat MoAb directed against components of the mould, LOU/c rats were immunized in the foodpats with 5.10^6 spores of Alternaria alternata (IHEM 18586) or Aspergillus fumigatus (IHEM 6117) or Stachybotrys chartratum (IHEM 22013). At the end of the immunization, lymphocytes were obtained from the poplietal lymph nodes. Lymphocytes were fused with the IR-983F cells. Growing hybridomas were selected in HAT medium. Positive clones were selected by fluorocytometry on various mould spores.

Five MoAb were selected from the rats immunized with Alternaria alternata and their characteristics are listed on 2. LO-ALT-1, -3 and -5 bind alternaria spores in cytometry and also recognize alternaria mould extract using an indirect ELISA. These MoAb are all IgM. LO-ALT-2 and -5 do not recognize mould extract by ELISA and are IgG2c and IgG1 respectively.

	Isotype	Spores cytom	Extrait Elisa
LO-ALT-1	IgM	Y	Y
LO-ALT-2	IgG2c	Y	N
LO-ALT-3	IgM	Y	Y
LO-ALT-4	IgG1	Y	N
LO-ALT--5	IgM	Y	Y

Table IV: Characteristics of the rat MoAb obtained after an immunization with alternaria spores.

The specificities of LO-ALT-1, -3 and -5 were further analysed using fluorocytometry (**figure 59**). LO-ALT-3 binds to alternaria spores IHEM 18586 but also to four other alternaria strains. However this antibody do not bind cladosporium, penicilium, aspergillus, stachybotrys nor candida and saccharomyces strains demonstrating that LO-ALT-3 is clearly species specific (while this antibody also recognize ulocladium botrytis IHEM 328, which are phylogenically very close to alternaria ssp). The two other MoAb (LO-ALT-1 and -5) do recognize all mould strains tested until now but not yeast strains tested (Candida albicans IHEM 3731 and Saccharomyces cerevisiae IHEM 6272) indicating that this two antibodies recognize an antigenic determinant common to the moulds.
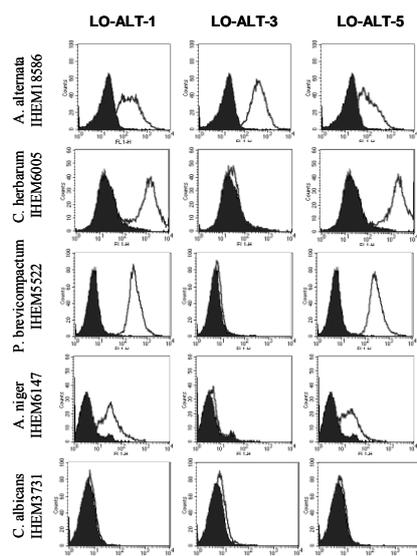
Figure 59: Fluorocytometric analyse of the specificities of LO-ALT-1, -3 and -5. Mould spores were incubated with the indicated antibodies. After washing bound antibodies were detected using an FITC labelled mouse MoAb directed against the rat kappa light chains. The fluorescence was analysed on a FACscalibur cytometer.

We then analysed the ability of the LO-ALT-1 (A1) and LO-MO-5 (F10) to detect mould componants in solution using a sandwich ELISA. Soluble extract from various mould species were prepared by overnight agitation of known numbers of mould spores in PBS. Insoluble material was removed by centrifugation. Supernatants containing the soluble antigens were tested using the various combinations of these two antibodies as capture antibody or secondary biotinylated antibody. As shown in **figure 60**, the four antibody combinations tested similarly detected antigens presents in the extract of Cladosporium herbarum (IHEM 6005) but the best results were obtained with LO-MO-5 both as a capture and as a detecting antibody.
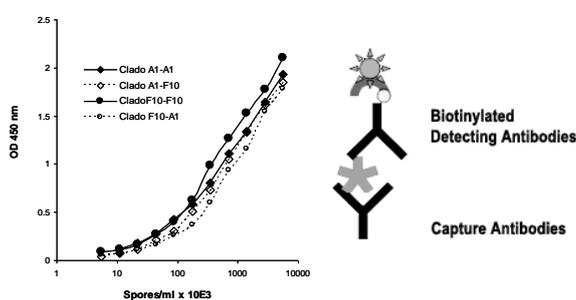
Figure 60: Detection of Cladosporium herbarum extracts using a sandwich ELISA with the LO-ALT-1 (A1) and LO-MO-5 (F10) as capture and detection antibodies. The detection antibody was labelled with biotin. Plates were revealed using peroxydase labelled avidin and OPD as substrate.

A sandwich ELISA using the LO-MO-5 both as a capture and as a detection antibody was used to detect the presence of the recognized antigen into various mould extract preparations. As shown in **figure 61**, this assay was able to efficiently detect a mould antigen in the extracts from Alternaria alternata (IHEM 21999), Cladosporium herbarum (IHEM 6005), stachybotrys chartratum (IHEM 22013), Penicillium chrysogenum (IHEM 220859). Aspergillus niger (IHEM 6147), Acremonium strictum (IHEM 19179) and Fusarium oxysporum (IHEM 3014) extracts were moderately recognized while extracts from Candida albicans (IHEM 3731) and saccharomyces cerevisiae (IHEM 6272) were not or almost not recognized.
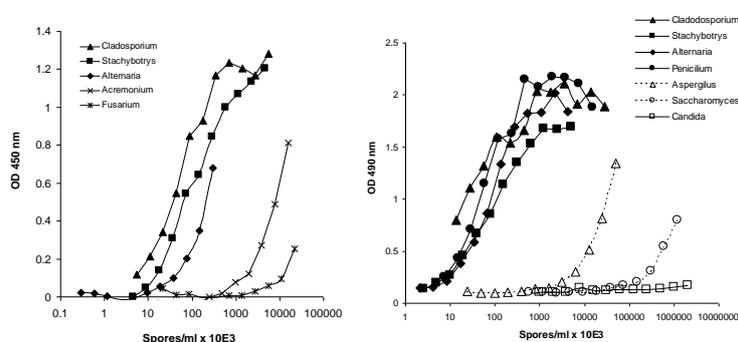
Figure 61: Analysis of various mould extracts using a sandwich ELISA with the LO-MO-5 as capture and biotin labelled LO-MO-5 as detection antibody. Plates were revealed using Peroxydase labelled avidin and OPD as substrate.

This assay was optimalized (coating of the antibody, saturation solution, incubation times, concentrations of revealing antibodies and peroxydase streptavidin) and we used an extract of *Cladosporium herbarum* spores as an internal standard for the quantification of field samples (**figure 62**). We used a "logit" regression to calculate the standard curve. Next we analysed the sensitivity and the coefficient of variation intra- and inter-assay. These coefficients are necessary to have an idea of the efficiency and reproducibility of this assay. We have run six duplicates of the same sample to measure the CV intra-assay, this assay was performed five times during five consecutive days in order to calculate the CV inter-assay. We obtained 9.81, 9.56 11.68, 12.05 and 6.31 for the CV intra-assay leading to an inter-assay CV of 20.58. The sensitivity of this assay was estimated to be between 2000 and 1000 equivalent *C. Herbarum* spores per ml. For the measurements in field samples, an extract of *C. Herbarum* spores was always used as an internal standard and for the calculation of the mould spore concentrations expressed therefore as equivalent *C. Herbarum* spores.
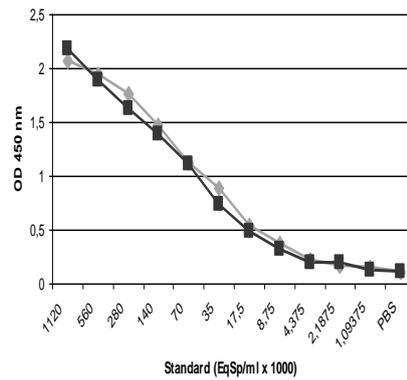
Figure 62: Standard curves obtained using a *Cladosporium extract* in a LO-MO-5 based sandwich ELISA.

Next we analysed the ability of this same assay to detect the antigen in environmental samples. The **figure 63** gives an example of such an experiment. One hundred centimetres square surface from ten different living rooms were vacuum cleaned and the dusts were solubilised in PBS. The quantity of LPS in these extracts was estimated by the limulus assay and the number of gram negative bacteria by standard microbiological cultures. Moreover the number of gram negative bacteria in 40 air litres of these living rooms was also estimated.

	LPS EU /100cm 2	BGN/ 100 cm2	Bact/40 litres air
C5	105.84	2160	74
C10	397.76	144	109
C8	**3.4**	**46080**	**17**
C9	**442.56**	**1152**	**57.5**
C7	40.68	2240	187.5
C2	13.84	20000	29
C3	5.36	880	16
C4	7	80	10
C6	4.16	7200	71
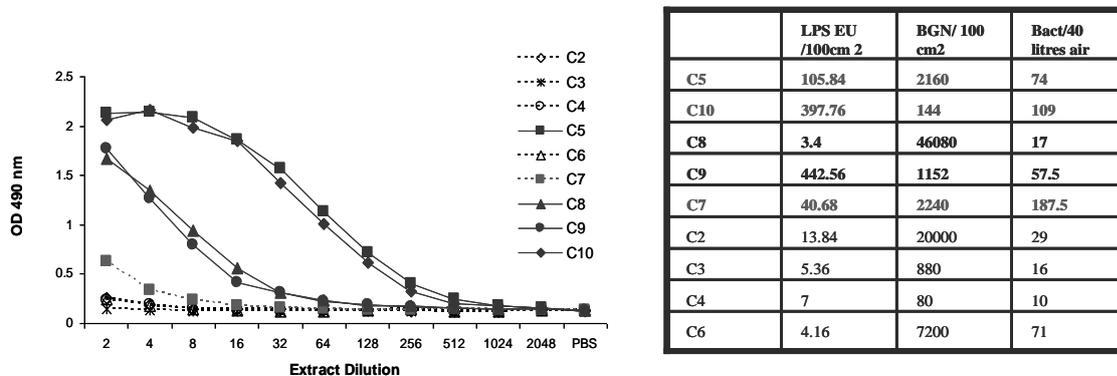
Figure 63: Analysis of various environmental samples using a sandwich ELISA with the LO-MO-5 as capture and biotin labelled LO-MO-5 as a detection antibody. Plates were revealed using Peroxydase labelled avidin and OPD as substrate. In the table the quantity of LPS and the number of gram negatives bacteria in the samples and the number of gram negatives bacteria in 40 litres of air.

As shown in **figure 63**, the LO-MO-5 based ELISA was able to detect the presence of an antigen in four out of the ten samples. Moreover the positives samples in ELISA were the most contaminated since they presented the highest level of LPS (samples

C5, C10 and C9) or a very high number of gram negative bacteria (C8). Therefore the LO-MO-5 antibody seems very interesting to detect a large array of mould species in environmental samples.

2.12. Monoclonal antibodies against mycotoxins.

Mycotoxins are small non protein components that are not able to induce the production of antibodies when injected "as this" in animals since the production of antibodies (at least for non repetitive antigens) requires the help of T helper cells recognizing linear peptides. Therefore Roridin A and Verrucarin A were conjugated to the BSA and OVA. Since these toxins do not have a functional group to facilitate their conjugations, they were treated with succinic anyhydride to generate bis-hemisuccinate. These products were immediately coupled to the proteins (BSA, OVA or KLH) using a water soluble carbodiimide (1-ethyl-3-3-dimethyl aminopropyl carbodiimide hydrochloride). LOU/c rats were immunized in the footpads with 50 µg of roridin A or verrucarin A conjugated to the BSA or OVA. At the end of the immunizations, lymphocytes were obtained from the poplietal lymph nodes and fused with the IR-983F cells. Growing hybridomas were selected in HAT medium.

Supernatants of the growing hybridoma were tested by ELISA on plated coated with BSA or OVA labelled with the Verrucarin A to detect mycotoxin specific antibodies. 8 different MoAbs were obtained (their characteristics are listed in the **table V**) but none were able to detect the free toxin in solution, an essential characteristics for the development of an ELISA assay specific for this toxin.

Nom	Isotype	BSA	BSA-Ver	BSA-Ror	OVA	OVA-Ver	OVA-Ror	KLH	KLH-Ver	KLH-Ror
F8-3E5	IgM	No	Yes	Yes	No	Yes	Yes	No	Yes	Yes
F14-3G8	IgG2a	No	Yes	Yes	No	Yes	Yes	No	Yes	Yes
F8-1H6	IgG2a	No	Yes	Yes	No	Yes	Yes	No	No	No
F8-3A1	IgG2a	No	Yes	Yes	No	Yes	Yes	No	No	No
F10-1B9	IgG2a	No	Yes	Yes	No	Yes	Yes	No	No	No
F8-4E4	IgG1	No	Yes	No	No	Yes	No	No	No	No
F8-3E1	IgG2a	No	Yes	No	No	Yes	No	No	No	No
F10-2E9	IgG1	No	Yes	No	No	Yes	No	No	No	No

Table V: Summary of the isotypes and specificities of the 8 positive clones obtained.

Therefore we started new fusion experiments with LOU/c rats immunized in the footpads with 50 µg of verrucarin A conjugated BSA. Of the 553 tested clones, 70 clones (13%) produced antibodies recognizing the verrucarin A bound to OVA. Only

one of these clones produced antibodies which were inhibited by the free verrucarin A (**Figure 64**).
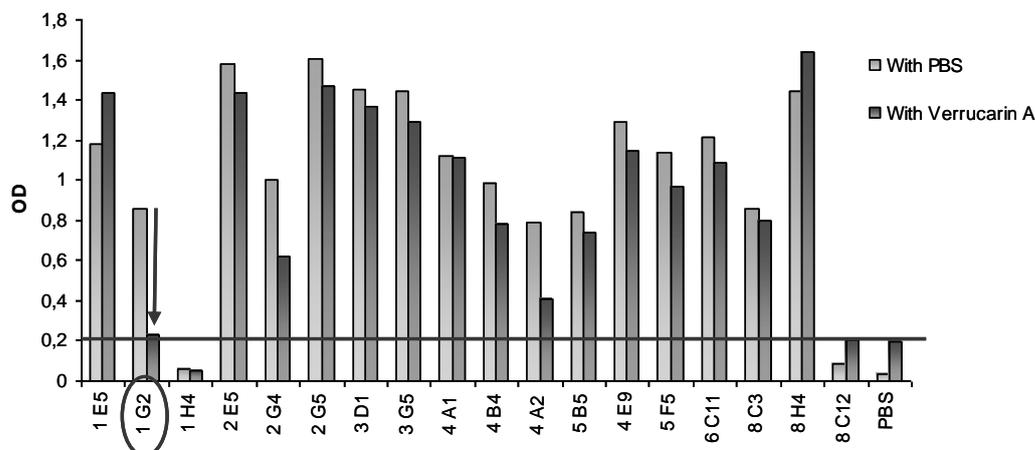
Figure 64: Screening of hybridomas supernatants on ELISA plates coated with OVA-verrucarin A in the presence or absence of free verrucarin A. Bound antibodies were detected using a peroxydase labelled-mouse MoAb directed against rat Kappa light chains and OPD as substrate.

The F24-1G2 antibody was then purified and its specificity was analysed in an indirect ELISA using verrucarin A or roridin A coupled BSA or OVA. This antibody was able to bind to OVA or BSA labelled verrucarin A but not to these same proteins labelled with roridin A or to the unlabelled proteins therefore demonstrating specificity towards verrucarin A only **(Figure 65A)**. In a competitive ELISA, neither free roridin A nor BSA labelled roridin A were able to inhibit the binding of the F24-1G2 antibody to BSA-verrucarin A. However this binding was efficiently inhibited by BSA labelled verrucarin A or by the free verrucarin A (**Figure 65B**).
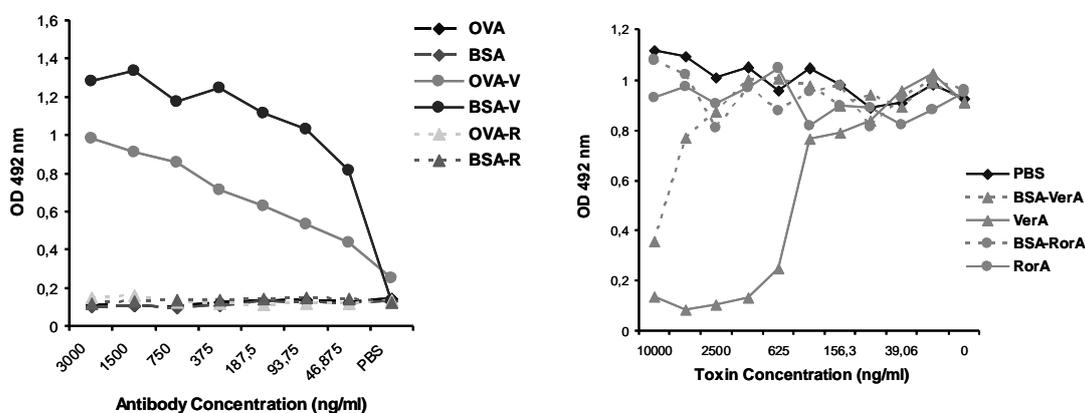
Figure 65: **(A)** Analyse of the specificity of the F24-1G2 antibody using an indirect ELISA. **(B)** Analyse of the inhibitory activity of the various carrier coupled toxins in a competitive ELISA using the F24-1G2 antibody.

Next we optimized this competitive ELISA in order to improve its sensitivity. We optimized the concentrations of BSA-verrucarin A for the coating, the detecting process with the F24-1G2 and the revelation process.

We analysed the sensitivity and the coefficient of variation intra- and inter-assay. We have run six duplicates of the same sample to measure the CV intra-assay, this assay was performed five times during five consecutive days in order to calculate the CV inter-assay. We obtained 55.3, 8.12, 26.5, 16.1 and 22.7 for the CV intra-assay leading to an inter-assay CV of 29.92. The overall sensitivity ranged between 3.9 and 1.95 ng/ml of free verrucarin A.

2.13. Detection of mycotoxins with FTIR-ATR

2.13.1. Detection of verrucarin-A in buffer solution (coupled or under free form)

It has been shown that using monoclonal antibody anti-verrucarin developed by ISP-WIV, the verrucarin A in solution is concentrated on the surface of a germanium or silicon internal reflection element (IRE).

We first studied the detection of mycotoxins (coupled and free) in buffer and then the detection of mycotoxins in complex media (environmental samples)

Verrucarin-BSA detection

$y = 4E{-}06x + 0{,}06$
$R^2 = 0{,}9631$
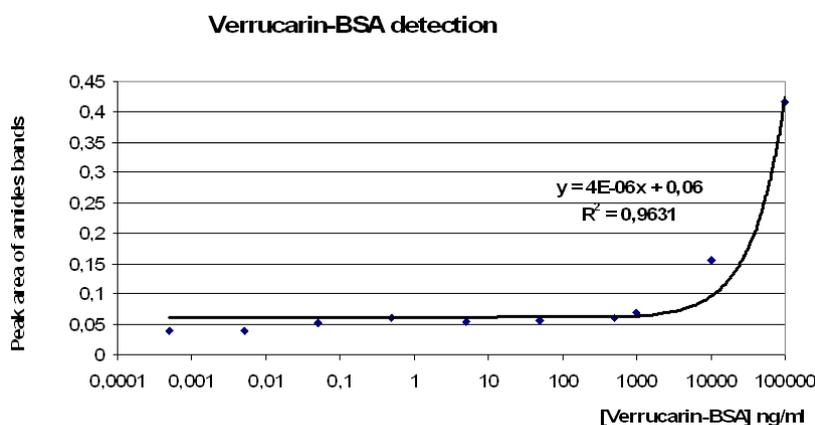
Figure 66: Detection of VERRU-A coupled to BSA

It is possible to monitor the binding of mycotoxins coupled to BSA as a function of time, by recording the evolution of amide bands. The assay curve in buffer solution is shown in **figure 66.**
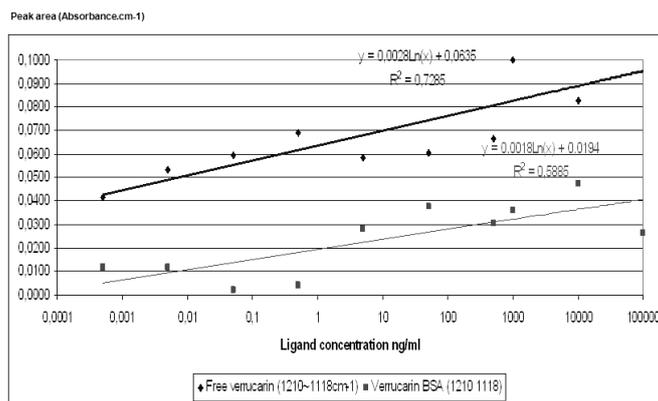
Figure 67: Detection of VERRU-A free or coupled in buffer solution.

Anti-Verrucarin mAb is more sensitive with free verrucarin as you can note in **figure 67**. The amount of Verrucarin-BSA bound to the mAb is less than the one of Verrucarin free for the same concentration because there are less verrucarin molecules under coupled form.

We determined the limits of detection as three times the spectral response with PBS, in this case (that is to say between 1210 and 1118 cm^{-1}) peak area with PBS equals 0.008 Absorbance.cm^{-1}

Therefore the corresponding limit of detection is equal at 0.024 Absorbance . cm^{-1}.

So we can theoretically detect free Verrucarin-A in buffer solution at femtogram level by plotting the ordinate at the origin. Here we clearly detect Verrucarin-A at 1pg/ml in buffer solution thanks to our sensors which is better than indirect Elisa sensitivity (about 1 ng/ml for free verrucarin A)

The sensitivity is about 1000 times higher for FTIR biosensors in comparison with indirect ELISA.

2.13.2 Specificity of anti-verrucarin antibody F24 :
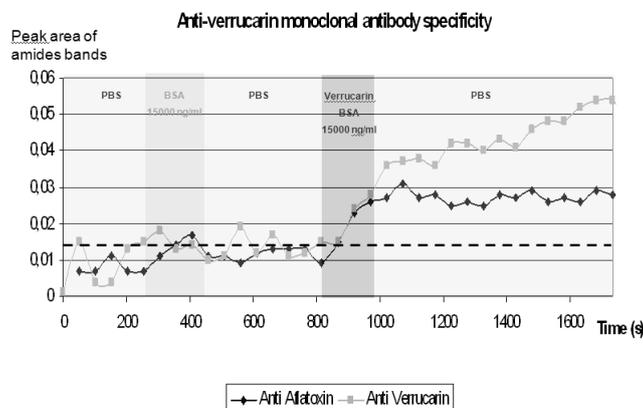
Figure 68: Specificity of MAB anti- verrucarin F24 with coupled verrucarin-A
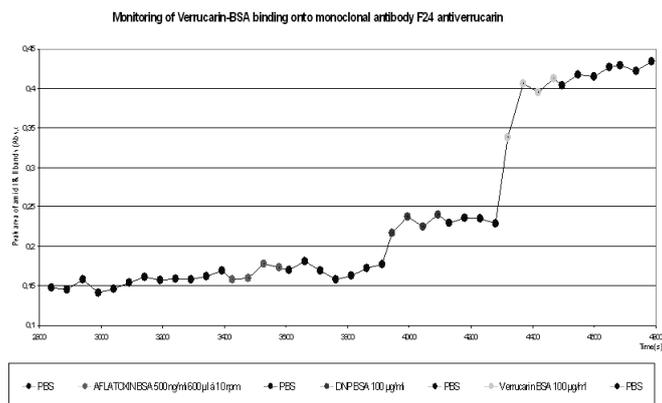
Figure 69: Specificity of anti-verrucarin mAb F24 with coupled verrucarin-A

The specificity of Anti-verrucarin mAb F24 was further analysed in **figures 68** and **69.** Only verrucarin-BSA binding onto mAb was monitored by peak area evolution of amide bands. The other ligands i.e. BSA, DNP-BSA or AFLA-BSA are not recognized by Anti-Verrucarin mAb F24.
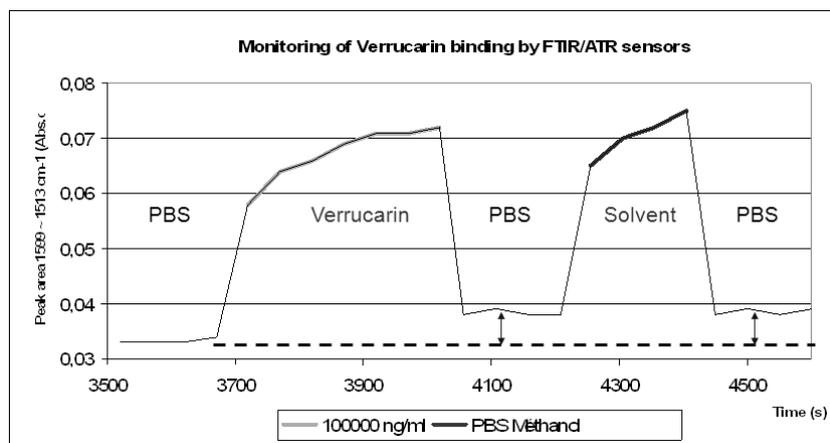
Figure 70: No impact of solvent onto verrucarin-BSA detection

In **figure 70**, we show that the signal has increased after Verrucarin-BSA around amide II band and moreover this is not due to solvent effects.

2.14. Mould genera found in symptomatic dwellings

2.14.1 Environmental sampling.

Environmental samplings have been coupled to the standard activities of HVS teams in indoor pollution prevention and diagnosis (LPI, Laboratoire de Prévention des Pollutions Intérieures). The LPI team is intervening on request of the general practitioner: an investigation is performed in the dwellings suspected to be the cause of health problems to their occupants, including systematic sampling for both chemical and microbiological pollutants and measuring of physical parameters. A questionnaire is filled-up with the patient and first advices are provided. After the analysis of the samples, a report is send to the patient and a copy to the medical practitioner with specific advices related to the results.

Figure 71: Vehicle used by the LPI for visiting symptomatic dwellings and example of the questionnaire filled up with the patient during the visit.

For air sampling, a high flow-rate pump (RAVEBO SUPPLY B.V) has been used in symptomatic dwellings (see **Figure 72**). It allows the sampling to be carried out at a flow rate of 100 to 600 litre/minute (6-36 m³/hour). The airborne toxins were collected on quartz filters (pore diameter: 2.2 µm) by sucking an air volume corresponding to that of half of the room at a flow rate of 400 L/min. Filters were then washed with extraction buffer and submitted to the different techniques developed and/or used during this project (FTIR-ATR, ELISA, EnviroLogix QuantiTox™ Kit). In parallel to the development of our analytical tools, a cross-validation was requested at the University of Ghent (Prof. S. De Saeger) who analyzed the air samples by liquid chromatography tandem mass spectrometry method (LC-MS/MS).

Airborne fungi were monitored with a portable RCS air sampler, usually called "impactor". Agar strips (YM agar strips, Biotest) are loaded into the rotor of the RCS sampler.

They are composed of a plastic holder with grids (wells) filled with a specific solid YM agar medium amended with Rose Bengal, which is a combination of the characteristics found in Malt Extract Agar, Sabouraud Dextrose Agar and the standard Rose Bengal Agar and allows for the increased recovery of organisms that are difficult to cultivate such as *Alternaria* species. Colony forming units were counted after 5 days incubation at 20°C.

Figure 72: High flow-rate pump

Figure 73: RCS sampler
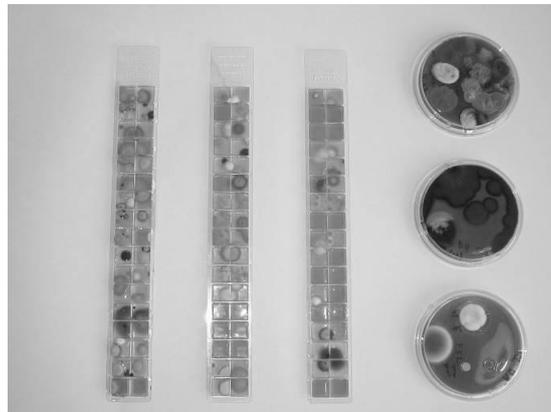
Figure 74: Colony Forming Unit (CFU) of molds on YM agar strips and RODAC plates after incubation at 20°C

For surface sampling, RODAC plates (Replicate Organism Detection and Counting) made with Rose Bengal Chloramphenicol Agar were used to sample mold contaminated areas (walls, ceilings,…). Plates were incubated to promote mold growth. After 5 days of incubation at 20°C, results are reported as the number of CFU (colony forming units) per area sampled and determination of mold genera is performed.

For dust sampling, a vacuum cleaner Philips FC model 9064 was used, whose tube was modified with additional accessories in order to hold a filter (made of cleansing cotton pads) to collect dust by sucking up a 0,25 m^2 surface using a pattern (50 cm x 50 cm) placed on the floor.

During the sampling campaign of MIC-ATR, 84 visits were made to symptomatic dwellings and 17 visits to "control" dwellings (meaning houses where habitants didn't complained about health problems and where there were no visible molds). Moreover, a specific campaign was conducted in social housing (located in the city of Hensies) as the request for an intervention was introduced by the Mayor following complains about dampness, probably due to construction defects.

Besides all the samples collected by our teams, we also received 95 dust samples from the Laboratoire d'Allergologie du Nouvel Hôpital Civil de Strasbourg (in collaboration with Prof. F. De Blay and Martine Ott, Conseillère Médicale en Environnement Intérieur).

2.14.2. Mould genera found in symptomatic dwellings: analysis of surfaces.

From the database containing all the parameters collected during the sampling campaign, it has been possible to extract the followings observations related to the surface analysis: depending on whether one owns or leases the symptomatic dwelling visited, the percentage of cases with visible molds is significantly higher in tenants (92%) than in owners (55%), shedding the light on a first discrepancy depending on the status of owner or not (see **figure 75**).
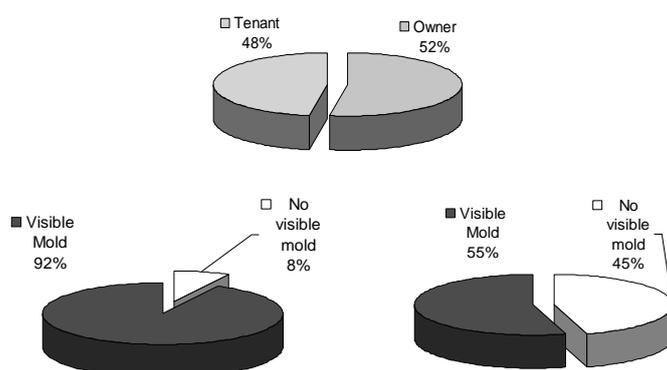
Figure 75: Presence of visible molds depending on whether one owns or leases the symptomatic dwelling visited

Going further in this study with the determination of the mold genera, we can observe that the three major genera found in the surface of the symptomatic dwellings are *Cladosporium*, *Penicillium* and *Aspergillus* in both owners and tenants, but with the tenants, a greater diversity and representativeness with the genera is found (36%) (see **Figure 76**). From these first observations, one can make the assumption that with the tenants a longer period elapses before visit of experts and remediation, offering to mold the possibility for a more extensive development. It can also be underlined that *Stachybotris*, the infamous mold associated with pulmonary hemorrhages was found in both groups, as well as *Alternaria* and *Ulocladium* known to be major allergy-causing molds.
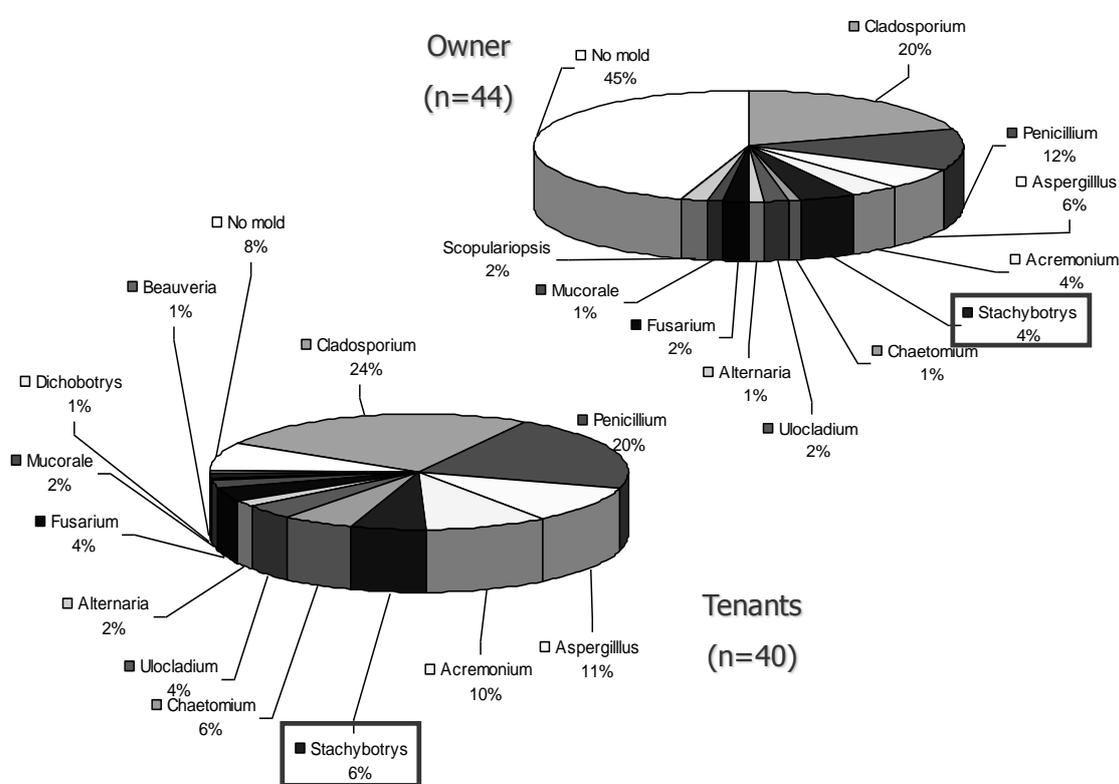
Figure 76: Diversity and representativeness of the mold genera found on surfaces in symptomatic dwellings of owners and tenants. n = number of houses visited.

2.14.3. Mould genera found in social houses from Hensies: analysis of air.

As explained earlier in the text, this specific campaign was conducted under the request of the Mayor of the town Hensies (Hainaut, Belgium) since inhabitants were complaining about dampness problems in their houses. In this specific case, 100% of the visited dwellings showed up visible molds on the surfaces (see **Figure 77**).

Two of the three major genera found in our previous study were also found in this specific case (*Cladosporium* and *Aspergillus*). *Stachybotris* was also found in 4 % of the cases.
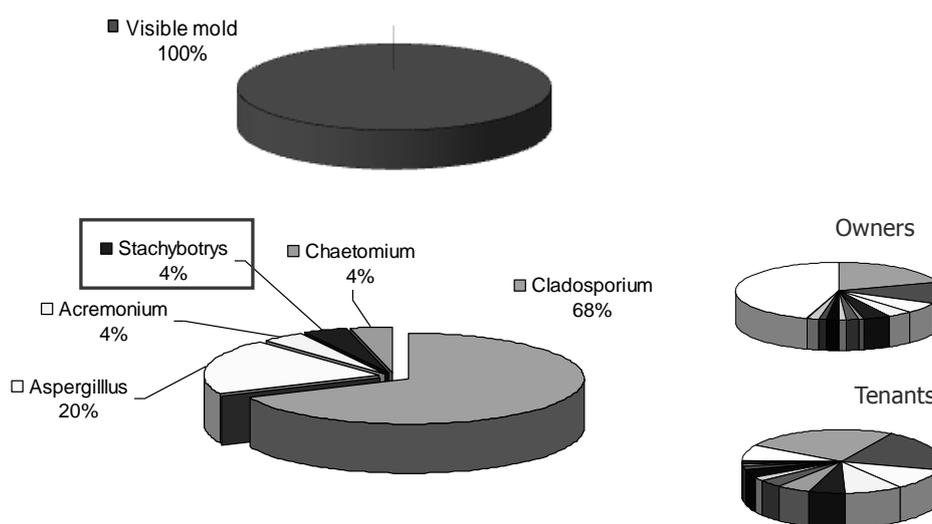
Figure 77: Diversity and representativeness of the mold genera found on surfaces in symptomatic dwellings of the social houses from Hensies (n= 24). The results obtained during the whole campaign are placed besides in order to compare with the social houses.

2.14.4. Mould genera found in symptomatic dwellings: analysis of air.

Airborne fungi were systematically monitored with a RCS air sampler, with one measurement for the indoor air and one for the outdoor air. In this way, it is possible to discriminate if contamination is rather coming from inside or outside de house. The external load (expressed in CFU) differs dramatically depending on the season and has to be considered when using data.

Our results show a massive contamination of the symptomatic dwellings (> 90%) while control houses only show up 6 % of air contamination (see **Figure 78**). Contrary to what appears with the surface study where there was a highly significant difference between owners and tenants among symptomatic dwellings, this discrepancy doesn't exist anymore with air where tenants as well as owners show high values of mold contamination.
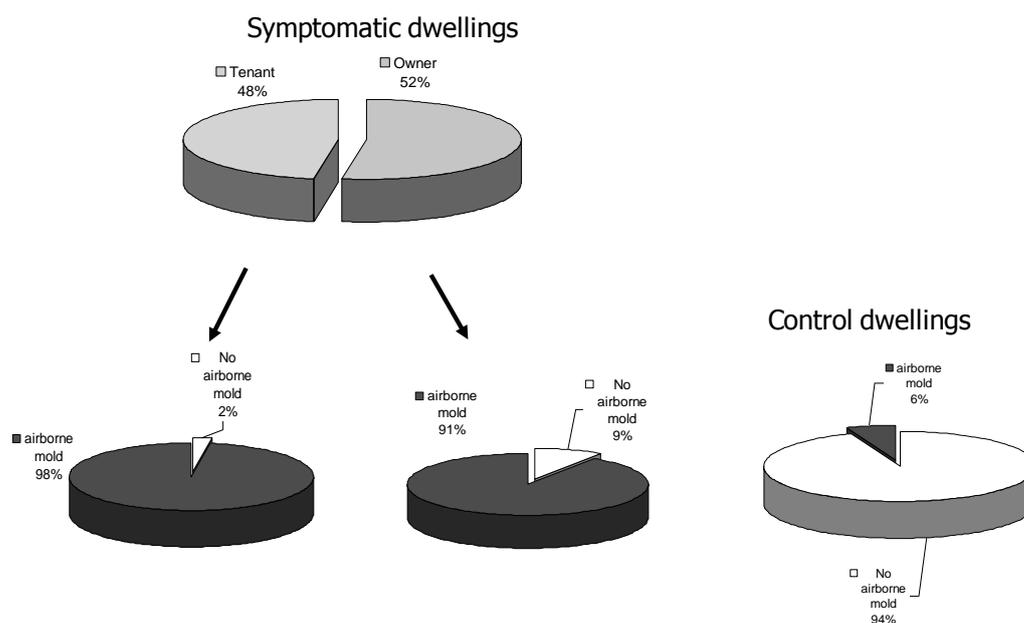
Figure 78: Air contamination with molds in symptomatic dwellings (divided into owners and tenants) and in control dwellings.

When analyzing the diversity and representativeness of mold genera in the air of symptomatic dwellings, we found the same three major ones than in surfaces, namely *Cladosporium, Aspergillus* and *Penicillium* in all cases (tenants, owners and social housing) (see **Figure 79**). In this study, all the data were considered, regardless of the external and internal mold load. We only considered genera that were assumed to come specifically from indoor, by analyzing the genera determination performed on incubated agar strips. We also conduct the same kind of study but only considering the data in the cases internal CFU values are higher than external ones. In this case, the representativeness of the three major genera doesn't change much whatever the case (owner, tenants, social housing) but there is less diversity in genera (see **Figure 80**). While the results seem clearest and easier to interpret in this way, it biases the analysis since this leads to leave out some important information like for example, the presence of *Stachybotris* in owner's dwellings.
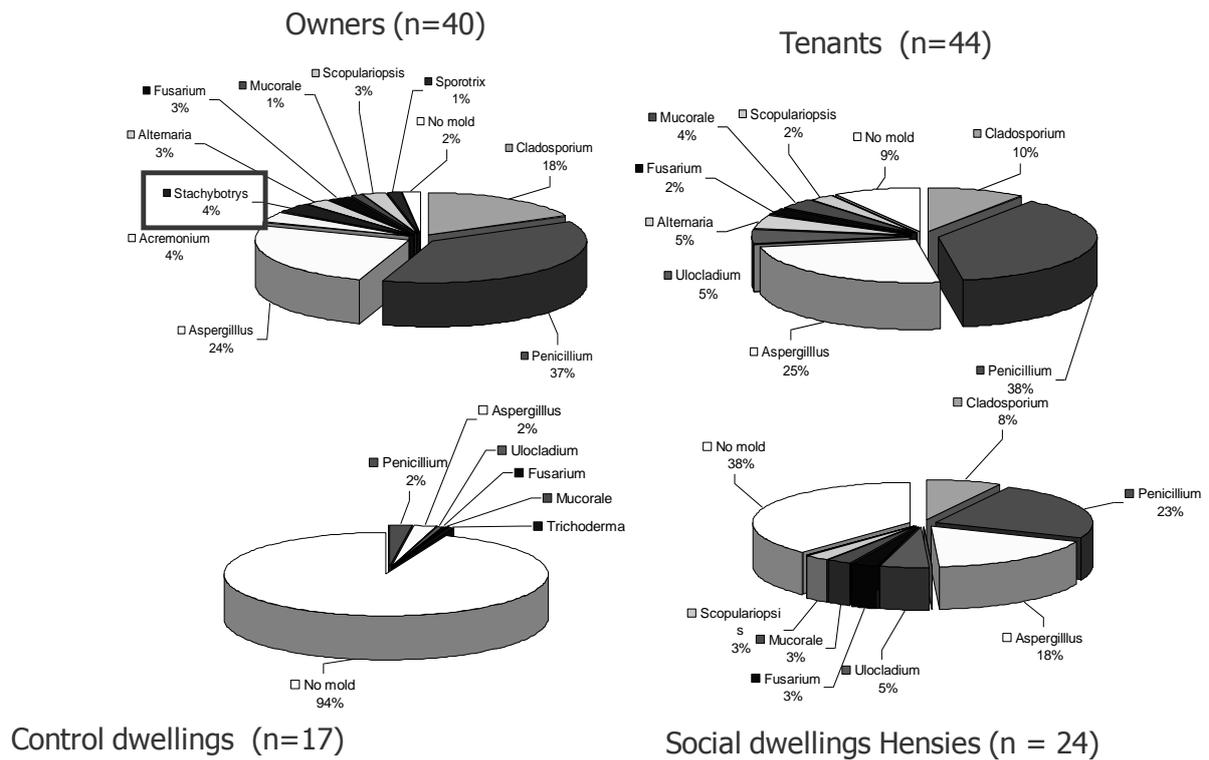
Figure 79: Diversity and representativeness of the mold genera found in the air of symptomatic dwellings and of social houses, compared to control dwellings.
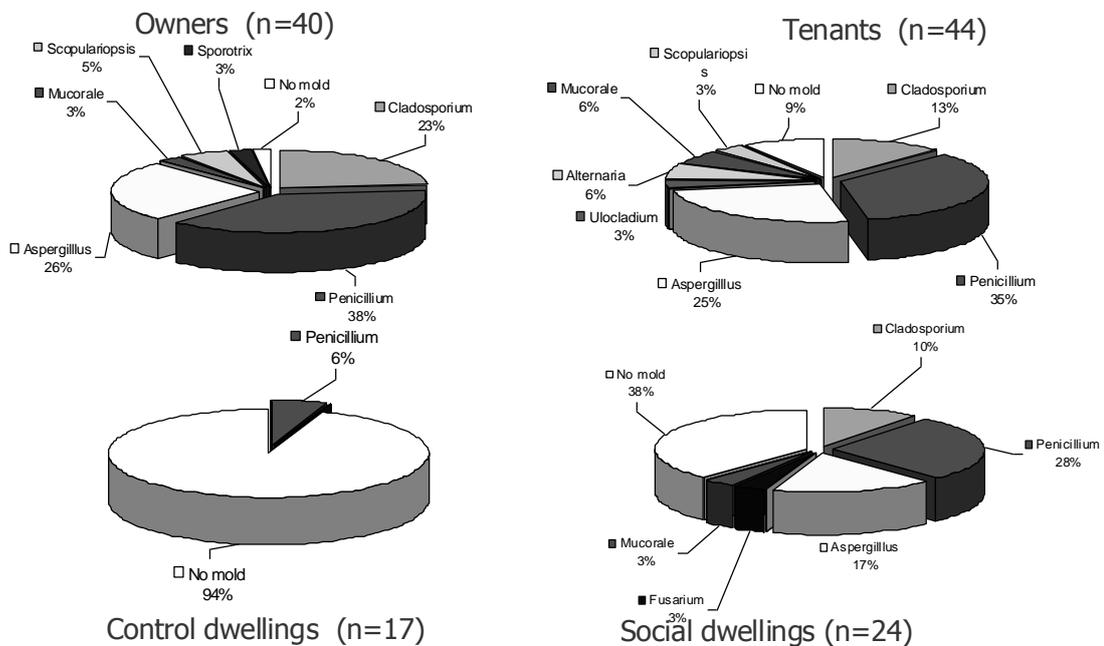
Figure 80: Diversity and representativeness of the mold genera found in the air of symptomatic dwellings and of social houses **if CFU int > CFU ext**.

2.14.5. Relationships between mould genera and health problems in symptomatic dwellings

In the initial request introduced by the general practitioner to ask the intervention of the LPI at a symptomatic dwelling, some information are usually collected regarding the complaints and health problems of the patients. This information has been systematically introduced in our database, together with the information directly collected from patients with the questionnaire during the visit. This constituted the medical records we crossed with the data about status of owner or tenant and with mold diversity and representativeness.

A first study was to check the frequency of diverse pathologies and symptoms. As we can see in **Figure 81**, the major health problems are asthma, bronchitis, rhinitis/sinusitis and cough, whatsoever in tenants as in owners.
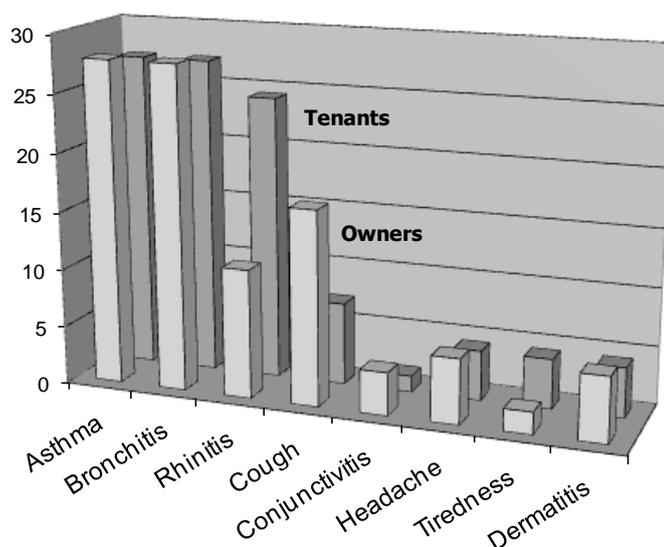
Figure 81: Statement of health problems as introduced in the initial request and in the questionnaire submitted during the visit of the LPI.

Going further with the analysis of the data, we checked for the correlation between pathologies and the presence of some specific genera of mold in the dwelling of the patient. We therefore associated on a graph the diversity of genera found corresponding to the pathologies declared by the patient, and this for each symptom and for surface and air molds (see **Figure 82**). At first sight, there is no obviousness of a systematic correlation between one or several specific health problems and the presence in air or in surfaces of specific mold. However, due to the scope and complexity of the data, some statistic tools should be used to clarify the situation.
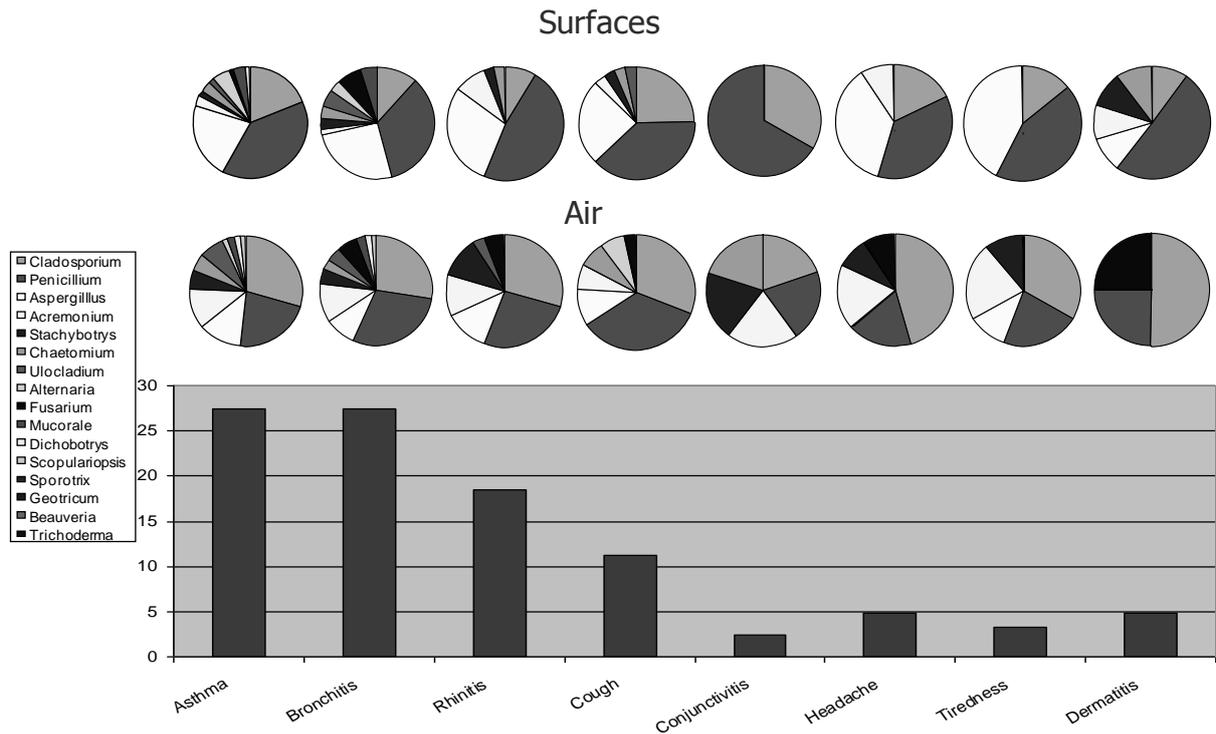
Figure 82: Correlation between the diversity of genera found in air and in surfaces of symptomatic dwellings and the pathologies declared by the inhabitants.

Nevertheless, to simplify the data processing, we grouped all the respiratory diseases in one category and all other problems in a second one and checked for a potential correlation in this new configuration. Results are shown in **Figure 83**: respiratory problems are associated with a larger diversity of genera compared to the group "other problems", in air as well as in surface, but this is not necessarily due to specific mold responsible for respiratory problems but simply because cases in this category are far more numerous than in the other category and therefore the diversity of mold genera found is also more important.
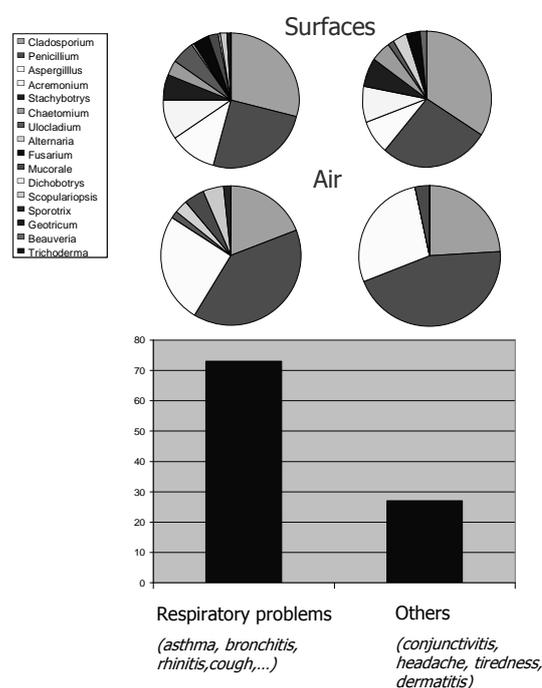
Figure 83: Search for a correlation between the diversity of genera found in air and in surfaces of symptomatic dwellings and the appearance of pathologies in a simplified version of data processing.

2.15. Indoor mould biomass quantified using immunoassays in symptomatic dwellings.

2.15.1. Measurements in air; comparison with the RCS sampler.

Classically the total mould biomass in dwellings is measured using special devices called" impactors" which inject allows the determination of airborne mould CFU after a period in culture. While straightforward, this technique is time-consuming and is not devoid of major drawbacks as for instance the problems of growth inhibitions between species, the problems of distinct optimal growing temperature between various species.

Immunoassays are more objective monitoring techniques allowing the quantitative determination of the target antigens. We used our LO-MO-5 based assay (specific for the classical mould species found indoor see 2.4.) in order to measure the amount of the target mould antigens in air samples from dwellings and we compared these results from the measurements with the RCS samplers.

For the measurements of the mould biomass in field samples, an extract of *C. herbarum* spores was always used as an internal standard and for the calculation of the mould spore concentrations expressed therefore as equivalent of *C. herbarum* spores.

When air samples from control dwellings (meaning dwellings without inhabitant's health problems) were analyzed, the total amount of mould CFU found outdoor was higher as compared to indoor CFU indicating that these dwellings were not contaminated. These results were confirmed with the LO-MO-5 immunoassay. However two dwellings showed a low presence of airborne mold antigens (below 10.000 Eq Clado spores/m^3). These two samples had the highest CFU when measured with the RCS sampler. Therefore in control air samples a good correlation was found between the results obtained with the RCS impactor and the LO-MO-5 immunoassay.
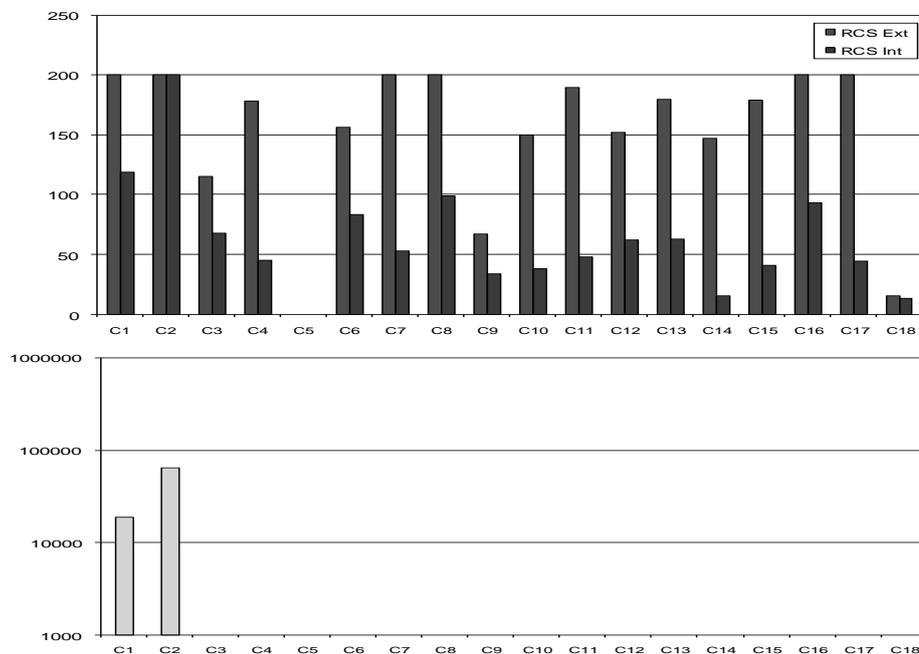
Figure 84: Quantification of the indoor mould biomass in control dwellings. Immunoassay measurements in air: comparison with the RCS sampler. Upper graph: Number (x10) of mould CFU outside (first bar) and inside (second bar) per cubic air meter obtained using the RCS sampler. Lower graph: Number of equivalent *Cladosporium* spores per cubic air meter calculated from the immunoassay. N=17.

We then compared in the same way air samples from symptomatic dwellings (meaning dwellings with inhabitant's health problems reported to HVS by general practitioners). The **figure 85 and 86** show the results from this analysis made in 49 symptomatic dwellings.

As shown on these figures, some air samples showed a correlation between increased mould CFU indoor and the presence of high airborne mould antigens. Other dwellings not recognized as contaminated with the impactor measurements showed high airborne mould antigens while in some others airborne mould antigens were not detected with the LO-MO-5 immunoassay while the RCS sampler found an increased presence of mould CFU indoor. This analysis showed the difficulty to correlate the living mould biomass in air (CFU results obtained after an *in vitro* culture) and the total quantity of a mould antigen airborne.
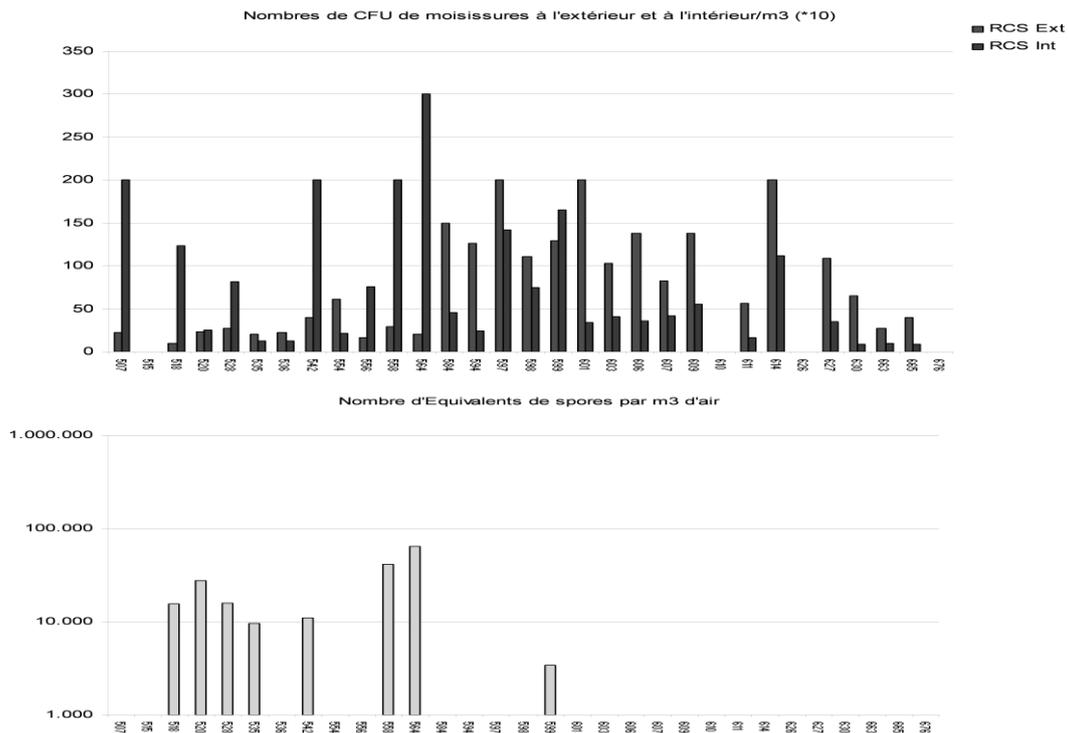
Figure 85: Quantification of the indoor mould biomass in symptomatic dwellings. Immunoassay measurements in air: comparison with the RCS sampler. Upper graph: Number (x10) of mould CFU outside (first bar) and inside (second bar) per cubic air meter obtained using the RCS sampler. Lower graph: Number of equivalent *Cladosporium* spores per cubic air meter calculated from the immunoassay. N=28.
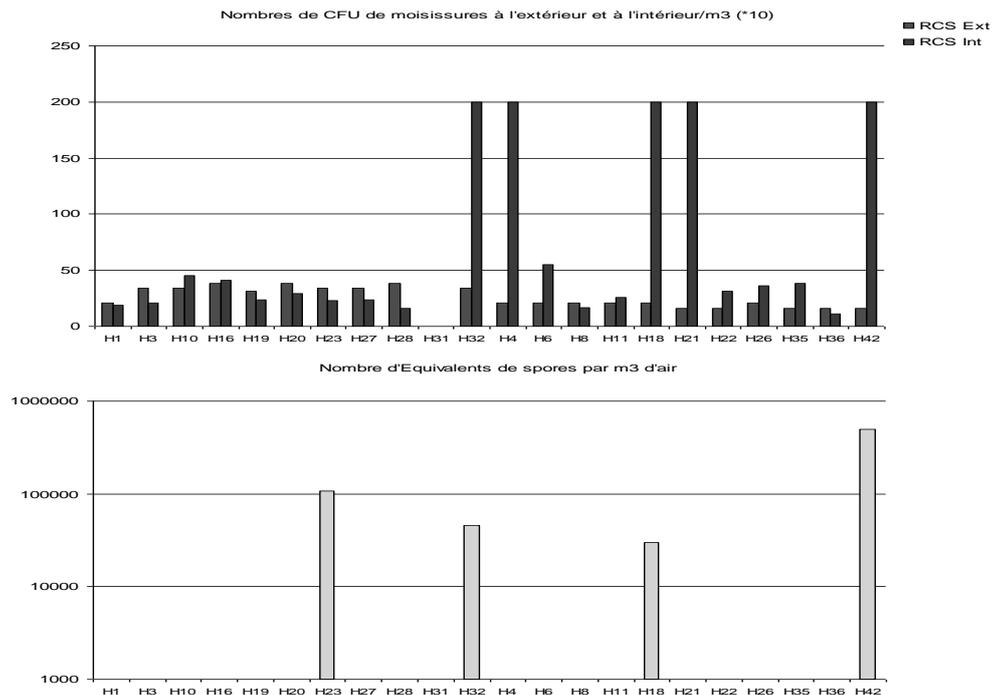
Figure 86: Quantification of the indoor mould biomass in symptomatic dwellings. Immunoassay measurements in air: comparison with the RCS sampler. Upper graph: Number (x10) of mould CFU outside (first bar) and inside (second bar) per cubic air meter obtained using the RCS sampler. Lower graph: Number of equivalent *Cladosporium* spores per cubic air meter calculated from the immunoassay. N=21.

2.15.2. Measurements in dust; comparison with the RCS sampler.

We then compared in the same way mould CFU found in air samples from symptomatic dwellings with mould antigens found in settled dust and quantified with the LO-MO-5 immunoassay. As shown on **figure 87**, the LO-MO-5 immunoassay detected the mold antigens in all dust samples while in this analysis of 12 dwellings, only 4 showed a higher mould CFU inside versus outside. The fact that airborne CFU measurements represent only a "moment" while dust samples are more representative of an accumulation in time of antigens can explain these discordances. Since the long term presence of mould antigens in dwellings can significantly affect the health of their inhabitants, the measurement of mould antigens accumulating in dust might be very interesting in term of health problems.

If lower and higher limits are sets for 10% of the sample population and 90% of the sample population respectively then the lower threshold are $1.1 \cdot 10^6$ Eq Clado spores per m^2 of vacuumed ground floor and the higher threshold is $3.5 \cdot 10^7$ Eq Clado spores per m^2 of vacuumed ground floor.
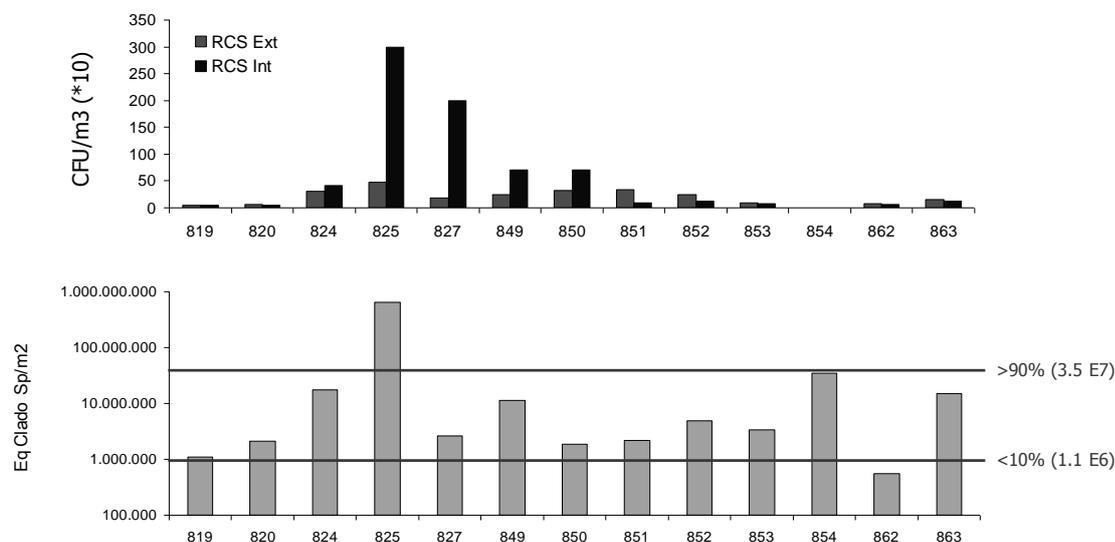
Figure 87: Quantification of the indoor mould biomass in symptomatic dwellings. Immunoassay measurements in settled dust: comparison with the RCS sampler. Upper graph: Number of mould CFU outside (first bar) and inside (second bar) per cubic air meter obtained using the RCS sampler. Lower graph: Number of equivalent *Cladosporium* spores per square meter of vacuumed floor (smooth floor) calculated with the immunoassay. N=13.

2.15.3. Measurements in dust; comparison with mite allergens.

It is well known that settled dust found in dwellings is contaminated with numerous compounds including mould spores, mycelia fragments, bacteria, LPS, mites allergens,...

In order to shed some lights on the eventual correlation (or lack of correlation) between mould antigens and other contaminants in settled dust, we compared the amounts of mould antigens and mite allergens. Mites allergens were relevant in this analysis because mites allergens are important allergens leading to major respiratory problems but also because there is a biological association between moulds and mites. Indeed mites are commonly found growing indoors on mouldy surfaces and therefore an association between mite allergens and mould contamination can be hypothesized.

Dermatophagoïdes pteronyssimus allergens (*Derp*) and *Dermatophagoïdes farinae* (*Derf*) allergens and mould antigens were quantified in dust vacuumed from carpets, mattress and smooth living floors. The **figures 88, 89** and **90** show the results of these comparisons.

There was no correlation between the presence of *Derp* and *Derf* allergens in dust, some samples showed high *Derp* allergens without *Derf* allergens and some show the opposite. There was also a group of samples showing no mite allergens at all in dust. Regarding the presence of mould antigens, there was no correlation between the presence of mould antigens and mite allergens. Divergent from the mite allergen results, mould antigens were found in every dust samples without correlation with the mite allergens.

When lower and higher limits were sets at 10% and 90% of the sample populations respectively then the lower threshold was $53 \cdot 10^6$ Eq Clado spores per gram of dust found in carpets and the higher threshold was $57 \cdot 10^7$ Eq Clado spores per gram of dust found in carpets. Regarding the mattress the lower thresholds was $29 \cdot 10^6$ Eq Clado spores per gram of mattress dust and the higher threshold was $22 \cdot 10^7$ Eq Clado spores per gram of mattress dust. Finally, in dust vacuumed from smooth living floors, the lower thresholds was $85 \cdot 10^6$ Eq Clado spores per gram of dust and the higher threshold was $25 \cdot 10^7$ Eq Clado spores per gram of dust. These results show the absence of correlation for the presence of contaminating compounds in settled dust, the accumulation of contaminants in carpets in contrast to smooth floors and the ubiquitous presence of mould antigens in dust samples.
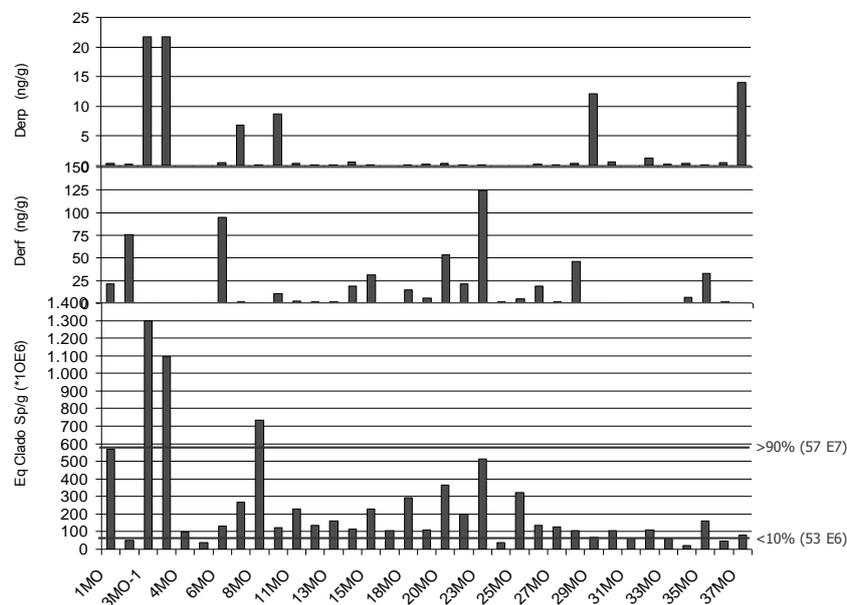
Figure 88: Quantification of the indoor mould biomass in carpets from symptomatic dwellings. Immunoassay measurements in dust: comparison with mite allergen concentrations. Upper graphs: Quantity of *Derp* and *Derf* in gram of vacuumed carpet dust. Lower graph: Number of equivalent *Cladosporium* spores per gram of vacuumed carpet dust calculated with the immunoassay. N=35.
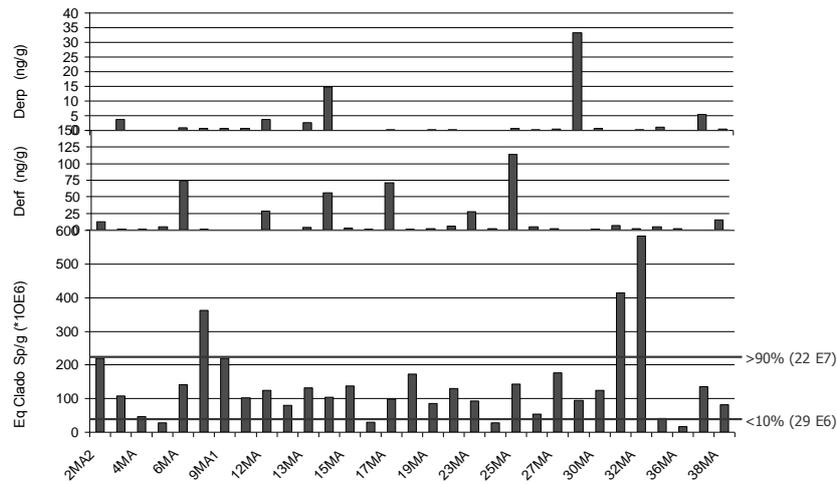
Figure 89: Quantification of the indoor mould biomass in mattress from symptomatic dwellings. Immunoassay measurements in dust: comparison with mite allergen concentrations. Upper graphs: Quantity of *Derp* and *Derf* in gram of vacuumed mattress dust. Lower graph: Number of equivalent Cladosporium spores per gram of vacuumed mattress dust calculated with the immunoassay. N=32.
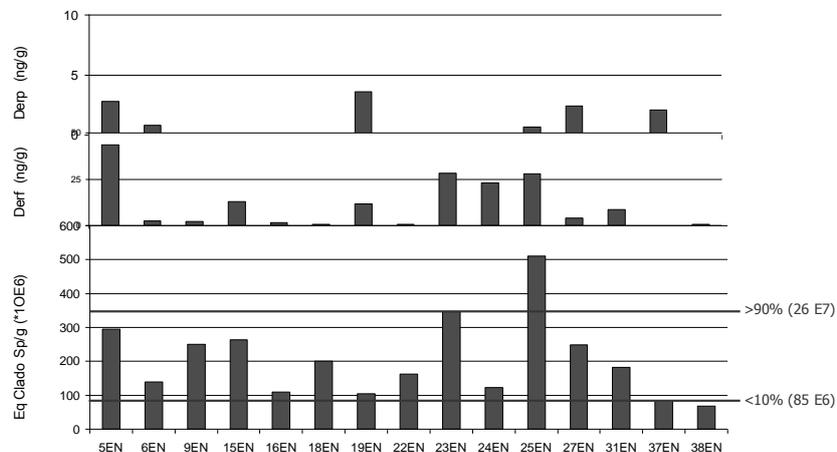
Figure 90: Quantification of the indoor mould biomass in smooth living room floors from symptomatic dwellings. Immunoassay measurements in dust: comparison with mite allergen concentrations. Upper graphs: Quantity of Derp and Derf in gram of vacuumed living room floors dust. Lower graph: Number of equivalent *Cladosporium* spores per gram of vacuumed living room floor dust calculated with the immunoassay. N=15.

2.15.4. Measurements in air and dust; symptomatic versus control dwellings.

We investigated and compared the concentrations of mould antigens, using the LO-MO-5 immunoassay, in air and dust from symptomatic and control dwelling (**Figure 91**). This analysis involved 17 control dwellings and 76 symptomatic dwellings for the air samples and 17 control and 43 symptomatic dwellings for the dust samples.

Regarding the air samples, 15 air samples from control and 25 air samples from symptomatic dwellings were under the limit of detection of the assay. In control dwellings, only two samples showed a low amount of airborne mould antigens while the majority of air samples from symptomatic dwellings showed a concentration of airborne mould antigens above the mean of control dwellings. Clearly symptomatic dwellings showed a significant higher concentration of airborne mould antigens.

Regarding the dust samples, mould antigens were found in every dust samples, from control and symptomatic dwellings. The discrimination between these two populations in term of mould antigens concentration was however again significant showing that both airborne and settled mould antigens are more present in symptomatic dwellings as compared to control dwellings.
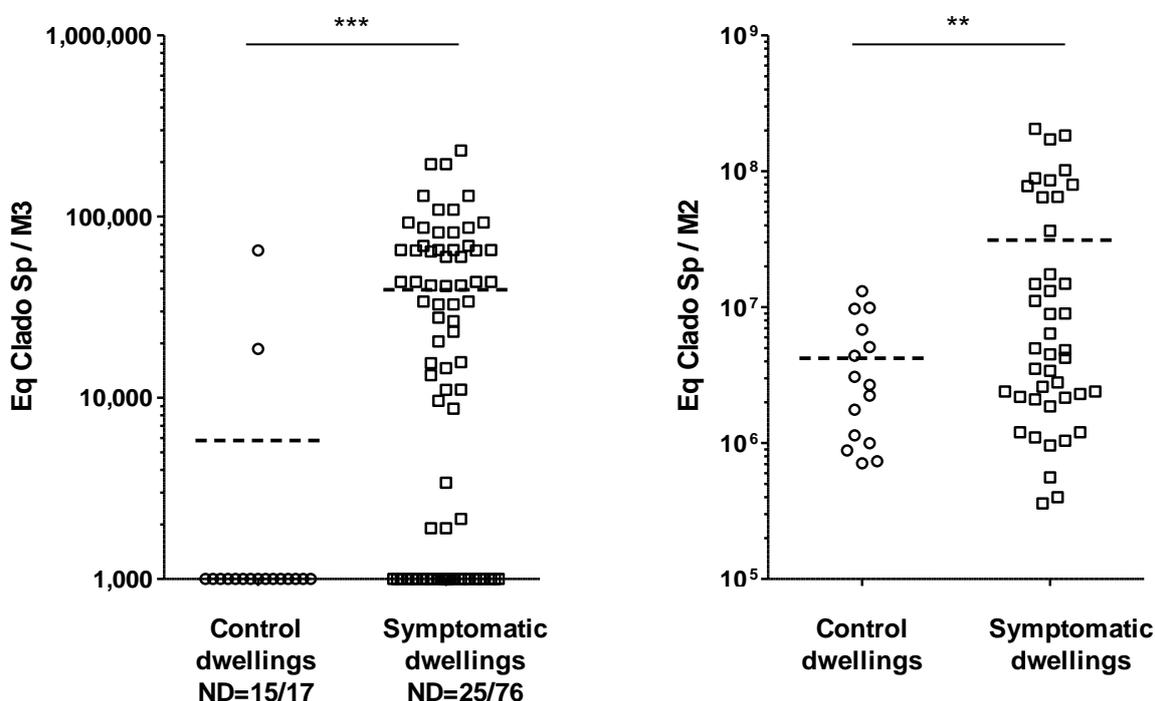
Figure 91: Comparison of the indoor mould biomass in air and dust from control and symptomatic dwellings. Immunoassay measurements in dust. ND= not detected. The limit of detection of this ELISA was 1000-2000 Eq. Clado Spores. *** p<0.01, ** p<0.05.

2.15.5. Measurements in air and dust; correlation with inhabitant's diseases/symptoms.

The total mould biomass, measured with the LO-MO-5 immunoassay in air samples from symptomatic dwellings were analysed in function of the health complains of their inhabitants (N=53). In this dwelling population, respiratory problems (asthma, bronchitis and rhinitis-sinusitis) represented 71 % of the health complains. The total airborne mould biomass in dwellings with respiratory problems (mean was 29.034 Eq Clado Sp/m^3) showed no difference as compared to the dwelling with other complains (mean was 26.575 Eq Clado Sp/m^3). The mean mould biomass found in the whole population of dwellings was 28.285 Eq Clado Sp/m^3. Therefore there is no correlation between the level of airborne mould antigens found in these dwellings and the kind of health problems (respiratory versus others) from their inhabitants (**Figure 92**).

When specific health problems were investigated, asthma represented 30%, bronchitis 24%, rhinitis and sinusitis 19%, cough 9%, conjunctivitis 2.5%, headaches 6.4%, fatigue 2.5% and dermatitis 6.3%.The total airborne mould biomass was analysed in function of the various diseases/symptoms from the inhabitants but no individual relationship between the total airborne mould biomass and the various diseases/symptoms from the inhabitants were observed (**Figure 92)**.
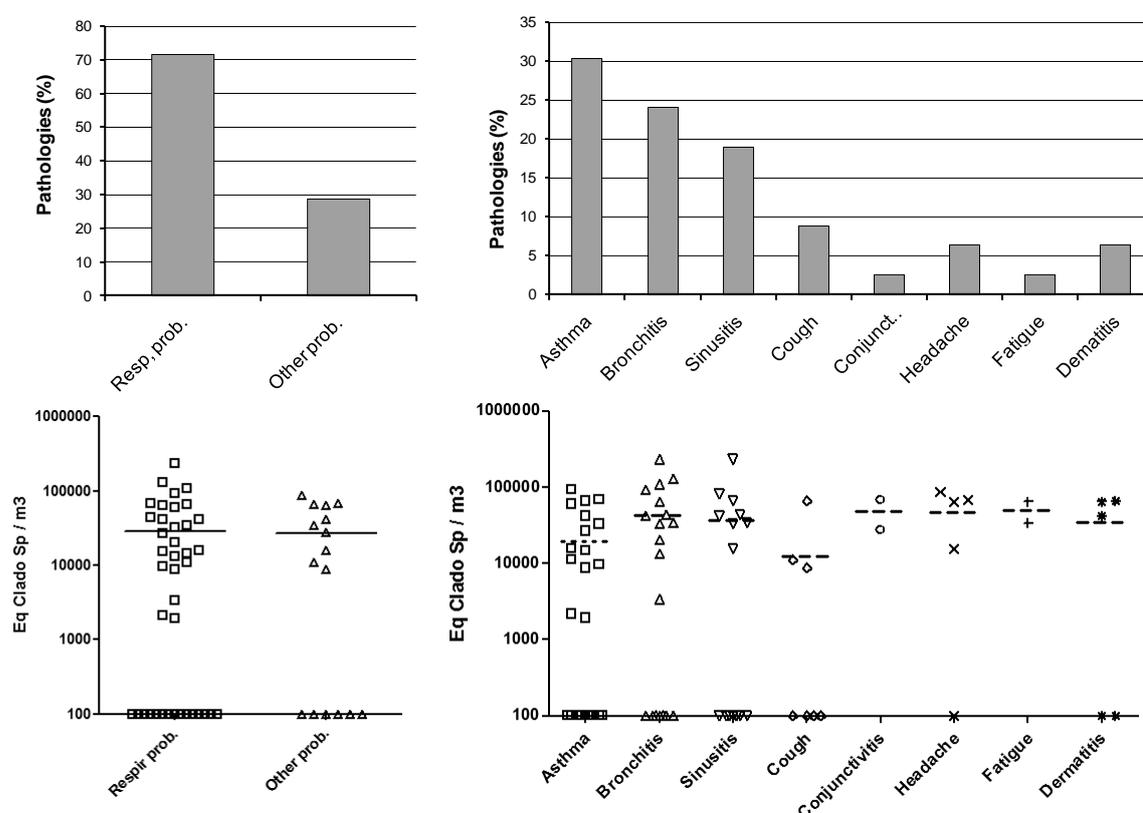
Figure 92: Analysis of the relationships between health complains of the dwellings inhabitants and the airborne mould biomass. LO-MO-5 based Immunoassay measurements in air samples. N=53 dwellings.

In another symptomatic dwelling population, the total mould biomass were measured with the LO-MO-5 immunoassay in dust samples and analysed in function of the health complains of their inhabitants (N=42). In this dwelling population, respiratory problems (asthma, bronchitis and rhinitis-sinusitis) represented 76 % of the health complains. The total mould biomass in dust from dwellings with respiratory problems (mean was $4.17 \ 10^7$ Eq Clado Sp/m^3) was higher as compared to the dwelling with other complains (mean was $9.52 \ 10^6$ Eq Clado Sp/m^3). However, this difference was not statistically significant (t test). The mean mould biomass found in the whole population of dwellings was $3.38 \ 10^7$ Eq Clado Sp/m^3. Therefore, even if a trend towards the association between higher mould biomass in dust and respiratory problems of the inhabitants could be suspected there is no statistical correlation between the level of mould antigens in dwellings and the kind of health problems (respiratory versus others) from their inhabitants (**Figure 92**).

When specific health problems were investigated, asthma represented 24.7%, bronchitis 26%, rhinitis and sinusitis 20.5%, cough 9.6%, conjunctivitis 2.7%, headaches 6.9%, fatigue 2.7% and dermatitis 6.8%. The pathologies/symptoms profile in this population was therefore very similar to the profile observed in the dwelling population analysed before. The total mould biomass in dust was analysed in function of the various diseases/symptoms from the inhabitants. Even if a trend towards a higher concentration of mould antigens in dust from dwellings with inhabitants complaining of asthma, bronchitis and rhinitis-sinusitis was observed, these associations were not statistically significant. Therefore no individual relationship between the total mould biomass in dust and the various diseases/symptoms from the inhabitants were observed (**Figure 93).**
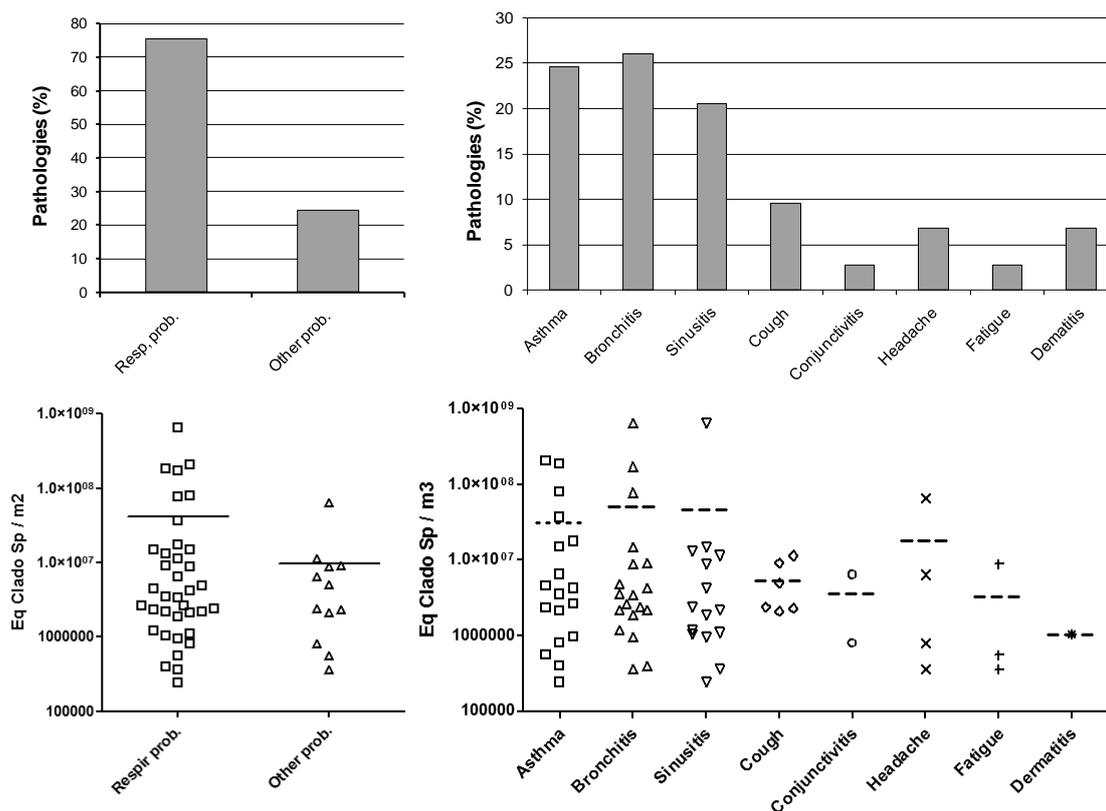
Figure 93: Analysis of the relationships between health complains of the dwellings inhabitants and the concentration of mould antigens in settled dust. LO-MO-5 based Immunoassay measurements in dust samples. N=42 dwellings.

2.16. Quantification of mycotoxins in dwellings.

In recent years, a great deal of interest has been generated regarding the study of mycotoxins. Historically, mycotoxins have been a problem related to agricultural, food, poultry and cattle industries. However, many toxigenic fungi have been found to infest buildings with indoor environmental problems. Several recent cases have related toxigenic fungi and mycotoxins to building occupant health problems caused by contaminated indoor environments and cases of pulmonary hemorrhage were reported in infants who were living in homes that were contaminated with toxigenic fungi (Flappan *et al.,* 1999, Vesper *et al.,* 2000, Van Emon *et al.,* 2003).

Mycotoxin exposures have been linked to a variety of acute and chronic adverse health effects. Generally, these effects include acute symptoms such as pulmonary hemorrhage, dermatitis, recurring cold and flulike symptoms, burning/sore throat, headaches, excessive fatigue and diarrhea.

Chronic effects include carcinogenicity, mutagenicity, teratogenicity, central nervous system effects, immune system damage, and specific effects of the heart, liver, kidneys and other organs. Therefore research and systematic field investigation are needed to provide an understanding of the presence of mycotoxins in dwellings.

2.16.1. Quantification of airborne mycotoxins indoors, relationships with the total mould biomass.

The presence of 17 different mycotoxins was analyzed in air samples from control (N=17) and symptomatic dwelling (N=50) using liquid chromatography - mass spectroscopy analyzers (LC-MS). The LC-MS represent a "gold standard" for the detection of mycotoxins and show a very good resolution allowing the simultaneous detection of several mycotoxins and a very good sensibility and reproducibility.

The 17 different mycotoxins investigated are given in **figure 94**. No airborne mycotoxin was detected in control dwellings. However, mycotoxins were found in air samples from 9 dwellings (18% of the investigated dwellings) and are indicated by arrows on the graph. We analyzed the potential relationship between the total airborne mould biomass obtained with the RCS sampler or the LO-MO-5 based immunoassay and the presence of mycotoxins. As shown on **figure 94**, there was no correlation between the presence of mycotoxins and the presence of airborne mould spores (RCS sampler) or airborne mould antigens (LO-MO-5 based immunoassay). Indeed, from the 9 dwellings in which mycotoxins were found, only 4 had an increased presence of mould CFU indoors when measured with the RCS sampler and only 3 detectable airborne mould antigens with the LO-MO-5 assay.
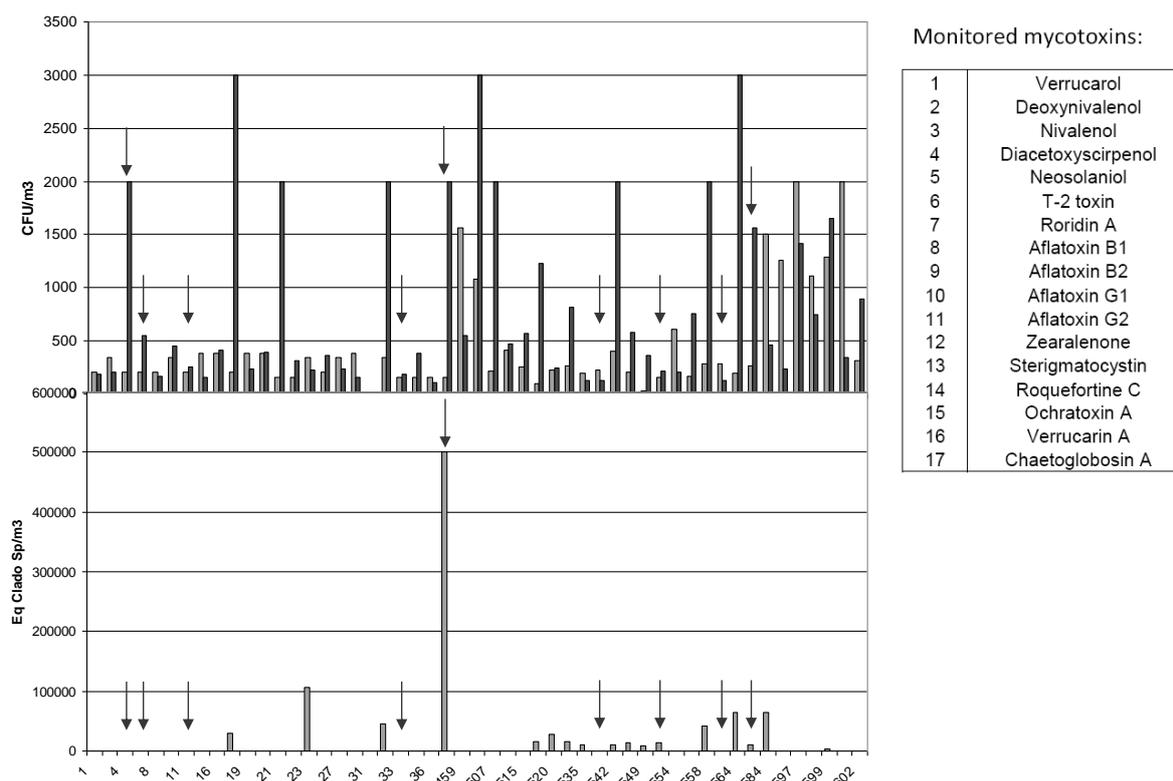
Figure 94: Analysis of the relationships between the presence of mycotoxins (shown by an arrow) in air sample and the mould biomass obtained with the RCS sampler (above, for each dwelling the first bar gives the amount of CFU outdoor and the second the amount of CFU indoor) or with the LO-MO-5 based immunoassay (below). N=50 dwellings.

2.16.2. Quantification of airborne mycotoxins indoors, correlation between the mass spectrometry and immunoassays.

Although the LC-MS readily detected airborne mycotoxins, the immunoassays that we developed previously with rat mAb specific for the verrucarin A were not sufficiently sensitive to detect the mycotoxins in the same air samples. We therefore investigated the ability of a commercial kit called "The EnviroLogix QuantiTox™ Kit" to detect the mycotoxins in air samples from the control dwellings (N=17) and the symptomatic dwellings (N=50). The QuantiTox™ Kit is designed for the quantitative detection of some tricothecenes, including Roridin A and Verrucarin A in bulk samples. This kit is a competitive immunoassay with a detection limit (LOD) of 0.14 ppb developed by EnviroLogix (Portland, USA). The QuantiTox™ kit detected mycotoxins in one air sample from the control dwellings and in 39 air samples from the symptomatic dwellings. When compared with the LC-MS results, the QuantiTox™ kit gave 23 false positive responses (46%) and 3 false negative responses (6%).

Therefore this kit could not represent an interesting tool for the rapid and easy detection of mycotoxins in air samples.
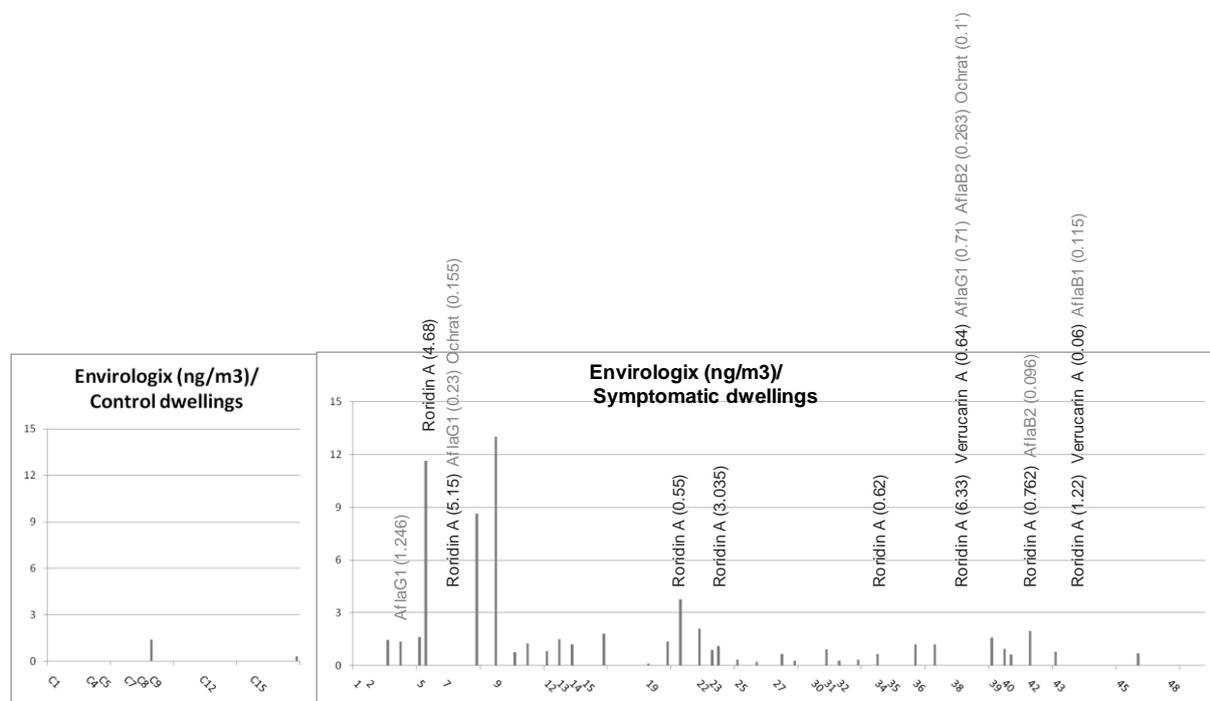
Figure 95: Analysis of the presence of mycotoxins in air samples from control dwellings (left, N=17) or from symptomatic dwellings (right, N=50). Each bar represents the concentration of mycotoxins in air samples (ng/m^3) obtained with the QuantiTox^{TM} kit. Mycotoxins detected by LC-MS are indicated above with the concentration in ng/m^3 between brackets.

2.16.3. Quantification of airborne mycotoxins indoors, summary.

Results from the analysis of airborne mycotoxins in dwellings are summarized in **table VI.** The presence of airborne mycotoxins was analysed in 17 control dwellings and in 50 symptomatic dwellings. Mycotoxins were detected in 9 symptomatic dwellings using the LC-MS. The major mycotoxins detected were roridin A, verrucarin A, and aflatoxins. All the dwellings contaminated with mycotoxins presented a development of mould on surfaces (walls, windows,...). 7 out of the 9 dwellings with mycotoxins presented the development of cladosporium on some surfaces. Aspergillus was found in 3 out of the 9 dwellings. Other minor genera found in these 9 dwellings were Penicillium, Chaetomium, Ulocladium and Acremonium. Only 3 out of the 9 nine dwellings showed an increased airborne mould biomass indoors as compared to outdoors (samples 1, 5 and 9).

The Cladosporium genus was found airborne in 9 out of the 9 dwellings containing airborne mycotoxins. The Aspergillus genus was found in 4 out of the 9 dwellings. Other minor genera found were Penicillium, Rhizopus, Fusarium and Sporotrix.The QuantiTox[TM] assay gave 3 negative responses for these 9 dwellings. This assay also overestimated the presence of mycotoxins and gave half of the time false negative responses.

Dwelling	Mycotoxins (LC ms/ms) ng/m3	Visible molds	Visible mold genera	RCS Ex/In CFU	Air molds Cla Sp/m3	Airborne molds Genera	QuantiTox ng/m3
1	Aflatoxines G1 (1,246)	Y	Aspergillus sp. Cladosporium sp.	21/>200	ND	Aspergillus sp Cladosporium sp	1,45
2	Roridines A (4,678)	Y	Cladosporium sp.	21/55	ND	Aspergillus sp Cladosporium sp Penicillium sp	1,35
3	Roridines A (5,148) Aflatoxines G1 (0,233) Ochratoxines (0,155)	Y	Cladosporium sp.	21/26	ND	Cladosporium sp Penicillium sp Rhizopus sp.	ND
4	Roridines A (0,548)	Y	Not defined	16/19	ND	Aspergillus sp Cladosporium sp Penicillium sp	3,77
5	Roridines A (3,035)	Y	Aspergillus sp.	16/>200	501.355	Aspergillus sp Penicillium sp Fusarium sp	1,1
6	Roridines A (0,622)	Y	Cladosporium sp. Chaetomium globosum	23/13	ND		0,67
7	Roridines A (6,318) Verrucarines A (0,640) Aflatoxines B1 (0,713) Aflatoxines B2 (0,263) Ochratoxines (0,140)	Y	Cladosporium sp.	16/22	14.596	Cladosporium sp Penicillium sp Sporothrix schenckii	ND
8	Roridines A (0,762) Aflatoxines B2 (0,096)	Y	Aspergillus sp. Penicillium sp. Cladosporium sp.	29/13	ND		1,98
9	Roridines A (1,221) Verrucarines A (0,059) Aflatoxines B1 (0,115)	Y	Cladosporium sp. Ulocladium sp. Acremonium strictum	27/156	11.090	Cladosporium sp Penicillium sp	ND

Table VI: Summary of the results concerning the analysis of airborne mycotoxins in dwellings.

2.16.4. Quantification of mycotoxins in dust.

The presence of mycotoxins was also investigated in settled dust obtained from symptomatic dwellings. Dust samples were obtained by vacuuming one hundred centimetres square surface. Dusts were solubilised in PBS and then analyzed using the verrucarin A-specific ELISA or with QuantiTox^{TM} kit.

To test the recovery properties of the immunoassays used, two dust samples (0.1g each) devoid of mycotoxins were spiked with 150 ng of verrucarin A before been extracted in 750 µl of PBS giving a theoretical concentration of verrucarin A of 2000 ng/gram of dust. These samples were analysed using the verrucarin A-specific ELISA and the QuantiTox^{TM}. The mean concentration of verrucarin A obtained with the ELISA in the two samples was 495 ng/gram of dust. The quanti Tox assay gave a mean of 619 ng/gram of dust. Therefore the recovery in both case was very low, 24.7% for the verrucarin A specific ELISA and 31% for the QuantiTox^{TM} assay (**figure 96**). This poor recovery is probably due to the complexity of the matrix since a plethora of compounds should be present in settled dust and this complexity probably affect the immunological recognition of the verrucarin A by the antibodies used.

	ELISA VerA (ng/ml)				Quanti Tox	
	Mean (ng/ml)	SD	Mean (ng/g)	SD	Mean (ng/ml)	Mean (ng/g)
3MA	0	0	0	0	2,13	15,97
3MA-S	76,2	18,3	571,5	137,25	81,8	613,5
8MO	0	0	0	0	3,67	27,52
8MO-S	55,8	2,3	418,5	17,25	83,27	624,52
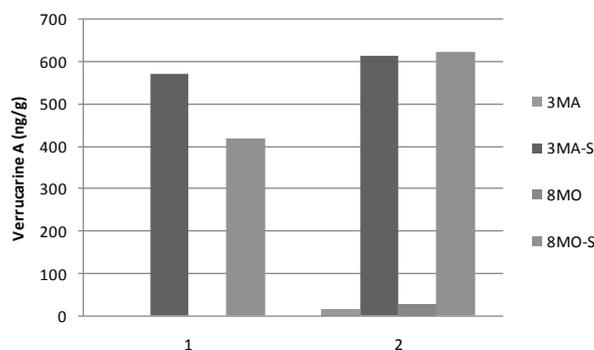
Figure 96: Analysis of the recovery of verrucarin A in dust samples using the verrucarin A specific ELISA or the QuantiTox^{TM} assay. Two dust samples were spiked, extracted and analysed with the two techniques. The theoretical concentration of verrucarin A in the dust samples was 2000 ng of verrucarin A per gram of dust. The measured concentrations of verrucarin A with the two techniques are indicated in the table and on the graph.

Despite this low recovery, we used these assays to monitor the presence of mycotoxins in the settled dust from symptomatic dwellings. A group of 95 vacuumed dust samples from symptomatic dwellings were analysed with the verrucarin A-specific ELISA. From these 95 samples, 13 samples (13.6%) gave a positive response. When these 13 samples were

analysed using the QuantiTox^TM kit, 12 samples gave a positive response but the concentrations of mycotoxins detected were each time lower as compared to the concentrations obtained with the verrucarin A-specific ELISA (**figure 97**). Importantly the presence of mycotoxins in these samples could not be confirmed by the LC-MS. Indeed the LC-MS showed a decreased limit of detection in dust samples (probably because of the complexity of the matrix) preventing the detection of mycotoxins in these samples.

	ELISA VerA (ng/ml)				Quanti Tox	
	Mean (ng/ml)	SD	Mean (ng/g)	SD	Mean (ng/ml)	Mean (ng/g)
14MA	34,2	8,5	256,5	63,75	1,99	14,92
15MO	46,8	18	351	135	10,49	78,67
15EN	52,4	5,7	393	42,75	57,93	434,47
24MA	70	14,6	525	109,5	2,35	17,62
28MO	19,2	7	144	52,5	4,37	32,77
28MA	7,8	1,8	58,5	13,5	2,04	15,3
29MO	20	7,3	150	54,75	4,12	30,9
29MA	5,4	1,9	40,5	14,25	2,44	18,3
36MO	29,5	7,2	221,25	54	6,72	50,4
MRIE	13,5	4,9	101,25	36,75	4,55	34,12
38MO	38,2	11,7	286,5	87,75	11,09	83,17
37EN	30	26,1	225	195,75	46,45	348,37
14MO	127,6	139,9	959	1049,25	ND	ND
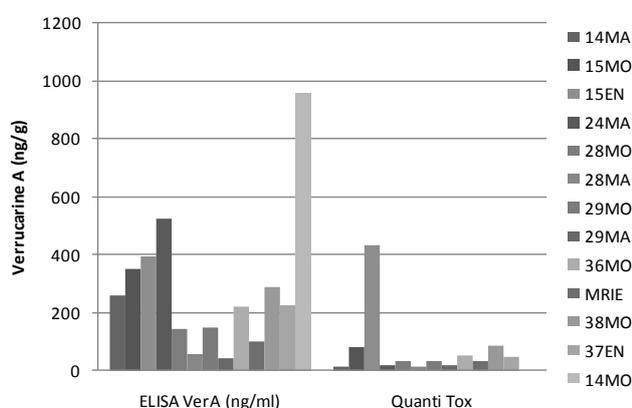
Figure 97: Analysis of verrucarin A concentrations in dust samples using the verrucarin A specific ELISA or the QuantiTox^TM assay. The measured concentrations of verrucarin A with the two techniques are indicated in the table and on the graph.

2.16.5. Quantification of mycotoxins in environmental samples by FTIR-ATR

The reference spectra of dried Verrucarin-A is in agreement with spectra obtained after detection in a complex media because we find the same peaks located in the same infrared regions (**figure 98**).
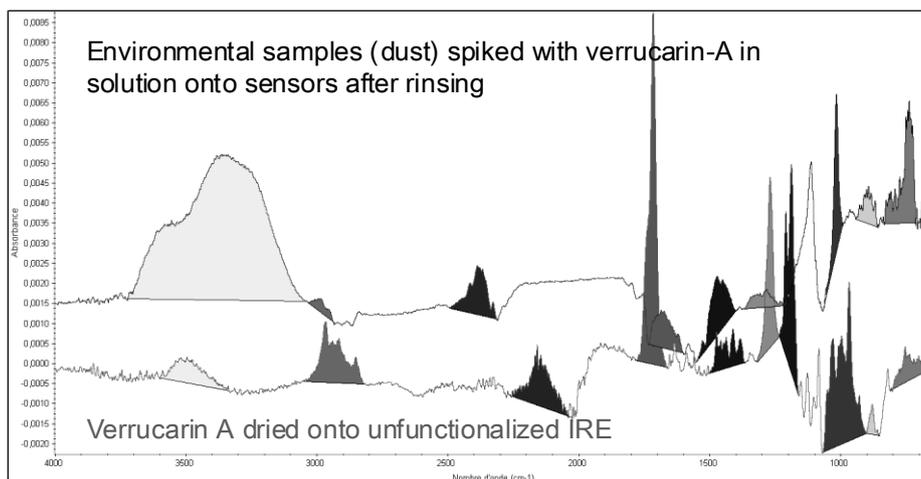
Figure 98: Comparison of reference peaks with the peaks detected with our sensors.

The reference spectra of dried Verrucarin-A is in agreement with spectra obtained after detection in a complex media because we find the same peaks located in the same infrared regions (**figure 98**).
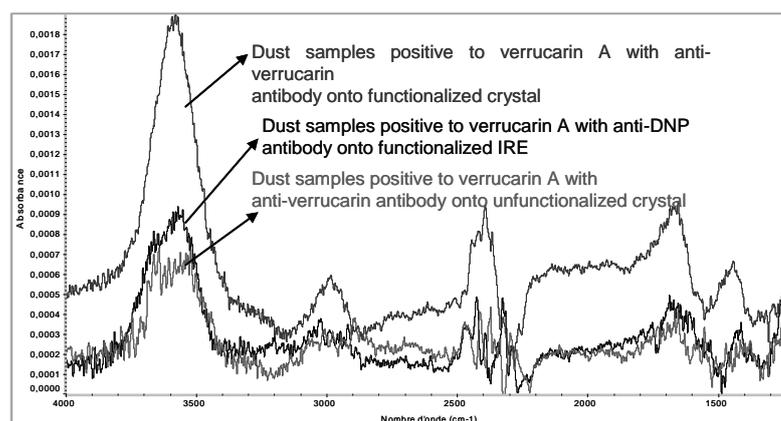
Figure 99: Detection of verrucarin-A in dust sample

In **figure 99**, if we compare average spectra after injecting 80 µl of dust sample (considered to be positive by Elisa and LC-MS-MS) at a flow rate about 12 µl/min we can observe a detection using appropriate antibody (anti-verrucarin F24) onto functionalized surface. Onto cleaned crystal (without grafting) anti-verrucarin F24 is not able to detect dust sample positive to verrucarin-A. Using non relevant antibody (anti-dinitrophenol) onto grafted FTIR sensors, we do not detect the presence of verrucarin-A in sample dust, like expected.
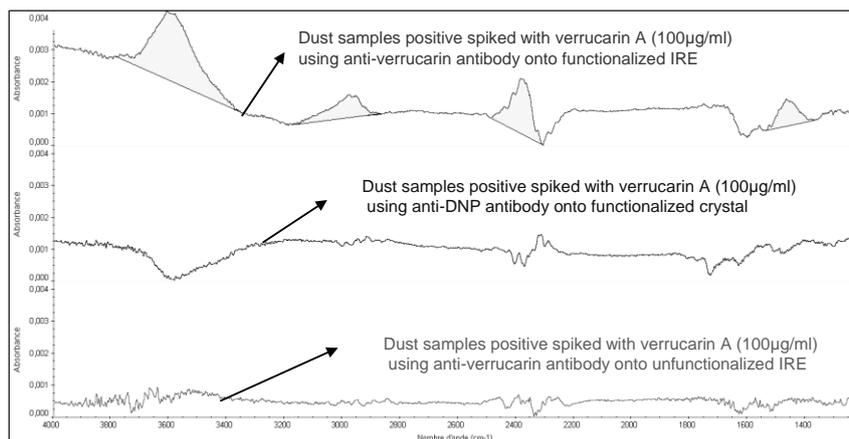
Figure 100: Specificity of the detection of dust samples spiked with Verrucarin-A

Comparing average spectra after rinsing, the verrucarin-A in positive dust samples and verrucarin-A spiked samples was detected only if the relevant antibody anti-verrucarin F24 was used as receptor onto our molecular construction as shown in **figure 100**. Without grafting, dust samples do not give significant peaks, even after spiking with verrucarin-A. If anti-DNP mAb is used, verrucarin-A is not detected demonstrating the specificity of this recognition
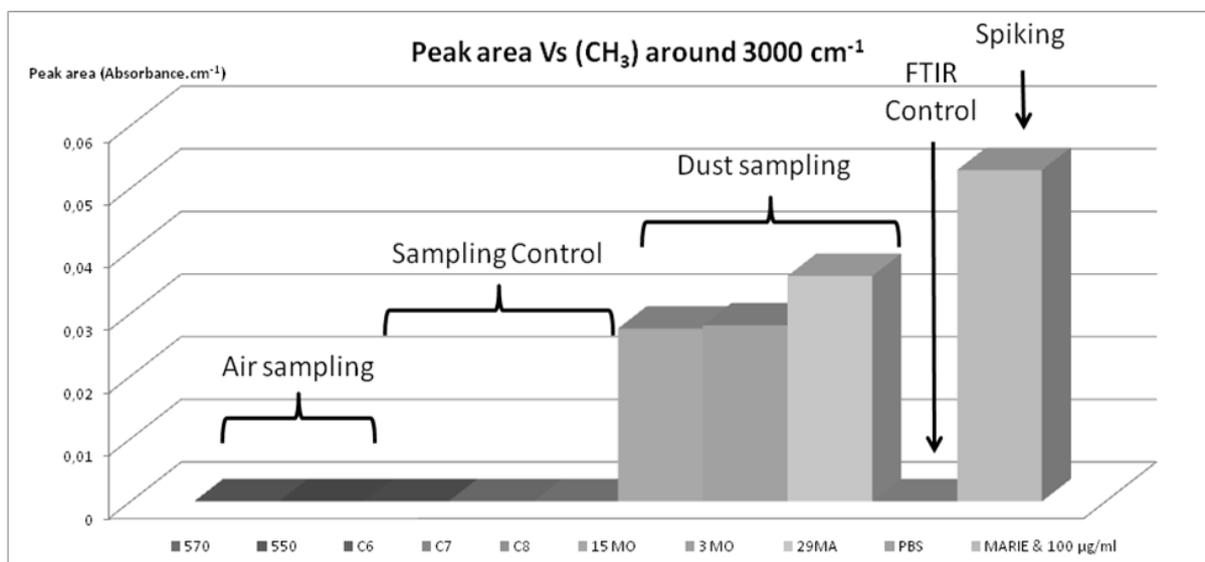
Figure 101: Mycotoxin detection around 3000 cm^{-1} in environmental samples.

We investigated the presence of Verrucarin -A in environmental samples using FTIR biosensors and the anti-verrucarin-A mAb F24.

We first focused on the CH stretching region around 3000 cm^{-1} (**in figure 101**) because this frequency is in agreement with chemical structure of the verrucarin-A.

Regarding the **dust samples**, CH peaks were found in all analyzed samples (15MO, 3MO, 29MA and spiked MARIE) after rinsing. This clearly indicates the presence of verrucarin-A in all dust samples. In all the control samples, no CH stretching vibrations were found showing there is no verrucarin-A.

Regarding the **air samples**, no peaks were found. The two samples (550 and 570) could be a priori considered as negative if we focused only on this infrared frequency. This discrepancy is probably due to the complexity of the media, but thanks to the large range of frequency explored by FTIR (between 4000 cm^{-1} and 850 cm^{-1}) other regions in agreement with chemical structure of verrucarin could be analyzed.
In the Hydroxyl stretching region (3300 cm^{-1}) (**figure 102)** these two samples show a strong significant peak (present in reference verrucarin-A spectra already shown on **figure 33**) unlike the control sample. So in this spectral region these samples can be considered as positive ones. Infrared detection in some infrared regions is thus in agreement with results obtained previously by ELISA.
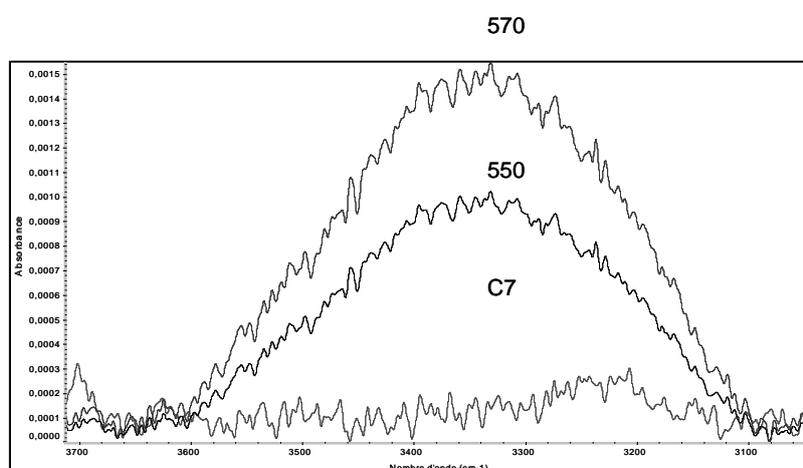
Figure 102: Mycotoxins detection in OH stretching region.
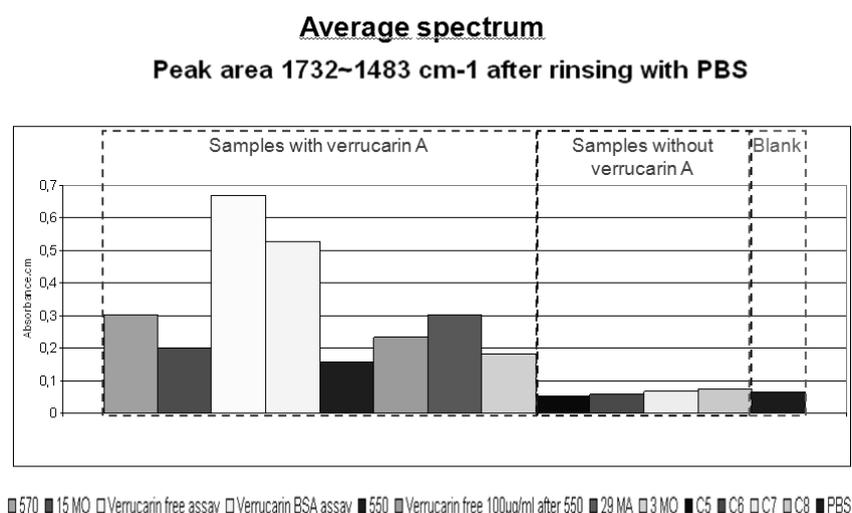
Figure 103: Mycotoxin detection between 1732 and 1483 cm^{-1} in environmental samples.

In **Figure 103**, we can also distinguish the positive samples for VERRU-A by analyzing the peaks area including C=C stretching and the C=O stretching.
You can note that the level of noise in this region is higher and therefore the peaks area of control samples is not equal to zero.

In conclusion, we have demonstrated that the FTIR biosensor is a promising technology able to detect mycotoxins in a complex matrix with a high sensitivity but the technique still needs further developments in order to validate the method, determine the limit of detection in environmental samples and quantify the ligands.

3. POLICY SUPPORT

The conclusions and recommendations arising from this study are the followings:

3.1. Investigation made on fungal flora in symptomatic dwellings and pathologies declared by the inhabitants

On surfaces, tenant's dwellings are far more contaminated by molds than owners ones (92% vs. 55%). This discrepancy has not been observed in air. However, the presence of mycotoxins has been clearly associated with the development of molds. 3 major genera of molds have been found but with the tenants, a larger diversity and representativeness is observed (36%), among which *Stachybotrys*, *Ulocladium* and *Alternaria,* known to cause adverse health effects, represent 12% of the total contamination.

- Recommendation: This mold proliferation should be avoided before health problems occur. Ideally, owners should be obliged to solve the problems of dampness and molds before putting a property for rent, and one way to make this item compulsory is to legalize it. When selling a property, the Walloon Region has to issue a Certificate with some points to be fulfilled about the state and energy performance of the dwelling for sale. Some requirement about dampness and fungal load might be added if not considered up to now. Tenants should also be more informed about of this problem, and when signing a new lease, a law should oblige to investigate the presence of mold or severe dampness problems leading to mold development.

Air contamination is massive (>90%) in symptomatic dwellings (*Stachybotrys, Ulocladium, Alternaria* represent 7 to 10%) while in control houses, the air presents a very low contamination (only in 6% of the dwellings)
The three major pathologies declared by the patients to their medical practitioner and to the LPI team during the intervention on site are asthma, bronchitis and rhinitis but we were not able in this study to find a direct correlation between a specific pathology and the presence of one or several specific mold genera.

- Recommendation: there is a need to conduct more studies to establish the causality between health problems and presence of peculiar genera of molds. There is also a need to study expression of biomarkers for indoor mold exposure but as reported in the literature, very few biomarkers exist at the current time that can aid in measuring human exposure to molds.

However, several studies are ongoing to develop appropriate methods (Van Emon *et al*, 2003; Jarvis and Miller, 2005; Pucheu-Haston *et al*, 2010).

3.2. Quantification of the indoor mold biomass

A Sandwich ELISA has been set up for the quantification of mold antigens (in air and dust).

In air, 88% of the control dwellings are below the sensitivity limit, 28-38% for symptomatic dwellings. The means values are lower in control than in symptomatic dwellings.

- Recommendation: It would be necessary to go further with the development of this test. One can imagine that a clean house should show a negative result in air. Further investigations should be conducted on the sampling methods to obtain negative results in control houses and positive ones in symptomatic dwellings, with appropriate sensitivity limits of detection and definition of thresholds values.

In dust, mold biomass has been found in all investigated dwellings, but the means values are significantly lower in control than symptomatic dwellings.
No correlation could be made between mold pollutants and dust mites pollutants, showing the large diversity of contaminants and situations.
Dust coming from carpets in symptomatic dwellings contains a highest *Cladosporium* spore equivalent quantity than in living and on mattresses, confirming the dust collecting properties of carpets versus smooth floor and mattresses.

- Recommendation: The spore antigens are present everywhere so the threshold value is not zero. It can reasonably be drawn from these data that values for mattresses and floor should not exceed $30 \ 10^6$ Eq clado sp/m2 and $85 \ 10^6$ Eq clado sp/m2 respectively. However, it would be more convenient to express results and threshold values per gram of dust. Therefore, a new study setting up an improved sampling method could be useful to achieve this aim. This method should ideally be independent on the way the inhabitants are cleaning their house, like the method described by Noss *et al* (2008, 2010) where a simple passive electrostatic dust fall collector is used to collect indoor dust, instead of vacuum dust sampling.

3.3. Quantification of mycotoxins indoors

In air, mycotoxins have been detected by LC-MS/MS in 18% of symptomatic dwellings but not in control dwellings. This value is of high concern since these compounds are the potential source of severe adverse effects on human health.

The major mycotoxins present in the analyzed samples are Roridin A and Verrucarin A. However, access to commercial mycotoxin standards for LC-MS/MS is very difficult and only a panel of 17 available standards was used (Polizzi *et al.*, 2009). We have no idea of the possible presence of other ones; we just can consider Verrucarin A and Roridin A as indicators of the potential contamination by mycotoxins.

The Quantitox kit from Envirologix overestimates mycotoxins in air, when compared to the results obtained in LC-MS/MS.
However, LC-MS/MS has shown limits with more difficult matrix like dust samples for which the limit of detection (LOD) was not sufficient.

- Recommendation: the existing tests and methods have all shown their limits and drawbacks, either with inadequate LOD or matrix effect problems.
  No correlation was found between mycotoxins and other parameters (airborne mold monitored by RCS sampler or by immunoassays), but only with the presence of mold visible on surface.

  Finally, a major recommendation could be simply to avoid the large spread of mold and therefore implement measures more quickly to avoid mold growth and synthesis of mycotoxins. This is more specifically recommended with tenants, since 100% of the mycotoxins found in air were in tenants dwellings and that 92% of the tenants' dwellings have mould on surfaces.
  This leads once again to stress on the need for a regulation regarding dampness and mold contamination of dwellings and the obligation that should be made to owners while hiring or selling a property to obtain some kind of certificate on sanitary condition after inspection, and make compulsory the remediation if dampness and molds are detected.
  This is maybe even more crucial in these times of repeated floods that will promote mold growth in dwellings where dampness problems are becoming recurrent.

Detection of mycotoxins in dust affects 13,6 % of symptomatic dwellings (results obtained by ELISA test)

- Recommendation: there is a need for a better comparison between LC-MS/MS and ELISA. Matrix effects are affecting the performance of the LC-MS/MS technique but the ongoing development of improved protocols should partly or totally overcome this drawbacks.

Based on these uncertainties, we do not dispose of sufficient and definitive information to predict human health exposure effects when dealing with inhalation of mycotoxins in a typical, nonindustrial indoor environment. Thus, further study is needed. This lack of definitive information creates the need to eliminate or reduce the potential for exposure. This can only be achieved via the proactive control of mold growth. As noted, mold growth requires an adequate substrate (food source), suitable temperature conditions and moisture. Controlling one - or all - of these parameters will help prevent mold growth. To do so, a facility should establish an effective preventive maintenance program that includes:

*systematic facility inspections that focus on typical moisture sources such as roofs, piping systems, HVAC systems, condensation sources and humidification systems;

*timely repair or elimination of identified water leaks or other unwanted sources of water;

*routine HVAC maintenance that includes filter change-outs, humidity control adjustments, airflow adjustments and cleaning;

*routine inspections to look for visible evidence of mold growth/water damage;

*adequate cleaning of mold growth/water-damaged nonporous materials with suitable cleaning agents such as a 10-percent bleach solution and/or the removal of potentially contaminated porous materials such as carpeting, drywall, furniture and ceiling tiles. These simple tips can also help a facility control mold growth;

*Repair plumbing and other building leaks as soon as possible;

*Watch for condensation sources and fix them. To achieve this,
1) increase the surface temperature by insulating or increasing air flow or 2) reduce indoor humidity levels by repairing leaks, increasing ventilation or dehumidification.

*Maintain HVAC drip pans, piping systems and other components in a clean, unobstructed condition.

*Vent moisture-generating appliances and processes directly to the outside.

*Maintain indoor relative humidity levels in the range of 30 to 50 percent.

*Clean and dry wet/damp spots as soon as possible.

*Keep foundations as dry as possible through proper drainage and sloping.

4. DISSEMINATION AND VALORISATION

4.1. Poster and abstracts presentation at international meetings

E. Gosselin, M.Gorez, M. Voué, O. Denis, J. Conti, A. Van Cauwenberge, E. Noël, J. De Coninck "Detection of small molecules in competitive immunoreactions monitored by BIA-ATR sensors" presented at the EUROSENSORS 2008 congress – Dresden – Germany 07.09-10.09.2008.

M. Gorez, E. Gosselin, N. Popovic, O. Denis, J. Conti, A. Van Cauwenberge, E. Noël, J. De Coninck, M. Voué. "Fourier-transform infrared immunosensors: mycotoxin analysis tools of tomorrow?" Presented at World Mycotoxin Forum 2008 (WMF), 17-18 November 2008, Noordwijk-aan-Zee, The Netherlands.

M. Voué, A. Van Cauwenberge, O. Denis, E. Gosselin, N. Popovic, J. De Coninck.. "Fourier transform infrared sensors: a breakthrough for immunodetection" presented at 1st Bio-Sensing Technology Conference, Bristol (UK) 10-12 November 2009.

E. Gosselin, A. Van Cauwenberge, O. Denis, N. Popovic, J. De Coninck. "FTIR-ATR biosensors: a new label-free method", presented in BIOSENSORS 2010, Glasgow (UK), 26-28 May 2010.

4.2. Symposium

- Organisation of the Workshop « Indoor Air Pollution and Health Problems », Brussels, Domaine de Latour de Freins, 25th May 2009.

5. PUBLICATIONS

Gosselin E., Gorez M., Voue M., Denis O., Conti J., Popovic N., Van Cauwenberge A., Noel E., De Coninck J. (2009) Fourier transform infrared immunosensors for model hapten molecules. *Biosensors and Bioelectronics*, 24, 2554-2558.

E. Gosselin, M. Gorez, M. Voué,*, O. Denis, J. Conti, A. Van Cauwenberge, E Noel, J. De Coninck. 2008. "Detection of small molecules in competitive immunoreactions monitored by BIA-ATR sensors" Poceedings of the EUROSENSORS 2008 congress.

Olivier Denis, Anne Van Cauwenberge, Greta Treutens, Bouazza Es Saadi, Françoise Symoens, Nathalie Popovic, and Kris Huygen. Characterization of new mold and *Alternaria alternata* specific rat monoclonal antibodies.
Will be submitted to *Mycopathologia* in January 2011

6. ACKNOWLEDGMENTS

We wish to thank the following persons for their helpful collaboration to this project:
- Prof. Sarah DE SAEGER, Department of Bioanalysis, Laboratory of Food Analysis, Ghent University.
- Svetlana MALYSHEVA and Dr Barbara DELMULLE, Department of Bioanalysis, Laboratory of Food Analysis, Ghent University.
- Prof. F. de BLAY and Mrs Martine OTT, Laboratoire d'Allergologie, Nouvel Hopital Civil, Strasbourg, FRANCE.
- Prof. Jacqueline MARCHAND-BRYNAERT, CHOM, Université Catholique de Louvain (UCL).
- Prof. Erik GOORMAGHTIGH Structure et Fonction des Membranes Biologiques – SFMB, Université Libre de Bruxelles (ULB).
- Prof. Jean-Jacques VANDEN EYNDE, Laboratory of Organic Chemistry, University of MONS (UMons).

7. REFERENCES

Ackermans, F., F. Nisol, and H. Bazin. 1990. Immunization of rats. In: Bazin H., editor. *Rat hybridomas and rat monoclonal antibodies.* Boca Raton, CRC Press; **1990**. pp. 75–85.

Akinbami, L.J., Moorman, J.E., Garbe, P.L., and Sondik, E.J. 2009. Status of Childhood Asthma in the United States, 1980–2007. *Pediatrics:* 123 (Supp 3), S131-145.

American Lung Association. 2007. Epidemiology & Statistics Unit, Research and Program Services. Trends in Asthma Morbidity and Mortality.

Andreescu, S., and O. A. Sadik. 2004. Correlation of analyte structures with biosensor responses using the detection of phenolic estrogens as a model. *Anal. Chem.* 76: 552-560.

Bartra, J., J. Belmonte, J. M. Torres-Rodriguez, and A. Cistero-Bahima. 2009. Sensitization to Alternaria in patients with respiratory allergy. *Front Biosci.* 14: 3372-3379.

Bazin, H., L. M. Xhurdebise, G. Burtonboy, A. M. Lebacq, C. L. De, and F. Cormont. 1984. Rat monoclonal antibodies. I. Rapid purification from in vitro culture supernatants. *J. Immunol. Methods* 66: 261-269.

Bex, V., A. Mouilleseaux, L. Bordenave, and F. Squinazi. 2003. [Environmental audits in Ile-de-France]. *Eur. Ann. Allergy Clin. Immunol.* 35: 259-263.

Black, P. N., A. A. Udy, and S. M. Brodie. 2000. Sensitivity to fungal allergens is a risk factor for life-threatening asthma. *Allergy* 55: 501-504.

Bornehag, C. G., J. Sundell, L. Hagerhed-Engman, T. Sigsggard, S. Janson, and N. Aberg. 2005. 'Dampness' at home and its association with airway, nose, and skin symptoms among 10,851 preschool children in Sweden: a cross-sectional study. *Indoor. Air* 15 Suppl 10: 48-55.

Brasel, T. L., J. M. Martin, C. G. Carriker, S. C. Wilson, and D. C. Straus. 2005. Detection of airborne Stachybotrys chartarum macrocyclic trichothecene mycotoxins in the indoor environment. *Appl. Environ. Microbiol.* 71: 7376-7388.

Cooley, J. D., W. C. Wong, C. A. Jumper, and D. C. Straus. 2004. Fungi and the indoor environment: their impact on human health. *Adv. Appl. Microbiol.* 55: 1-30.

Dales, R., L. Liu, A. J. Wheeler, and N. L. Gilbert. 2008. Quality of indoor residential air and health. *CMAJ.* 179: 147-152.

Devouge, S., C. Salvagnini, and J. Marchand-Brynaert. 2005. A practical molecular clip for immobilization of receptors and biomolecules on devices' surface: synthesis, grafting protocol and analytical assay. *Bioorg. Med. Chem. Lett.* 15: 3252-3256.

Digneffe, C., F. Cormont, B. Platteau, and H. Bazin, 1990. *Fusion cell lines* In: Bazin H. , editor. *Rat hybridomas and rat monoclonal antibodies.* Boca Raton, CRC Press; 1990. pp. 69-74.

Drusch, S., and W. Ragab. 2003. Mycotoxins in fruits, fruit juices, and dried fruits. *J. Food Prot.* 66: 1514-1527.

European lung white book. 2003 European Respiratory Society and the European Lung Foundation. Brussels, Belgium.

Flappan, S. M., J. Portnoy, P. Jones, and C. Barnes. 1999. Infant pulmonary hemorrhage in a suburban home with water damage and mold (Stachybotrys atra). *Environ. Health Perspect.* 107: 927-930.

Goldzstein, A., A. Aamouche, F. Homble, M. Voue, J. Conti, C. J. De, S. Devouge, J. Marchand-Brynaert, and E. Goormaghtigh. 2009. Ligand-receptor interactions in complex media: a new type of biosensors for the detection of coagulation factor VIII. *Biosens. Bioelectron.* 24: 1831-1836.

Goormaghtigh, E., V. Raussens, and J. M. Ruysschaert. 1999. Attenuated total reflection infrared spectroscopy of proteins and lipids in biological membranes. *Biochim. Biophys. Acta* 1422: 105-185.

Institute of Medicine of the National Academy of Sciences. 2004. Damp indoor Spaces and Health, Report from the committee from the board on health promotion and diseases prevention, The national academies press, Washington DC. http://www.nap.edu/openbook.php?isbn=0309091934

Jarvis BB and Miller JD.2005. Mycotoxins as harmful indoor air contaminants. *Appl Microbiol Biotechnol.* 2005. 66(4):367-72

Jennessen, J., K. F. Nielsen, J. Houbraken, E. K. Lyhne, J. Schnurer, J. C. Frisvad, and R. A. Samson. 2005. Secondary metabolite and mycotoxin production by the Rhizopus microsporus group. *J. Agric. Food Chem.* 53: 1833-1840.

Jonsson, U., L. Fagerstam, B. Ivarsson, B. Johnsson, R. Karlsson, K. Lundh, S. Lofas, B. Persson, H. Roos, I. Ronnberg, and . 1991. Real-time biospecific

interaction analysis using surface plasmon resonance and a sensor chip technology. *Biotechniques* 11: 620-627.

Kroger, D., M. Liley, W. Schiweck, A. Skerra, and H. Vogel. 1999. Immobilization of histidine-tagged proteins on gold surfaces using chelator thioalkanes. *Biosens. Bioelectron.* 14: 155-161.

Lebacq-Verheyden, A. M., A. Neirynck, A. M. Ravoet, and H. Bazin. 1983. Rat hybridoma technology: culturing of rat myeloma cell line IR983F prior to cell fusion. *Hybridoma* 2: 355-358.

Liley, M., J. Bouvier, and H. Vogel. 1997. Incorporation and Antibody Recognition of a Lipid-Anchored Membrane Protein in Supported Lipid Layers. *J. Colloid Interface Sci.* 194: 53-58.

Malmqvist, M. 1993. Biospecific interaction analysis using biosensor technology. *Nature* 361: 186-187.

Marchand-Brynaert, J., E. Goormaghtigh, F. Homblé, M. Voué, and J. De Coninck, J. 2002. Surface chemical modification of optical elements for the spectroscopic detection of molecules and organic components, PCT WO 02/056018A1.

Mirabella Jr F.M. (editor), 1993. *Internal Reflection Spectroscopy, Theory and Applications*, Mar-cel Dekker, New York.

Niemeier, R. T., S. K. Sivasubramani, T. Reponen, and S. A. Grinshpun. 2006. Assessment of fungal contamination in moldy homes: comparison of different methods. *J. Occup. Environ. Hyg.* 3: 262-273.

Nolard, N., H. Beguin, and C. Chasseur. 2001. [Mold allergy: 25 years of indoor and outdoor studies in Belgium]. *Allerg. Immunol. (Paris)* 33: 101-102.

Noss I, Wouters IM, Visser M, Heederik DJ, Thorne PS, Brunekreef B, Doekes G. 2008. Evaluation of a low-cost electrostatic dust fall collector for indoor air endotoxin exposure assessment. *Appl Environ Microbiol.* 74(18):5621-7.

Noss I, Doekes G, Sander I, Heederik DJ, Thorne PS, Wouters IM. 2010. Passive airborne dust sampling with the electrostatic dustfall collector: optimization of storage and extraction procedures for endotoxin and glucan measurement. *Ann Occup Hyg.* 54(6):651-8.

Ozcelik, S., N. Ozcelik, and L. R. Beuchat. 1990. Toxin production by Alternaria alternata in tomatoes and apples stored under various conditions and quantitation of the toxins by high-performance liquid chromatography. *Int. J. Food Microbiol.* 11: 187-194.

Perzanowski, M. S., R. Sporik, S. P. Squillace, L. E. Gelber, R. Call, M. Carter, and T. A. Platts-Mills. 1998. Association of sensitization to Alternaria allergens with asthma among school-age children. *J. Allergy Clin. Immunol.* 101: 626-632.

Polizzi V, Delmulle B, Adams A, Moretti A, Susca A, Picco AM, Rosseel Y, Kindt R, Van Bocxlaer J, De Kimpe N, Van Peteghem C, De Saeger S. 2009. JEM Spotlight: Fungi, mycotoxins and microbial volatile organic compounds in mouldy interiors from water-damaged buildings. *J. Environ Monit.* 11(10):1849-58.

Pucheu-Haston CM, Copeland LB, Vallanat B, Boykin E, Ward MD. 2010. Biomarkers of acute respiratory allergen exposure: screening for sensitization potential. *Toxicol Appl Pharmacol* 15; 244(2):144-55

Resano, A., M. L. Sanz, and A. Oehling. 1998. Sensitization to Alternaria and Cladosporium in asthmatic patients and its in vitro diagnostic confirmation. *J. Investig. Allergol. Clin. Immunol.* 8: 353-358.

Robine, E., I. Lacaze, S. Moularat, S. Ritoux, and M. Boissier. 2005. Characterisation of exposure to airborne fungi: measurement of ergosterol. *J. Microbiol. Methods* 63: 185-192.

Scudamore, K. A., S. Nawaz, and M. T. Hetmanski. 1998. Mycotoxins in ingredients of animal feeding stuffs: II. Determination of mycotoxins in maize and maize products. *Food Addit. Contam* 15: 30-55.

Seltzer, J. M., and M. J. Fedoruk. 2007. Health effects of mold in children. *Pediatr. Clin. North Am.* 54: 309-3ix.

Van Emon, J. M., A. W. Reed, I. Yike, and S. J. Vesper. 2003. ELISA measurement of stachylysin in serum to quantify human exposures to the indoor mold Stachybotrys chartarum. *J. Occup. Environ. Med.* 45: 582-591.

Vesper, S., D. G. Dearborn, I. Yike, T. Allan, J. Sobolewski, S. F. Hinkley, B. B. Jarvis, and R. A. Haugland. 2000. Evaluation of Stachybotrys chartarum in the house of an infant with pulmonary hemorrhage: quantitative assessment before, during, and after remediation. *J. Urban. Health* 77: 68-85.

Vigano, C., J. M. Ruysschaert, and E. Goormaghtigh. 2005. Sensor applications of attenuated total reflection infrared spectroscopy. *Talanta* 65: 1132-1142.

Voue, M., E. Goormaghtigh, F. Homble, J. Marchand-Brynaert, J. Conti, S. Devouge, and C. J. De. 2007. Biochemical interaction analysis on ATR devices: a wet chemistry approach for surface functionalization. *Langmuir* 23: 949-955

WHO, 1990. Selected mycotoxins: Ochratoxins, Trichothecenes, Ergot. Environmental Health criteria 10. International Programme on Chemical Safety, World Health Organisation, Geneva, pp. 71-154.

Zureik, M., C. Neukirch, B. Leynaert, R. Liard, J. Bousquet, and F. Neukirch. 2002. Sensitisation to airborne moulds and severity of asthma: cross sectional study from European Community respiratory health survey. *BMJ* 325: 411-414.